

MODELLING OF SEASONAL THERMAL ENERGY STORAGE SYSTEMS

by

DIANE LU KOZLOWSKI

A thesis submitted in partial fulfillment of the
requirements for the degree of

Master of Science
(Mechanical Engineering)

at the

UNIVERSITY OF WISCONSIN - MADISON

May, 1989

Abstract

High investment costs and and complex thermal interactions of Central Solar Heating Plants with Seasonal Storage (CSHPSS) subsystems dictate careful planning and numerical predictions of the thermal performance of system designs. The work presented here has brought CSHPSS modelling capabilities to the TRNSYS simulation program.

The Lund University (Sweden) Stratified Storage Temperature (SST) computer model was adapted for use in TRNSYS. The model uses a "plug flow" storage volume coupled to a finite differenced surrounding ground. It is very adaptable to different storage volume shapes and control strategies. A detailed description of the SST and other models used in CSHPSS systems simulations is presented.

Predictions with the new TRNSYS version of the SST model were compared to several years of hourly data from the Lyckebo system in Sweden, the world's largest operational CSHPSS. The computer simulation of this system was complicated by the presence of a thermosiphon phenomenon in the storage cavern. Nonetheless, good predictions of monthly storage losses and cavern temperature profiles where obtained. The problem of numerical dispersion associated with stratified store computer models is discussed.

A detailed analysis of the modelling incorporated into the MINSUN computer program was made. The MINSUN program was developed specifically for the design optimization of CSHPSS systems. It is less detailed than the TRNSYS computer program. Simulations performed with the TRNSYS and MINSUN versions of the SST were compared for two CSHPSS systems. The SST models for each program gave identical results. The addition of other subsystem models gave somewhat different simulation results for the two programs, most notably the useful energy collected.

Acknowledgements

This work was funded by a grant from the United States Department of Energy. Let's keep the dough coming, George.

I would like to thank the following people for their help:

- The many participants in the Swedish Solar Heating Program with whom I communicated.
- Mr. Dwayne Breger, without whom the MINSUN computer work would not be possible.
- Professor Jack Duffie, whose reputation for excellence in the field of solar energy brought me to the SEL. I am grateful to have worked with him.
- Professor Bill Beckman, who made this thesis possible. Not only is he the most impeccably dressed man I've ever known, he is the best teacher I have had in my 21 years as a student. (Thank you, too, Sandy.)
- These citizens of the Federal Republic of Germany: Frank-Detlef, Manfred (the "Skull"), and the ever talented Harald.
- Doug-R, Ph.D, for his many insights, Mark-Cake, for being the best, Tim, for the many conversations, and Blake, for teaching me the words to "The Bowling Song".

I must thank with all my heart and soul my most fabulous husband Kenny and the members of our family. *Moja Droga Ja Cię Kocham.*

Table of Contents

Abstract, ii

Acknowledgements, iii

Chapter 1 Introduction 1

- 1.1 IEA Task VII, 3
- 1.2 Swedish Council for Building Research, 6
- 1.3 CSHPSS Design Considerations, 7
- 1.4 Operational Considerations, 9
- 1.5 Objective of This Study, 10

Chapter 2 Seasonal Storage Simulation Models 12

- 2.1 Previous Stratified Tank Models, 12
- 2.2 Stratified Storage Temperature Model, 15
 - 2.2.1 Ground Calculations, 18
 - 2.2.2 Storage Volume Calculations, 24
 - 2.2.3 Buffer Strategy, 28
 - 2.2.4 Storage Control Strategy, 30
 - 2.2.5 Component Startup, 33
- 2.3 Collector Model, 36

- 2.4 Pipe Model, 36
- 2.5 House Load Model, 37
- 2.6 Heat Pump Model, 38

Chapter 3 SST Model Validation

44

- 3.1 The Lyckebo CSHPSS, 44
- 3.2 Available Data , 51
- 3.3 Description of Validation Simulation, 55
- 3.4 Lyckebo Cavern Thermosiphon, 57
- 3.5 Simulation Procedure, 61
- 3.6 Simulation Results, 63
 - 3.6.1 Results Without Use of Buffers, 63
 - 3.6.2 Results With Use of Buffers, 68
- 3.7 Equivalent Conductivity of Thermosiphon, 72
- 3.8 Effect of Buffer Size and Number of Nodes, 76

Chapter 4 Comparison of TRNSYS and MINSUN CSHPSS Simulations 83

- 4.1 Program Descriptions, 84
- 4.2 Previous Comparison Study, 85
- 4.3 Description of Test Simulations, 86
- 4.4 Results of SST Test Simulations, 90

4.5	Results of Subsystem Test Simulations, 92	
4.5.1	Collector Subsystems, 93	
4.5.2	Load Distribution Subsystems, 101	
4.6	MINSUN and TRNSYS Results of Lyckebo Simulation, 105	
4.7	MINSUN and TRNSYS Results of Franklin System Simulation, 110	
Chapter 5	Discussion and Conclusions	121
5.1	Validation of the SST Model	121
5.2	Comparison of TRNSYS and MINSUN	125
5.3	Future Work	126
Appendix A	Flow Diagram of TRNSYS SST	128
Appendix B	Grid Pre-Processor Program	134
Appendix C	Computer Code for Selected SST Subroutines and for Other Models Used in This Study	147
Appendix D	Comparison of MINSUN and TRNSYS April 15 Predictions of Useful Energy Collected	177
Appendix E	Comparison of MINSUN and TRNSYS April 15 Predictions of Total House Load	180
Appendix F	TRNSYS Deck for Comparison Simulation of Lyckebo System	182
Appendix G	TRNSYS Deck for Comparison Simulation of Franklin System	193

List of Figures	204
List of Tables	207
Nomenclature	209
References	212

Chapter 1

Introduction

Variations in energy supply and demand can be offset by the use of energy storage. For this reason, Seasonal Thermal Energy Storage (STES) systems are gaining acceptance as an alternative technology in the production of space heating and hot water. A wide variety of storage structures are used for the collection of plentiful solar energy in the summer and the subsequent discharge of this stored energy in the winter when system loads are greatest. These systems are most applicable at northerly latitudes where large seasonal differences in temperature and solar radiation exist. Seasonal storage technology has burgeoned in the last decade, with much effort by participants of an international collaboration and researchers in several Scandinavian nations. The type of system employed will depend on the climate, geology, and economics of a given location. These systems can serve a single large building or an entire community.

STES has been employed with centralized heating systems, which is an established technology in Europe. The terms *group heating* and *district heating* are used to distinguish between small (a few hundred residential units) and large (a few thousand residential units) centralized heating plants. When solar energy is used as a heating source for STES - centralized heating plants, the term *Central Solar Heating Plant with Seasonal Storage* (CSHPSS) is employed. (The term is sometimes used in reference to

small, single facilities which employ solar - STES.) There are 32 identified CSHPSS systems worldwide (Bankston, 1987); several more are currently in the planning stages (Öfverholm, 1988).

CSHPSS district heating systems rely on the technology of low temperature load distribution systems. Space heating and domestic hot water needs are met at temperatures of 60 to 90 °C, rather than the relatively high temperatures required for process steam.

Underground thermal energy storage is usually employed with STES systems and can take several forms. Tubes, coils or ducts may be used in either a horizontal or vertical configuration. Above ground, buried, or partially exposed tanks may be utilized. Storage volumes may be excavated from the ground. Smaller excavations may require lining and insulation to lessen heat losses. Partial excavation storage volumes are also possible for smaller systems, with the top portion of the storage volume built up from the ground by berms. Large uninsulated excavations may be located in stable rock formations and be of such a size which ensures a small surface area to volume ratio. Thermal energy may also be stored in confined aquifers.

The present study concentrates on the modelling of CSHPSS designs which use earth pit and cavern storage types. Although site-specific storage types such as aquifers and vertical pipes with heat pumps could offer the lowest solar cost at low solar fractions, the earth pit and cavern storage systems are the most widely applicable technologies (Lund, 1987). The latter systems offer high solar fractions and a higher degree of energy independence.

1.1 IEA Task VII

Interest in CSHPSS systems has grown tremendously in the international community within the past decade. Much of the experience gained internationally has been shared in a collaborative effort coordinated by the International Energy Agency (IEA) Solar Heating and Cooling Program, under Task VII of this program. The activities of the program have included comprehensive feasibility and system evaluation studies and economic analyses. Because the investment costs of these systems are considerable, a systematic examination of the thermal and economic performances of different CSHPSS configurations via computer simulation was a major contribution of the program.

The IEA Task VII work, while still ongoing, can be divided into two initial phases (Bankston, 1986). Phase I emphasized development of preliminary designs, collection of data, and development of numerical tools. The MINSUN computer program was developed by Task members specifically for the analysis and optimization of CSHPSS designs. Modelling assumptions are built into the program and are specific to CSHPSS systems. Phase II compared results of simulations, examined system configurations and operational strategies, and location dependent parameters. Economics of configurations were investigated for a number of locations, and specific recommendations for further development made.

The MINSUN program is able to perform repetitions of a simulation for a given configuration while varying key parameters over a specified range. Optimal designs are

then found by minimizing the total investment and operating costs to meet a specified load or solar fraction. A brief summary of the work performed during Phase II of IEA Task VII serves as an example of both the type of optimization available with the MINSUN program and the economic considerations made in the design of CSHPSS systems.

The approach of the location dependent evaluations by Task members was standardized for the combined comparison of many system designs. A set of system configurations was first chosen for simulation. The system configuration was defined by specifying the types of solar collector, storage volume, and load distribution system, use of a heat pump, and total load (including domestic hot water fraction). Parametric analysis and optimization of configurations were then performed and ranked for different localities. The summarized results thus represented thousands of computer simulations.

Optimizations were based on minimizing a levelized annual cost for a given load. These costs represented only the investment of collector and storage subsystems and heat pump, if any. Assumptions on the actual cost of auxiliary energy or fuel price escalation rate were not included at this step in the optimization. The costs were compared for different systems by defining a *unit solar cost* as

$$\text{Unit Solar Cost} = \frac{\text{Levelized Annual Solar Costs}}{\text{Annual Energy Delivered from Storage}}$$

Simulations were performed to find the solar fraction yielded. Least unit solar cost designs for a given load and set of common parameters were then identified at a given solar fraction by plotting unit solar cost versus solar fraction.

The specification of actual auxiliary energy costs was the final step in the design optimization process. Systems with the highest cost-effective solar fraction were then determined by use of marginal cost analysis. Marginal cost curves represent the cost of an additional unit of solar fraction. Systems with a minimum unit solar cost less than the auxiliary fuel cost were cost-effectively increased in solar fraction until the marginal cost equalled the fuel cost per unit of output. One would choose the minimum unit solar cost system for a system which is not cost-effective unless the reason for building is not economic (e.g., independence from oil as an energy source).

Results for the design of small and large CSHPSS systems from the Swedish national contribution to the IEA study are of particular interest (Bankston, 1986). It was found that the use of a heat pump and associated high costs mandated the use of inexpensive unglazed flat plate collectors. Systems with no heat pumps could cost-effectively make use of new high efficiency flat plate collectors. Above ground tanks were found to be expensive, forcing small storage volumes and inefficient collector operation. Lower unit cost systems favored larger storage volumes, rather than larger collector arrays. The lowest system (and hence highest cost-effective solar fraction) costs were found for non-heat pump systems with new, highly efficient flat plate collectors. There are increasing thermal and economic benefits with large systems, associated with decreasing storage losses as the surface area to volume ratio decreases and with relatively low costs of excavation per volume.

The value of this work is seen in that promising configurations can be easily identified. MINSUN has thus shown to be a useful tool in the sizing of collector arrays, storage volume, and other system parameters.

1.2 Swedish Council for Building Research

The management of IEA Task VII has been conducted by the Swedish Council for Building Research. The Swedish government has a policy of pursuing energy sources which are alternatives to the use of nuclear energy and will reduce oil dependence. As a result of both referendum and parliamentary decision, nuclear power will be phased out in Sweden by the year 2010. Approximately 20% of that nation's electricity budget is used for heating (Andersson, 1988). Consequently, the Swedish government has expended much effort toward the development of CSHPSS systems. A series of increasingly larger heating plants have been built for research purposes. There currently exist over a dozen such systems in Sweden, including Lyckebo, the world's largest CSHPSS facility. The solar heating plants with seasonal heat stores being developed in Sweden are intended for future retrofit to existing group and district heating systems. In this manner, solar energy can potentially make a substantial contribution to the nation's energy needs.

Considerable experience in the design and performance of CSHPSS systems has been acquired through the Swedish effort. Thermal performance of collectors and storage volumes has been greatly improved by the Swedes, with resultant reduced costs. A major step toward cost effectiveness has been the development of large collector arrays specific to CSHPSS which exhibit very high efficiencies.

1.3 CSHPSS Design Considerations

The technical and economic performance of CSHPSS system vary with geology, climate, choice of sub-system, and load specific features; however, some general design considerations can be made. Presented here are findings from Swedish design experience (Dalenbäck, 1987a and 1987b).

The load distribution system can be classified according to the design temperature of the fluid extracted from the storage volume. The somewhat misnomered terminology of High Temperature Distribution System, or HTDS, and Low Temperature Distribution System, or LTDS, is sometimes used. In LTDS systems, the distribution outlet temperature is boosted to meet space heating and DHW loads, presumably via a heat pump. HTDS can meet the required load temperatures directly. Smaller earth pit systems make best use of LTDS, whereas larger cavern systems can make use of HTDS.

A size comparison of pit and cavern CSHPSS systems defining parameters is presented in Table 1.1. Larger cavern stores are nearly cost competitive with current (Swedish) energy prices because of an economy of scale in both construction costs and thermal performance. Projected costs for both storage types are shown, assuming a further price reduction in collector arrays. Because a transition between optimally sized pit and cavern storage volumes occurs between 60,000 and 100,000 m³, studies showed that storage volumes which fall within this range are not economically justified.

Table 1.1: Comparison of Pit and Cavern CSHPSS Systems

<u>Characteristic</u>	<u>Small System</u>	<u>Large System</u>
Storage Type	Insulated Pit	Rock Cavern
Storage Volume (m ³)	2000 - 60,000	100,000 minimum
Nominal Demand	100 - 3000 kW	5 MW
Annual Load	300 - 8000 MW-h	12 GW-h
Distribution System	HTDS or LTDS with use of Heat Pump	HTDS
*Projected Cost (SEK/kW-h)	0.40	0.30

*Projected costs assume a 30% future price reduction in collector arrays at 1987 price levels converted at an exchange of 1 SEK = \$ 0.16 U.S.

Swedish studies have also found a sensitivity to the size and distribution of heating load. The unit solar cost decreases with increasing total load and fraction of DHW. There is less seasonal dependence of the load profile with an increasing percent DHW, as possible in a community which includes light industrial loads.

Design guidelines for the building of Swedish CSHPSS systems can be extracted from much analytical and experimental work (Dalenbäck, 1987):

- 6 m² of collector area required per kW load
- 15 m² of ground space per kW load

- 18 m³ of storage volume per kW load
- Solar Fraction at design = 70 to 80%

Solar fractions above this value have very expensive additional unit costs. Also, there is a large uncertainty of annual variation of irradiation and load demand. Therefore, the optimal seasonal storage design is usually for less than 100% solar fraction.

Advantages for the connection of supplementary heating equipment directly to the store have been found. Equipment can be rated for lower output power than the power demand of the load. Lower capital and operating costs are then obtained. An industrial heat source may be used, and could supply energy on a schedule different than that of the demand. Many options for the use of energy sources in combination with solar collectors have been investigated, including incineration and co-generation (Sellberg, 1988).

The solar collectors used with auxiliary direct-to-store systems are designed and operated to yield high outlet temperatures of 90 - 95 °C. The load can then be met directly (without boosting) with the high temperatures obtained. Thus, in such systems, high temperature auxiliary energy must be added to the store if the maximum storage temperature falls below the minimum necessary to meet the demand.

1.4 Operational Considerations

The maintenance of thermal stratification in large scale CSHPSS storage volume is important for efficient thermal performance of the collector and load distribution systems.

Low temperatures must be available for efficient operation of the collector array, while high temperatures must be available to meet the load demand. A review of stratified tank models for computer simulations is presented in Chapter 2.

Thermal performance of a CSHPSS system is greatly influenced by the strategy employed in the operation of the collector array. High collector flow rates (ca. 0.015 l/s-m^2) decrease the turnover time of the storage volume. High flowrates encourage mixing in the storage volume with subsequent loss of stratification. These flow rates yield a low temperature rise in the collectors, and thus are unsuitable for high temperature distribution applications. Variable collector flowrates may be used to obtain a set temperature value in a relatively small storage volume in order to meet the temperature required by the load. This control strategy achieves a high temperature, rather than high (efficient) thermal yield from the system. Low constant flow rates (ca. 0.005 l/s-m^2) will produce a large temperature rise of the medium passing through the collector and help maintain stratification. An increase in system solar fraction can be obtained because high temperatures are available for distribution to the load earlier in the annual cycle.

It is recommended to operate the load distribution system such that heating takes place at a temperature level which is close to the lower limit of utility. Lower distribution losses will then be observed. Because distribution systems are of considerable length in CSHPSS systems, these losses cannot be neglected. The return temperature from the load should be as low as possible for two reasons: efficient utilization of the distributed thermal energy will be realized and collector efficiency will be maintained.

1.5 Objective of This Study

High investment costs and complex thermal interactions of Central Solar Heating Plants with Seasonal Storage subsystems dictate careful planning and numerical predictions of the thermal performance of system designs. Therefore, the main objective of this work is to bring CSHPSS modelling capabilities to the TRNSYS simulation program.

The Task VII participants, in cooperation with Lund University (Sweden) developed several STES computer models, including those for duct, aquifer, and Stratified Storage Temperature (SST) storage volumes. These have been incorporated into the MINSUN program. The Lund Stratified Storage model was shown to be very sophisticated and superior to existing TRNSYS stratified storage models for CSHPSS systems simulations. The TRNSYS models were not intended to be used for long-term storage.

The Lund Stratified Storage Temperature model was adapted for use in TRNSYS. This computational model was then tested and compared to versions already in use. Predictions with the new TRNSYS version of the model were compared to data from the Lyckebo system in Sweden, which has had extensive monitoring on it since the beginning of its operation. A detailed analysis of the modelling incorporated into the MINSUN program was made. Simulations performed with the TRNSYS and MINSUN versions of the SST were compared for two CSHPSS systems.

Chapter 2

Seasonal Storage Simulation Models

This chapter describes the models which were developed for use in TRNSYS CSHPSS simulations. A TRNSYS component for seasonal thermal energy storage has been developed based on the Lund University Stratified Storage Temperature (SST) model. Previous TRNSYS tank models did not include heat loss and thermal storage calculations for surrounding ground. This chapter also discusses other components that were written or modified to be comparable to those used in the MINSUN program for the TRNSYS - MINSUN comparison presented in Chapter 4.

2.1 Previous Stratified Tank Models

Kuhn et al. (1980) reviewed the Thermal Energy Storage (TES) models available for computer simulations. A usual assumption of TES models is one dimensional heat transfer within the liquid in the vertical direction. This assumption presumes horizontal isotherms in the tank and represents a higher storage efficiency than three-dimensional models. It was noted that some versions of these models did not include conductive and convective heat transfer in the tank liquid. In reality, degradation of stratification during periods of inactivity will occur due to conduction within the tank liquid. The lack of

these thermal processes within the tank liquid make these models unsuitable for the simulation of energy storage with annual charge-recharge cycles.

Two major types of mathematical TES models are extensively used. One type is a differential equation solution to the thermal energy balance based on the net flow to each horizontal layer in the store. This is shown in Figure 2.1 where tank horizontal layer (node) i is subject to as many as 2 incoming and 2 outgoing flows, depending on the relative position of the node in the tank and whether the node serves as an inlet and/or outlet. The governing differential equation (without loss terms) for the temperature T_i of each node of volume V_i is then

$$V_i \rho C_p \frac{dT_i}{dt} = \begin{cases} (\dot{m}_1 - \dot{m}_3) C_p (T_{i-1} - T_i) & \text{net flow downward} \\ (\dot{m}_3 - \dot{m}_1) C_p (T_{i+1} - T_i) & \text{net flow upward} \end{cases} \quad (2.1)$$

where ρ and C_p have their usual meanings.

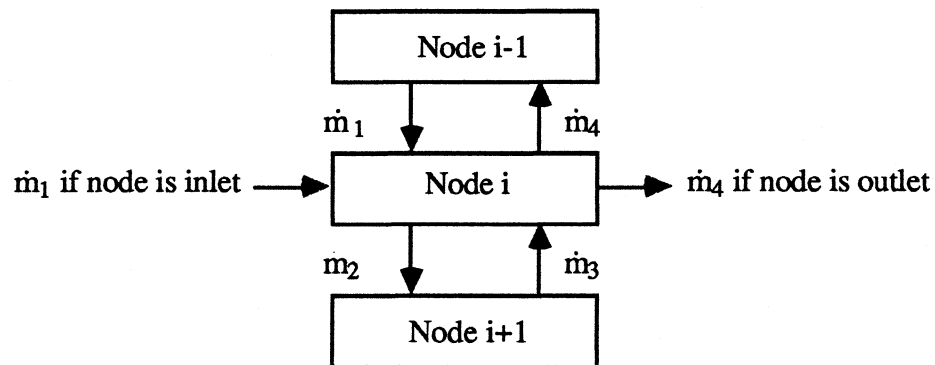


Figure 2.1: Node Representation of Net Flow Stratified Tank Model.

The second type is an algebraic model in which horizontal isotherms are formed by volume segments which remain distinct. A volume "plug" is inserted into the tank profile in proper order of temperature, pushing out another segment of the same volume. Figure 2.2 depicts the concept of a "plug flow" storage volume. Here the tank has 4 isothermal volume segments ("plugs") at some point in time. The number of tank isotherms will vary with time. As one plug is injected into the store over a timestep at the appropriate tank level (i.e., variable position of inlet), another plug (or likely part of one) of the same volume is extracted. The entire temperature profile between the injection and extraction levels shifts in the direction of the flow. The plugs remain distinct; there is no mixing between segments except for the amalgamation of small segment parts. There is no intermixing of flowstreams, so that the tank profile is shifted once for each of the two possible flowstreams present during a timestep.

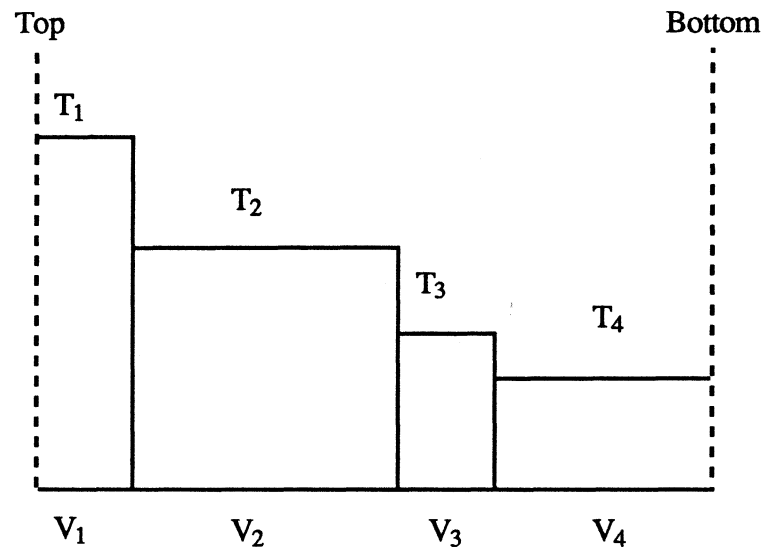


Figure 2.2: "Plug Flow" Algebraic Tank Model. Adapted from Kuhn (1980).

A wide array of control strategies for the injection and extraction of fluid from a storage volume exist in CSHPSS systems. They can vary from the simple to the complex. Obviously simple systems will have a first cost advantage. The simplest systems have storage inlets and outlets which are fixed in position. More complex control mechanisms allow injection and extraction to occur at various positions in the store. This may consist of a choice of one or more additional positions or a continuum of positions.

Two TRNSYS stratified tank models, based on the algebraic and plug flow models, are available and have similar storage inlet and outlet control strategies. These models have fixed outlet positions and fixed or continuously variable inlet positions. Fluid extraction to the collector is fixed to take place from the bottom of the tank. Fluid extraction to the load is fixed to take place from the top of the tank. These models thus draw the hottest available water to the load. If a fixed temperature drop across the load is modelled, then return flow from the load will be at a temperature other than the lowest possible.

2.2 Stratified Storage Temperature Model

The new TRNSYS version of the SST model takes features of two other versions, an original "Long Version" and the more recent MINSUN version (updated 01/14/85). The major difference between the Long Version and the MINSUN version is the ability to describe ground parameters in great detail and also have non-cylindrical storage volume shapes. Table 2.1 lists features of the two versions and those which were incorporated

Table 2.1: SST Versions and Their Features

Feature	Original Long Version	MINSUN Version	TRNSYS SST
Timestep	Hourly	Daily	Hourly
Number of Nodes in Storage Volume	3 to 100	10 only	3 to 100
Extraction Position	Fixed at top and bottom	Variable to load; Fixed at bottom to collector	Fixed or variable to load; Fixed at bottom to collector
Injection Position	Fixed at top and bottom	Variable	Fixed or variable
Flowstreams into Storage	Use net flow	Treated separately	Treated separately
Injected Volume	Accumulated until equal to volume of a node	Accumulated daily volume	Accumulated daily volume
Grid generation	User-specified or automatic	Automatic only	User-specified or automatic
Storage Volume shapes	Variable	Cylindrical only	Variable
Ground Parameters	Detailed	Vary by horizontal layers	Detailed or vary by horizontal layers

into the TRNSYS SST. Further description of the TRNSYS SST features follows. A flow diagram of the TRNSYS version of the SST appears in Appendix A. A new, independent "grid pre-processor" program which converts the TRNSYS SST from an automatic grid generator to an acceptor of detailed grid and ground parameters is presented in Appendix B. Additional TRNSYS SST subroutines which differ from the MINSUN version are presented in Appendix C, along with the computer code of other TRNSYS components which were developed for this study. A comparison of the TRNSYS and MINSUN SST versions is presented in Chapter 4.

The SST model can simulate the thermal processes of uninsulated caverns, insulated pits, ponds, or partially buried tanks (by specifying a negative value for depth). It models a modified "plug flow" storage volume coupled to a finite differenced surrounding ground. The program can use either two dimensional cylindrical or Cartesian coordinates. The following description of the SST model assumes cylindrical coordinates (Eftring, 1983).

The SST model can accurately simulate the shape and position of an underground thermal energy storage volume. If the user assumes a vertical cylindrical storage volume, a finite difference grid for the surrounding ground is automatically generated by the program. The generated mesh has variable-distanced vertical and horizontal lines; the grid spacing is finer near the storage region where large temperature gradients may be expected. Alternatively, the user may enter her own grid into the program for other shapes using the additional "grid pre-processor" computer program. Most probable storage volume shapes are compatible with the SST model, with the stipulation that the

radius of the store may not increase with depth. Example cross sections of revolution in 2-D space which can be simulated are shown in Figure 2.3.

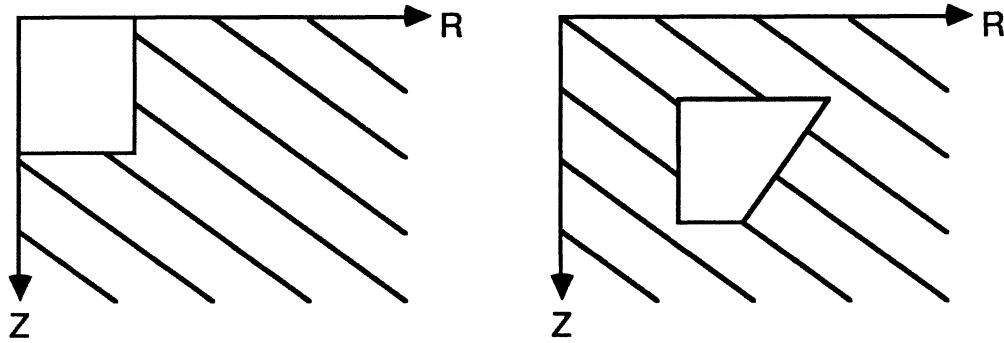


Figure 2.3 Example Cross-Sectional Storage Volume Shapes Compatible with the SST

2.2.1 Ground Calculations

The conduction of heat into the ground is represented in two dimensions, R and Z . Groundwater flow and other heat convection mechanisms are neglected. Thermal insulation may be placed at the boundaries of the storage volume and at the ground surface. The boundary conditions are the time dependent prescribed temperatures at the ground surface and zero heat flow at the axis of revolution. The grid is sufficiently large such that adiabatic boundary conditions may be assumed at the far side and bottom; when these boundaries are placed at a minimum distance of 5 store radii when automatic grid generation is used

An example grid for the ground is shown in Figure 2.4. The indices are given as i in the radial direction and j in the vertical direction. The ground cell (i,j) has an inner

radial boundary at $R(i)$, an outer boundary at $R(i+1)$, an upper depth of $Z(j)$, and a lower depth of $Z(j+1)$. The innermost radial boundary occurs at $R(2)$ and the vertical boundary of the ground surface at $Z(2)$ because the indices $i=1$ and $j=1$ are reserved for boundary conditions. The node for the temperature calculation is at the midpoint of the cell. Grid spacing is constant throughout the simulation.

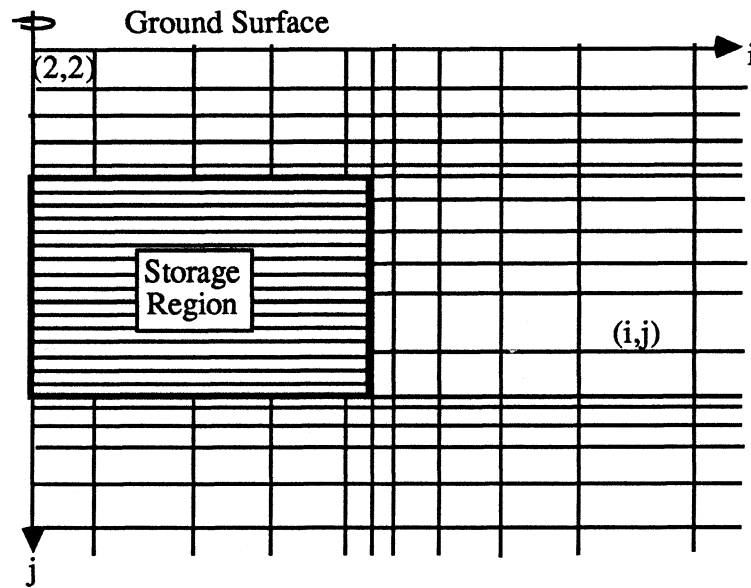


Figure 2.4: Example Ground Mesh Generated by the SST

The thermal properties of the ground surrounding the storage volume may be entered as homogeneous or as any number of different horizontal strata. Further detail in the ground cells may be input with the "grid pre-processor" program. In the latter case, the program then requires the number of rectangles with homogeneous properties which can be defined.

Figure 2.5 shows adjacent cells in the ground structure. Different thermal properties are shown in the two cells $(i-1,j)$ and (i,j) , and a thin thermal insulation is

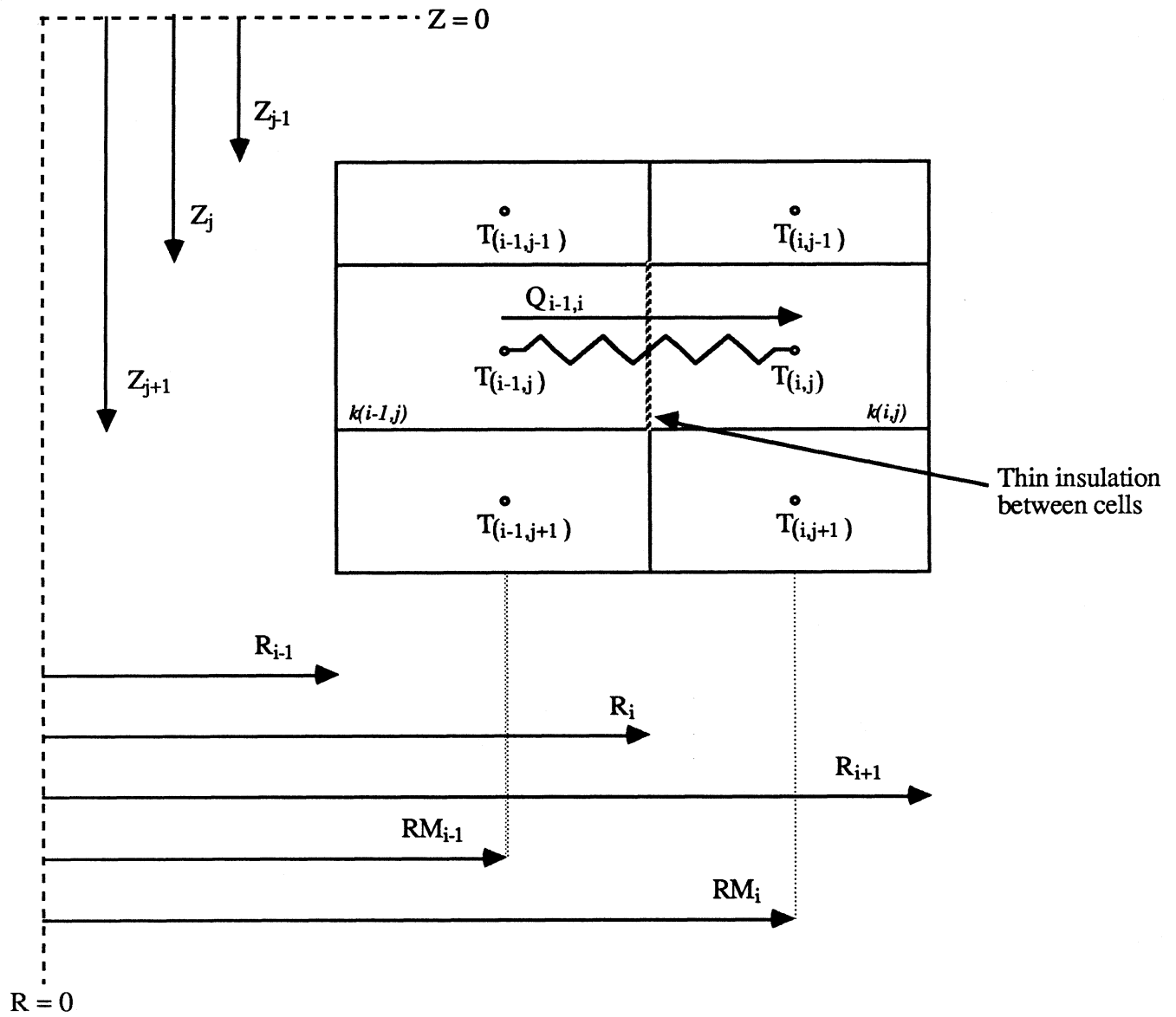


Figure 2.5: Heat Flow Between Adjacent Ground Cells

placed between them. The conductive heat flow Q (W) from ground cell (i-1,j) to ground cell (i,j) in Figure 2.5 is

$$Q_{(i-1,j),(i,j)} = (T_{i-1,j} - T_{i,j}) * G_R(i,j) \quad (2.2)$$

where

$$T_i = \text{temperature of ground cell } i \quad (^\circ\text{C})$$

$$G_R(i,j) = \text{thermal conductance between the cells in the radial direction (W/}^\circ\text{C),}$$

which can be expressed as

$$G_R(i,j) = 2\pi [Z(j+1) - Z(j)] \left[\frac{\ln\left(\frac{R(i)}{RM(i-1)}\right)}{k(i-1,j)} + \frac{\ln\left(\frac{RM(i)}{R(i)}\right)}{k(i,j)} + \frac{RI_R(i,j)}{R(i)} \right]^{-1} \quad (2.3)$$

and where

$$Z(j) = \text{vertical coordinate of the top of ground cell } (i,j) \quad (\text{m})$$

$$R(i) = \text{inner radial coordinate of ground cell } (i,j) \quad (\text{m})$$

$$RM(i) = \text{radial coordinate of the midpoint of ground cell } (i,j) \quad (\text{m})$$

$$k(i,j) = \text{thermal conductivity of ground cell } (i,j) \quad (\text{W/m-}^\circ\text{C})$$

$$RI_R(i,j) = \text{heat resistance due to thermal insulation between ground cells } (i-1,j) \text{ and } (i,j) \quad (\text{m}^2\text{-}^\circ\text{C/W})$$

Similarly, the conductive heat flow Q (W) from ground cell (i,j-1) to ground cell (i,j) is

$$Q_{(i,j-1),(i,j)} = (T_{i,j-1} - T_{i,j}) * G_Z(i,j) \quad (2.4)$$

where

$G_Z(i,j)$ = thermal conductance between the cells in the vertical direction ($W/^\circ C$),
which can be expressed as

$$G_Z(i,j) = \pi [R(i+1)^2 - R(i)^2] \left[\frac{Z(j) - ZM(j-1)}{k(i,j-1)} + \frac{ZM(j) - Z(j)}{k(i,j)} + RI_Z(i,j) \right]^{-1} \quad (2.5)$$

and where

$ZM(i)$ = vertical coordinate of the midpoint of ground cell (i,j) (m)

$RI_Z(i,j)$ = heat resistance due to thermal insulation between ground
cells (i,j-1) and (i,j) ($m^2-^\circ C/W$)

Ground cells (i,j) and (i,j+1) bounding a storage volume cell jj, as shown in Figure 2.6, will have a heat flow from the cells to the adjacent storage volume of H_{jj} , where

$$H_{jj} = (T_{(i_b,j)} - T_{jj}) G_R(i_b,j) XX_j \Delta\tau + (T_{(i_b,j+1)} - T_{jj}) G_R(i_b,j+1) XX_{j+1} \Delta\tau \quad (2.6)$$

and where

T_{jj} = temperature of storage volume cell jj

As shown in Figure 2.6, XX_j is the fraction of the ground cell (i,j) radial conductance which is in contact with node jj.

Ground properties are assumed constant throughout the simulation. Thus, the SST program needs only to calculate the radial and vertical conductances once.

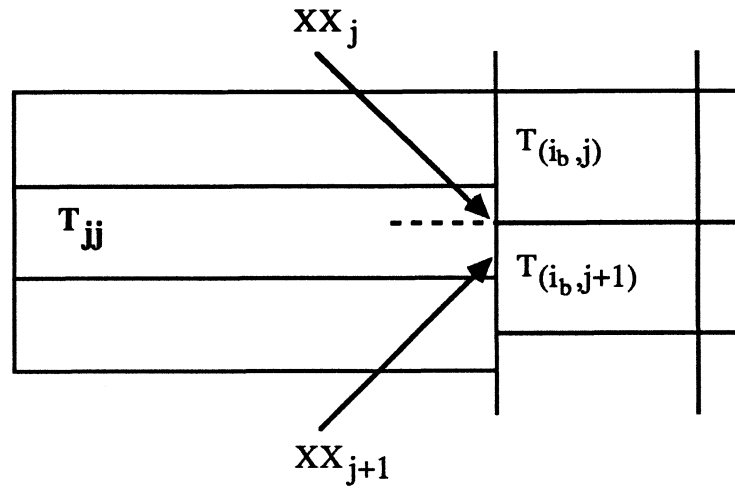


Figure 2.6: Conduction Flow from Ground Cell (i,j)
to Storage Node jj is Proportional to Fraction XX_j

The explicit forward difference method is used to solve the set of finite difference equations. In order to maintain numerical stability, this method has a restriction of the length of the time step $\Delta\tau$ (seconds) at which temperature updates are calculated. Two maximum timesteps are used in the SST model: one for the storage volume and another for the surrounding ground. The maximum stability timestep for the ground is found by

$$\Delta\tau_{\max} = \min_{\text{all } i \text{ \& } j} \frac{\bar{C}(i,j)}{\sum_k G(i,k)} \quad (2.7)$$

where

$$\bar{C}(i,j) = \rho(i,j) C_p(i,j) \Pi [R(i+1)^2 - R(i)^2] * [Z(j+1) - Z(j)]$$

$$C_p(i,j) = \text{cell heat capacity} \quad (\text{J/kg-}^\circ\text{C})$$

$$\rho(i,j) = \text{cell density} \quad (\text{kg/m}^3)$$

$$G(i,j) = \text{cell conductances } G_R(i,j) \text{ and } G_Z(i,j) \quad (W/^{\circ}C)$$

The calculated maximum timestep, which is generally on the order of many days for CSH PSS systems, is used in the simulation unless the default value given in the program is shorter. The default minimum timestep for the update of ground temperatures is currently set to three days.

2.2.2 Storage Volume Calculations

Stratification in the storage volume is modelled by N nodes (horizontal isotherms). All nodes are equal in volume, regardless of the shape of the store, and remain constant throughout the simulation. Thus, the shape of the finite difference grid and the storage volume do not change. The number of nodes chosen and the resultant degree of stratification (i.e., fully mixed or highly stratified) may affect subsystem performance and ground temperature profiles.

Thermal insulation may be placed around the store, and can vary in its thermal properties for the top, bottom, and sides.

Storage volume heat transfer processes are modelled using both conduction and mixing between nodes due to temperature inversions. Conduction occurs between nodes in the vertical dimension. Two modes of mixing are used to represent natural convection wherever an inversion occurs. One mode calculates an average mixed temperature for inverted nodes while the other switches node temperatures into the "correct" order.

Because radial conductance in a storage volume cell was not modelled, the temperatures of the fluid in the cell and that of the wall-fluid interface are assumed to be the same. The convection heat transfer coefficient at the boundary of the storage volume is therefore considered to be infinite for non-insulated storage volumes.

Figure 2.7 shows three storage volume cells and their relative position in the surrounding ground. In general, the storage volume cells may have different radii, but are depicted here with equal radii.

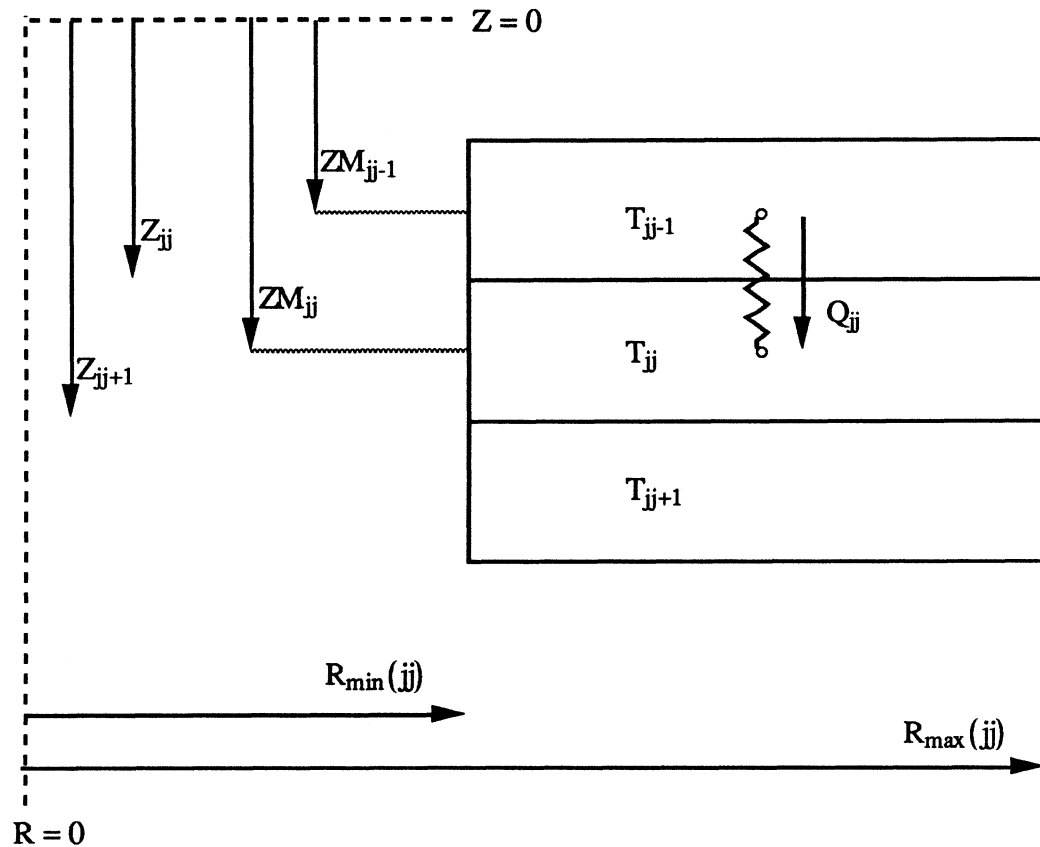


Figure 2.7: Storage Volume Cells in the Ground

The conductive heat flow Q_{jj} (W) from storage volume node (jj-1) to storage volume

node (jj) in Figure 2.7 is

$$Q_{jj} = (T_{jj-1} - T_{jj}) * G_s(jj) \quad (2.8)$$

where

$G_s(jj)$ = thermal conductance of a storage volume node, which can be expressed as

$$G_s(jj) = \frac{k_s * \pi [R_{\max}^2(jj) - R_{\min}^2(jj)]}{ZM(jj) - ZM(jj-1)} \quad (2.9)$$

and where

$$k_s = \text{thermal conductivity of fluid in storage volume} \quad (\text{W/m}^\circ\text{C})$$

New temperatures are found for storage cells at the end of the storage volume finite difference timestep $\Delta\tau$. The maximum value of $\Delta\tau$ is found by

$$\Delta\tau = \min_{\text{all } jj} \frac{\rho C_p V_{\text{cel}}}{\bar{G}_{jj}} \quad (2.10)$$

where,

$$\bar{G}_{jj} = G_s(jj) + G_R(i_b, j) XX_j + G_R(i_b, j+1) XX_{j+1}$$

with XX_j defined in equation 2.6.

The value of $\Delta\tau$ is currently set to the default value of one day. If the calculated maximum timestep is shorter than the default value, then the storage volume temperature

profile changes before 24 hours. In this case, a warning message is issued because errors in load and collector subsystem calculations will occur when buffers are used (Section 2.2.3). A new temperature, T_{jj}^t , of the storage volume cell (jj) due to conduction between nodes and conductive heat flow from the store to the surrounding ground is found at the end of the period $\Delta\tau$ by

$$T_{jj}^t = T_{jj}^{t-1} + [Q_{jj} - Q_{jj+1} + H_{jj}] * \frac{\Delta\tau}{\rho C_p V_{cel}} \quad (2.11)$$

In the SST model, the storage volume is divided into a user-defined number of cell volumes (i.e., isotherms). In contrast to the plug flow strategy shown in Figure 2.2, the storage cells in the SST are of equal volume and constant in number over the course of a simulation.

The incoming flow may or may not be great enough to completely fill a storage cell during a single hourly timestep in the SST model. When the flow is large enough to completely fill a cell, there is a net shift in the storage profile (i.e., "plug flow"). Otherwise, "cell volume mixing" occurs, where the incoming volume collected during a timestep is mixed with the node closest in temperature. New temperatures are calculated for all nodes jj through which there is a flowstream using

$$T_{jj} = \frac{T_i * V_{in} + T_{jj} * (V_{jj} - V_{in})}{V_{jj}} \quad (2.12)$$

where

T_i = temperature of either the injected flowstream or the previous node in the

direction of the flowstream

V_{in} = volume of injected flowstream

Hence, whether "plug flow" or "cell volume mixing" occurs over a timestep depends on the size of storage cells and the flowrates of flowstreams in the storage volume.

Since TRNSYS normally is run with an hourly timestep, "cell volume mixing" is likely to occur. Depending on the number of storage nodes, hourly flows may be very small in comparison to the size of storage cell volumes for CSH PSS systems. It will be shown in Chapter 3 using data from the Lyckebo CSH PSS that numerical dispersion may develop in the simulation storage volume profile when there is extensive cell volume mixing.

2.2.3 Buffer Strategy

An optional system of buffers which retains the incoming flow over a 24 hour period (one day) was devised to partially resolve numerical dispersion. This system is depicted in Figure 2.7. The size of a buffer is determined by the number of nodes and can contain a maximum volume equal to that of a node.

Buffers which are fixed to inject into the top and bottom of the storage volume when containing a volume equal to that of a storage node appear in the Long Version of the SST model. Therefore, plug flow always occurs in this version of the model. Only the net flow of the load and collector flowstreams is considered in the Long Version.

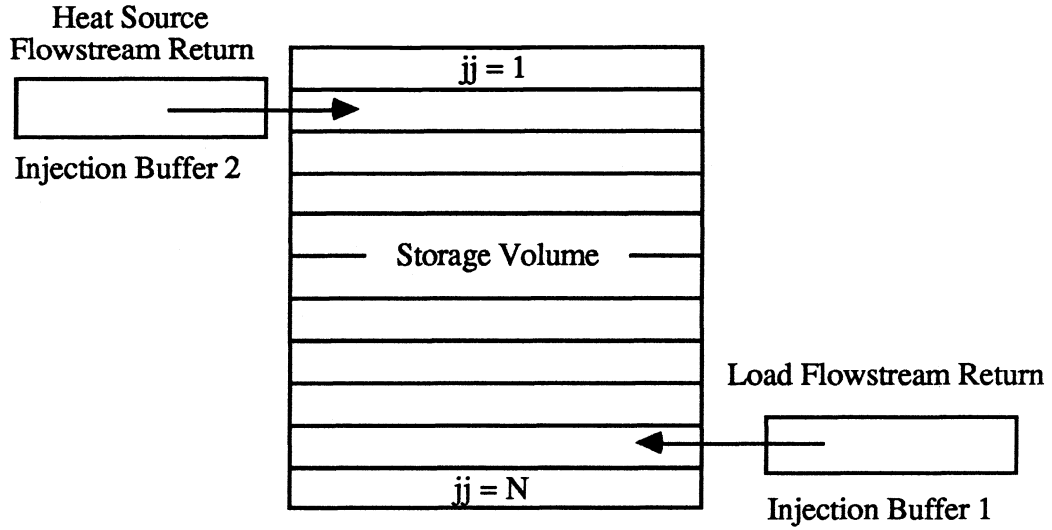


Figure 2.7: 24 Hour Buffer System

In the TRNSYS SST model, a buffer fills over the 24 hour period to a buffer volume V_B according to

$$V_B = \sum_{\tau=0}^{\tau=T} V_{in} = \sum_{\tau=0}^{\tau=T} \dot{V}_{\tau} \Delta\tau \quad (2.13)$$

The temperature of the fluid inside the buffer at time τ , T_B^{τ} , is averaged over the injection period:

$$T_B^{\tau} = \frac{T_i^{\tau} V_{in}^{\tau} + T_B^{\tau-1} V_B^{\tau-1}}{V_{in}^{\tau} + V_B^{\tau-1}} \quad (2.14)$$

When buffers are in use, the storage volume temperature profile does not change until the end of a 24 hour period. First, the contents of the collector side and load side buffers are injected into the storage volume. Each buffer will cause either a net shift in

the storage profile or an update of the profile according to equation 2.12. Daily energy losses of the storage volume to the surrounding ground are calculated after injection of the buffers. Additionally, the temperature profile of the store may change at this time without change in overall internal energy by means of conduction and mixing between nodes.

2.2.4 Storage Control Strategy

The TRNSYS SST model features various modes for the operation of the storage volume. Flowstream inlets and outlets may be held at fixed positions or varied in position. Variable inlet position directs the inflow to the storage node closest in temperature. Variable outlet position allows extraction from a node closest to a desired temperature. The outlet to the collector is normally fixed to extract from the bottom of the store. Outflow to the load can originate from the top of the storage volume or vary. A combination of fixed and variable inlets and outlets is accepted in the model, making simulation of most probable configurations possible.

For the case of variable load outlet, the temperature of the node at which extraction occurs is determined by a demand temperature T_D . This temperature is an input to the SST component. Whether the demand temperature is a constant or varies will depend on the strategy used in other components.

As an example, consider the space heating load \dot{Q}_L met by extraction from the SST

$$\dot{Q}_L = \dot{V}_L \rho C_p (T_D - T_R) \quad (2.15)$$

where

$$\dot{V}_L = \text{load volumetric flow rate} \quad (\text{m}^3/\text{s})$$

$$T_D = \text{demand extraction temperature} \quad (^\circ\text{C})$$

$$T_R = \text{return temperature from the load} \quad (^\circ\text{C})$$

Two common control strategies are used in conjunction with the load demand temperature concept. One is to fix the demand temperature T_D and the flow rate to the load, consequently letting the return temperature T_R vary. The other strategy is to fix the demand and return temperatures and thus let the load flow vary.

Figure 2.8 illustrates that the same demand temperature can be delivered to the load using either fixed or variable extraction. When the flow originates from the top of the store at a temperature hotter than the demand it can be tempered by mixing with an appropriate amount of the load return flowstream. A lower flowrate from the store is then required. (The actual presence of a mixing valve is not required in simulations where the distribution losses are not modelled, but the load return bypass flowstream is conceptually present with the reduced flowrate calculation.)

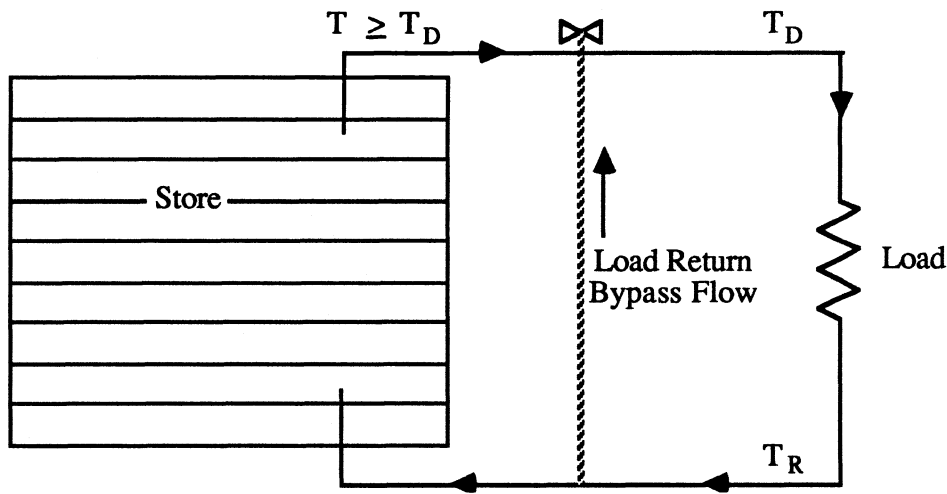


Figure 2.8: Demand Temperature Delivered to Load is Available
with Either Fixed or Variable Extraction

When variable extraction is used, the flow originates from a node closest to (at or above) the demand temperature. If the temperature of the extraction node is warmer than the demand temperature, then the SST model assumes an appropriate amount of the load return flowstream is mixed with the forward flowstream to deliver the exact demand temperature.

Variable inlets and outlets which use a demand temperature do occur in CSH PSS systems. The Lyckebo system in Sweden uses two pairs of moveable standpipes which control the position where injection and extraction occur.

The thermal load on the storage volume may consist of both space heating and domestic hot water (DHW). These loads may appear in series or parallel. In the latter case, two separate flow loops are used. Similar control logic for the positioning of the

two load inlets and outlets applies if a separate DHW loop is used.

2.2.5 Component Startup

CSHPSS systems may require several annual cycles before annual heat losses from the store reach a roughly steady value, after which variation is dependent solely on weather and load conditions. (It was predicted by designers that the Lyckebo system would require at least 5 years to reach such a state). The annual heat losses from the store decrease as the temperature profile of the ground surrounding a seasonal storage volume becomes increasingly stratified.

The thermal behavior of the storage volume over many annual cycles can be divided into two distinct periods, the startup phase and an approximate steady state. During the startup phase, heat transfer between the store and the surrounding ground is high. The thermal losses experienced by the system are highly transient during this period. As the temperature profile of the surrounding ground approaches the stratified profile of the storage volume fluid, annual thermal losses decrease, and the transience exhibited during the startup phase is largely damped out. The remaining transient behavior in annual losses, due to variations in injected and extracted energies, is small relative to the transience exhibited in the startup phase. The thermal behavior during the indefinite period following startup can therefore be referred to as an approximate steady state.

Computer simulations of CSHPSS systems may serve either of two purposes in which the importance of accurate modelling of the startup phase differ. Simulations that

are used in the design of systems focus on the long term thermal performance of a seasonal storage volume, which can be exemplified by steady state losses. Because there is little interest in the transient period, forcing functions which drive the energy flows in the storage volume can be repeated until steady state is attained. Simulations which are part of a study of an operational system require more accurate modelling, as heat losses may not be damped during the period of interest. Errors in the prediction of ground losses will then occur if the model ground temperature profile is unlike the actual profile.

Several approaches to modelling startup cycles may be taken, each resulting in different ground profiles and ground losses during this period. The input driving the storage volume may be in the form of several years of data, the repetition of a typical year, or some simplified approach. The effect that input has on predicted heat losses will depend on how close the system is to steady state. It is foreseen that the most accurate results would be obtained during the transient phase if it were possible to input a known ground temperature profile at the beginning of a simulation and use several years of system data. The resulting ground temperature profile at any time will then be "correct", with error limited to that of the mathematical model.

Upon initialization of the SST model, the ground cells may be given a uniform profile or a linear gradient with depth. Any initial ground temperature profile may be entered using the "grid pre-processor" program.

When only the periodic steady state heat losses are of interest in a simulation, a simple model which has been included in the SST component for the "pre-heating" of the ground can be used rather than repeating several years of data. Several pre-heat cycles

can be used to simulate transient store losses. In the pre-heat model, the storage volume is given a sinusoidally varying lumped temperature and only the thermal diffusion in the ground cells is calculated. The user defines the amplitude of the sinusoid by giving the expected minimum and maximum annual average temperatures. As shown in Figure 2.9, the period of the sinusoid is one year with the minimum assumed to occur on April 1st. This model was also used in the SST validation simulations (Chapter 3) previous to the input of available operational data.

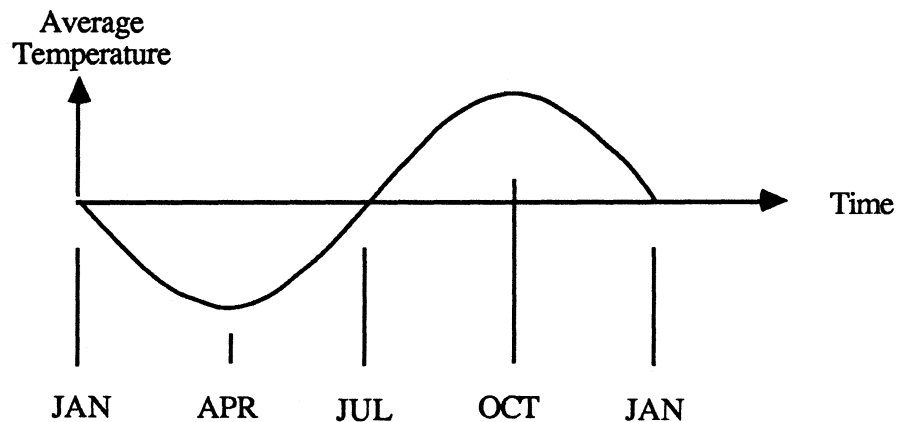


Figure 2.9 Sinusoidally varying lumped temperature imposed on store during Pre-heat

A feature of the MINSUN SST model insures that a system is being simulated under steady state ground conditions. The program reruns a simulation with new pre-heat maximum and minimum average annual storage temperatures if the average storage temperature is not within a specified number of degrees (typically 5 °C) from the initial value given at the start of the simulation.

2.3 Collector Model

While only minor changes were made to the available collector model (Type 1 of TRNSYS Version 12.1), a second component was developed which would change the control strategy of the collector to deliver a constant outlet temperature, T_o . The user specifies a desired outlet temperature, minimum and maximum collector flowrate, and the minimum acceptable outlet temperature at the minimum flowrate. The strategy for the calculation of a constant outlet temperature is outlined in section 4.5.1. An array factor was added to the collector model which reduces the useful energy collected. This adjustment represents an estimate of the annual energy delivery of an array of the specified module relative to the output of a single module (Bankston, 1986). It is used in lieu of modelling such collector array details as header and feeder pipes, row spacing, and pipe insulation. The value of the reduction factor ranges from 0.66 to 0.88, depending on the type of collector. These values were based on operational experience as analyzed by participants of IEA Task VII.

2.4 Pipe Model

A pipe model was written assuming buried pipes which encounter a constant surface temperature, T_∞ . The log mean temperature difference of fluid over the pipe length was then taken. The mean temperature difference between the fluid inlet and outlet states, ΔT_o , is described as

$$\Delta T_o = (T_i - T_\infty)[1 - \exp\{-UA/\dot{m}C_p\}] \quad (2.16)$$

where the pipe overall loss coefficient, UA, is

$$UA = \frac{2\pi k L}{\ln\left(\frac{r_o}{r_i}\right)} \quad (\text{W/m}^2\cdot^\circ\text{C})$$

and where

k = thermal conductivity of pipe insulation (W/m-°C)

L = length of pipe (m)

$(r_o - r_i)$ = difference between outer and inner pipe radii due to the thickness of pipe insulation

The thermal resistance of the pipe material itself is considered negligible compared to that of the pipe insulation.

2.5 House Load Model

An hourly house load rate \dot{Q}_L (kJ/hr) was calculated using the degree day concept, accounting for a constant rate of internal gain and domestic hot water load (rather than a varying "Rand"-type profile)

$$\dot{Q}_L = [UA (T_s - T_a) - \dot{Q}_{\text{Gain}}]^+ + \dot{Q}_{\text{DHW}} \quad (2.17)$$

where

$$T_s = \text{room set temperature} \quad (^\circ\text{C})$$

Two features were added to the model: a defined space heating season outside of which the space heating component of the house load (bracketed in equation 2.17) is zero and a threshold ambient temperature (several degrees below the room set temperature) above which the heating degree days are also zero. The control strategy for the variable flowrate used in the load subsystem, based on user specified demand and return temperatures, is discussed in section 4.5.2.

2.6 Heat Pump Model

Rather than making use of existing TRNSYS models which use manufacturer supplied performance data for specific heat pumps, a theoretical Carnot cycle water to water heat pump model was implemented for use with the SST based on an IEA supplied subroutine (Krischel, 1986 and Bankston, 1986). The components of the heat pump model and its interface between the storage volume and the load is shown in Figure 2.10. The temperature out of the condenser $T_{C,o}$ is equal to the load demand temperature T_D (of Figure 2.8). The resultant heat pump coefficient of performance is reduced by a user-defined "effectiveness" (equation 2.23). As shown in Figure 2.11, the user specifies an effectiveness curve which is a function of the difference between the condenser and the evaporator operating temperatures, T_H and T_L .

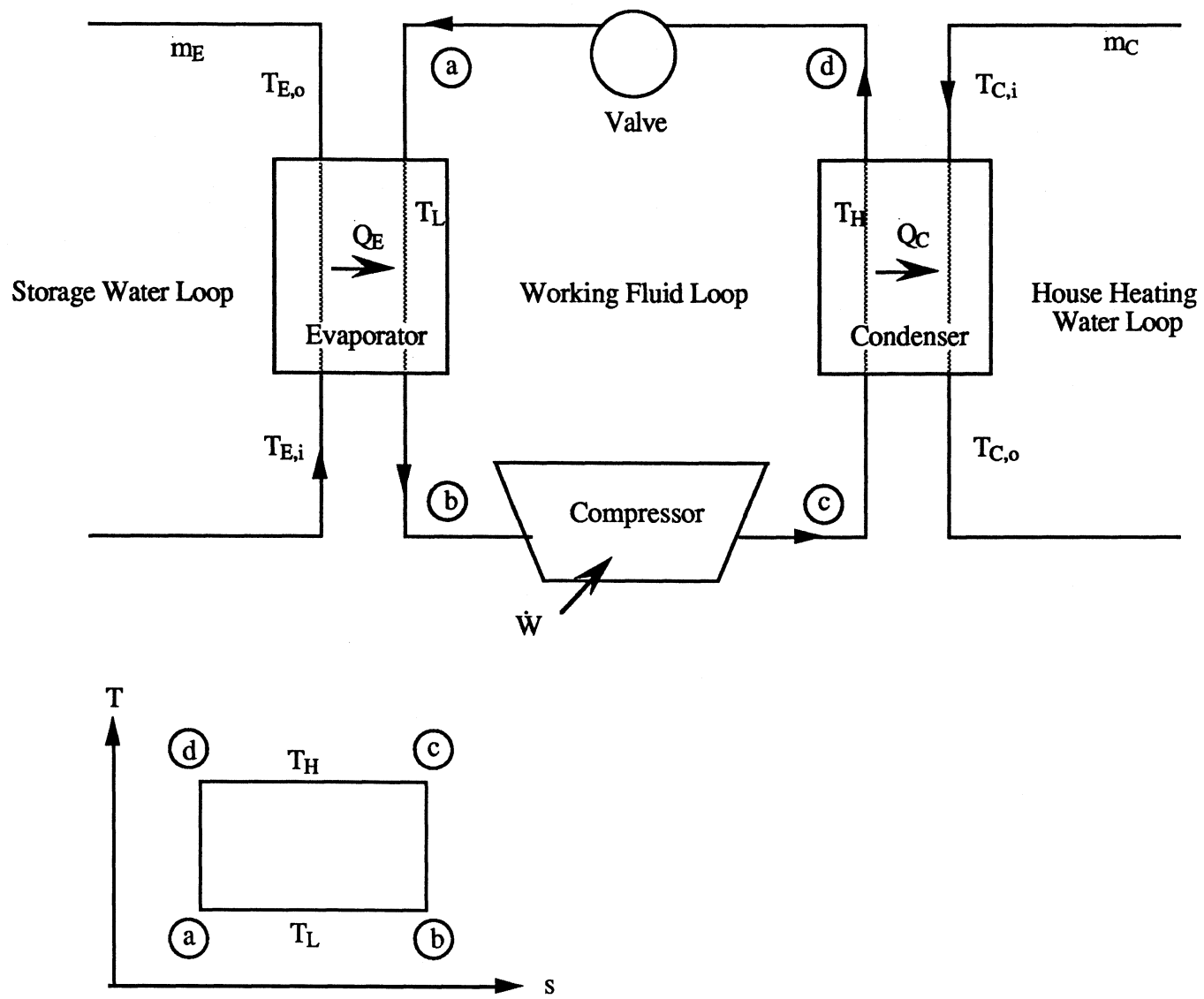


Figure 2.10: Heat Pump Model

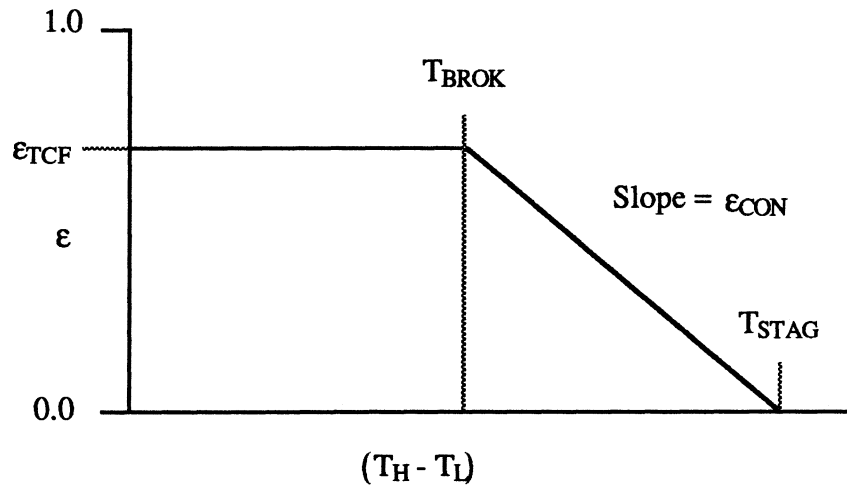


Figure 2.11: Heat Pump Effectiveness Curve

Three variables which fully describe the curve are specified by the user:

- ϵ_{TCF} = value of constant portion of the heat pump effectiveness curve
- T_{BROK} = temperature difference where the effectiveness begins to decrease
- T_{STAG} = temperature difference where stagnation occurs

The slope of heat pump effectiveness curve, ϵ_{CON} , is then known.

The operation of the heat pump is represented as follows:

Condenser

$$\begin{aligned} \dot{Q}_C &= \dot{Q}_{LOAD} \\ &= \dot{m}_C C_p (T_{C,o} - T_{C,i}) \end{aligned} \quad (2.18)$$

$$= h_C A_C \left[T_H - \left(\frac{T_{C,i} + T_{C,o}}{2} \right) \right] \quad (2.19)$$

where

$$\dot{Q}_C = \text{rate of energy liberated by the condenser} \quad (\text{kJ/hr})$$

$$h_C A_C = \text{condenser heat transfer coefficient times heat transfer surface area} \quad (\text{kJ/hr-}^\circ\text{C})$$

$$T_{C,o} = \text{outlet temperature of condenser delivered to load} \quad (^\circ\text{C})$$

$$= T_D, \text{ the user specified load demand temperature (section 2.5)}$$

$$T_{C,i} = \text{inlet temperature of condenser returned from load} \quad (^\circ\text{C})$$

$$= T_R, \text{ the load return temperature (section 2.5)}$$

Evaporator

$$\dot{Q}_E = \dot{m}_E C_p (T_{E,i} - T_{E,o}) \quad (2.20)$$

$$= h_E A_E \left[\left(\frac{T_{E,i} + T_{E,o}}{2} \right) - T_L \right] \quad (2.21)$$

where

$$\dot{Q}_E = \text{rate of energy consumed by the evaporator} \quad (\text{kJ/hr})$$

$$h_E A_E = \text{evaporator heat transfer coefficient times heat transfer surface area} \quad (\text{kJ/hr-}^\circ\text{C})$$

$$T_{E,o} = \text{outlet temperature of evaporator returned to the store} \quad (^\circ\text{C})$$

$$T_{E,i} = \text{inlet temperature of evaporator supplied by the store} \quad (^\circ\text{C})$$

Coefficient of performance

$$\text{COP} = \frac{\dot{Q}_C}{\dot{W}} \quad (2.22)$$

$$= \varepsilon \left(\frac{T_H}{T_H - T_L} \right) \quad (2.23)$$

where, if $T_H - T_L \leq T_{BROK}$,

$$\varepsilon = \varepsilon_{TCF}$$

or, if $T_H - T_L > T_{BROK}$,

$$\varepsilon = \varepsilon_{TCF} - \varepsilon_{CON}(T_H - T_C - T_{BROK}) \quad (2.24)$$

and where

$$\dot{W} = \text{rate of energy consumed by the compressor} \quad (\text{kJ/hr})$$

The temperature of the working fluid in the condenser, T_H , is a function of known condenser variables:

$$T_H = f(\dot{Q}_C, h_C A_C, \dot{m}_C, T_{C,o})$$

One must hold either the evaporator mass flow \dot{m}_E or the evaporator outlet temperature $T_{E,o}$ constant to complete the calculations. The choice of constant evaporator massflow \dot{m}_E was made such that

$$\dot{m}_E C_p = h_E A_E \quad (2.25)$$

When an energy conservation equation is added

$$\dot{W} = \dot{Q}_C - \dot{Q}_E \quad (2.26)$$

the systems of equations 2.18 through 2.26 can be used to find the resulting performance of the evaporator. The storage volume node of the SST which can supply water to the evaporator at the lowest utilizable temperature is found by the heat pump model.

Chapter 3

SST Model Validation

A 5 year simulation of the Lyckebo CSHPSS system near Uppsala, Sweden was performed as a validation of the TRNSYS SST model. Measured hourly data for the system were used as input to the model. Difficulties in modelling the system are discussed. The effect of buffer size and the number of nodes are investigated.

3.1 The Lyckebo CSHPSS

Figure 3.1 and Table 3.1 describe the Lyckebo system. The Lyckebo CSHPSS system is located near Uppsala, Sweden at a latitude of 60° North. It is currently the world's largest operational CSHPSS system, serving 550 residences. The 100,000 m³ uninsulated storage volume is excavated out of rock. Its toroidal shape has a diameter of 75 m. Space heating and DHW are 100% supplied from the storage volume. About 15% of the required energy comes from solar collectors. An electric boiler is used both to simulate up to 28,800 m² of collector area and to supply "auxiliary" energy to the store.

The control strategy used in the operation of the solar collectors is such that low, variable collector flowrates are used to obtain a nearly constant, high collector outlet

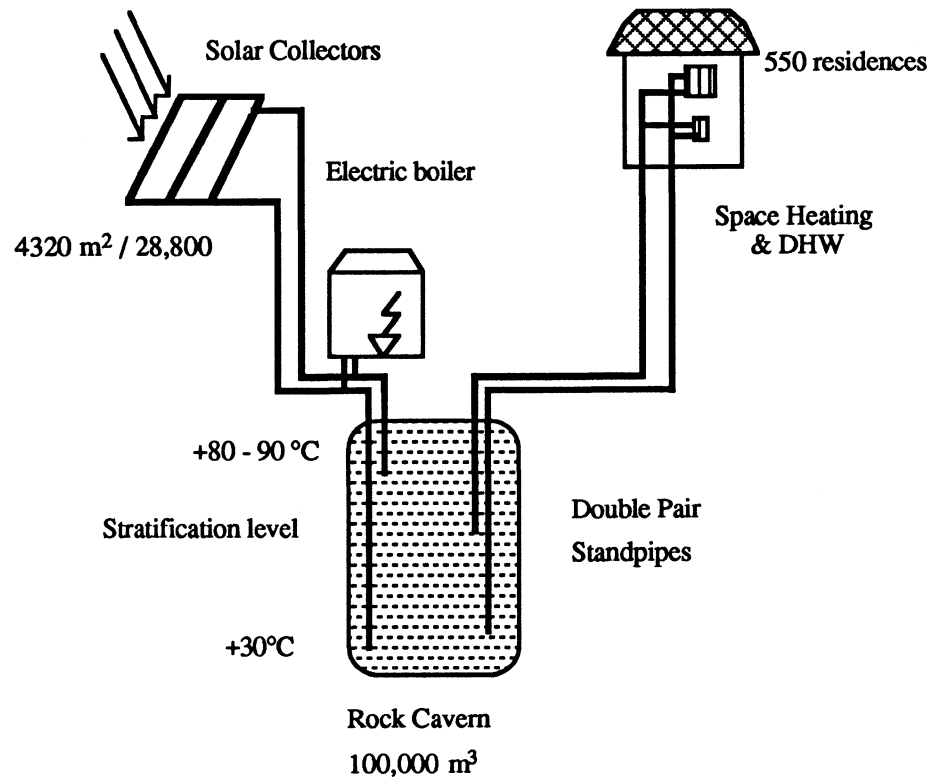


Figure 3.1 The Lyckebo CSHPSS system

temperature at set points between 75 and 95 °C (Wallentun, 1985). Flow to the store begins (at some minimum pump flowrate) after warming the interconnecting pipe system to a circulation temperature between 60 to 65 °C. The collector set point is then maintained by a speed-regulated pump. In theory, operation of the electric boiler would follow the same energy pattern as daily insolation in an experiment to determine the performance of the store if it were supplied with 100% of its energy from solar collectors. This has not been always possible, however, for reasons that are unknown to the author. Much of the boiler energy is instead supplied continuously during the autumn season.

Table 3.1: Description of Lyckebo CSHPSS system

Storage Volume

Type	Uninsulated Cavern
Size	100,000 m ³
Configuration	Toroid
Diameter	75 m with 39 m central pillar
Height	30 m

Collectors

Type	High Efficiency MEGA flat plate
Area	4320 m ²
$F_{av}U_L$	rated 2.8 W/m ² -C
$F_{av}(\tau\alpha)$	rated 0.75
Yield	330 kWh/m ²

Auxiliary Heat Source

Type	Electric Boiler
Operation	Simulate Solar Energy up to 28,800 m ² "theoretical" collector area Supply Auxiliary Energy directly to Store

Load

Type	Space heating + DHW
Size	8 GW-hr annually (20% = DHW)
Number Residences	550

Representative data for the Lyckebo system are shown in Figures 3.2a through 3.2d. Three extremes in heat source energy are shown by thermocouple recorded temperatures at the storage volume side of the heat exchangers, regardless of the presence of flow. The relative contribution of solar and boiler energies for a month in which daily insolation is mimicked by the electric boiler can be seen for September 1987 in Figure 3.2a. A plot of heat source temperatures for November 1987 in Figure 3.2b shows the nearly continuous supply of boiler energy for this month. Figure 3.2b shows a month (January 1987) where no energy was supplied to the storage volume. The spike at hour 350 for this figure is an operational control error, as verified by the presence of flow. Both the delivered and return temperatures of the water in the load distribution system are carefully controlled; Figure 3.2d shows typical, near constant values of storage extraction and return load distribution temperatures for a representative month (January 1987).

A high degree of stratification is maintained in the Lyckebo cavern by four telescopic standpipes that can be raised and lowered. The pipes can supply or extract water at the appropriate temperature and correct level in the store. The success of the standpipe operation is demonstrated by Figure 3.3 which shows actual cavern temperature profiles for March 1 and November 1, 1987. These two days are representative of two extreme states of energy charge in the store. Several notable features are present in the figure. A hot layer is maintained above a cool layer, and between them lies a sharp transition zone. A 30 °C drop occurs along a 2 meter change in depth in the transition zone. This 2 meter zone moves up and down the depth of the cavern, depending on the the extent of energy charge.

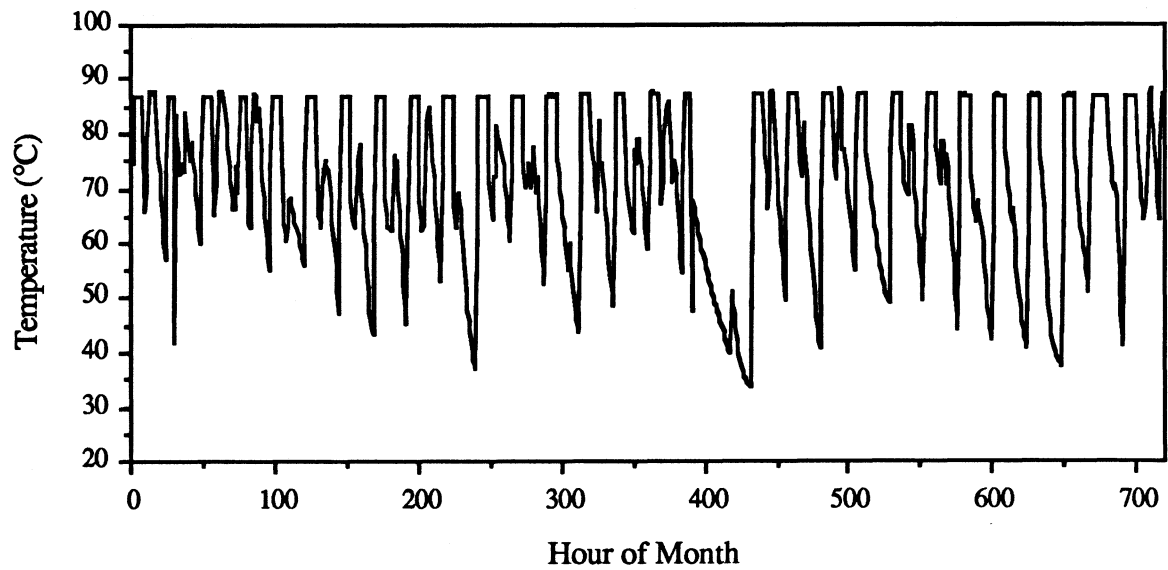


Figure 3.2a: Hourly Heat Source Injection Temperatures for September, 1987;
Electric Boiler Energy Mimics the Daily Contribution of Solar Energy.

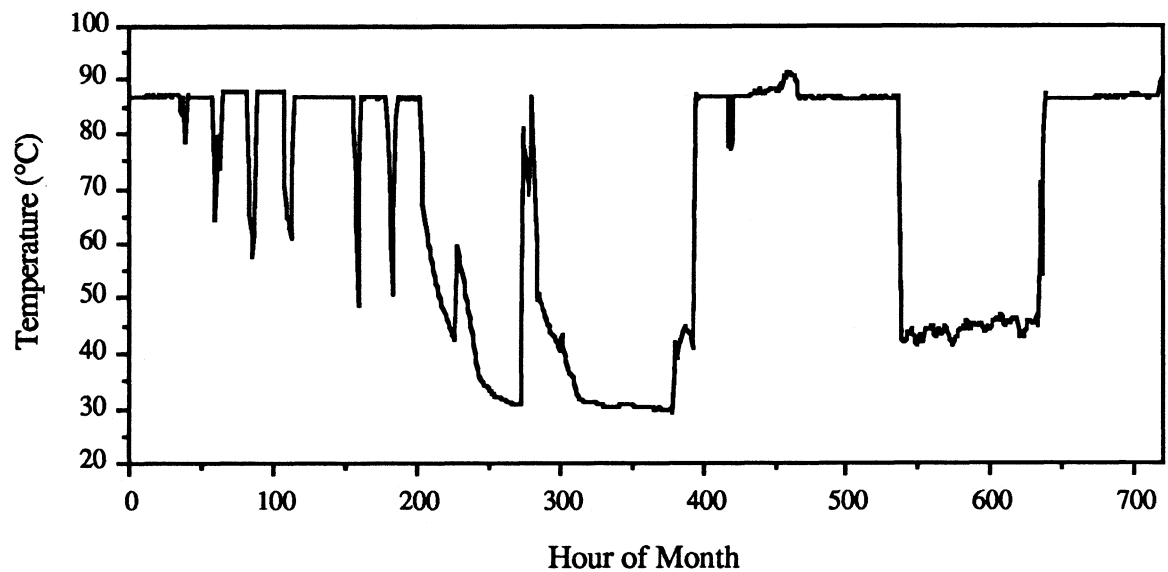


Figure 3.2b: Hourly Heat Source Injection Temperatures for November, 1987;
Electric Boiler Continuously Supplies Energy to the Storage Volume.

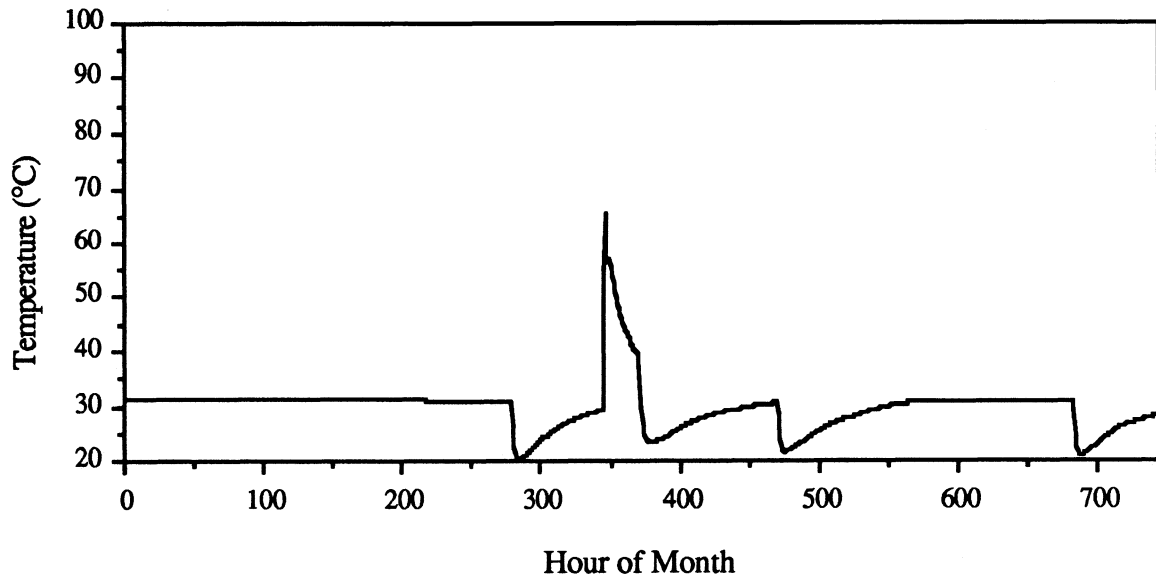


Figure 3.2c: Hourly Heat Source Temperatures for January, 1987; No Energy is Supplied to the Storage Volume.

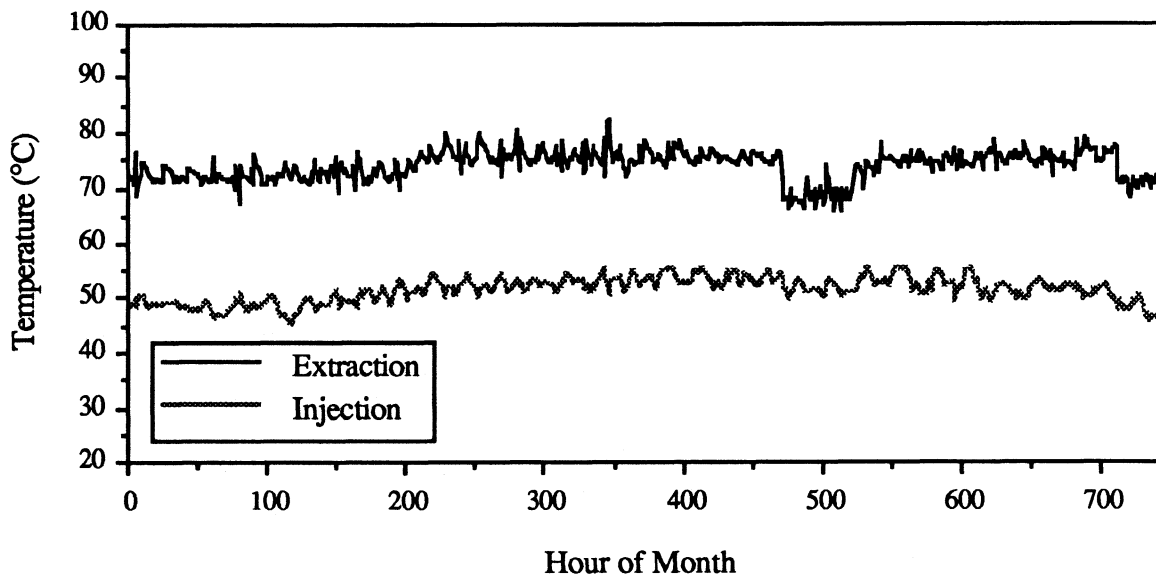


Figure 3.2d: Hourly Load Flowstream Storage Extraction and Return Injection Temperatures for January, 1987.

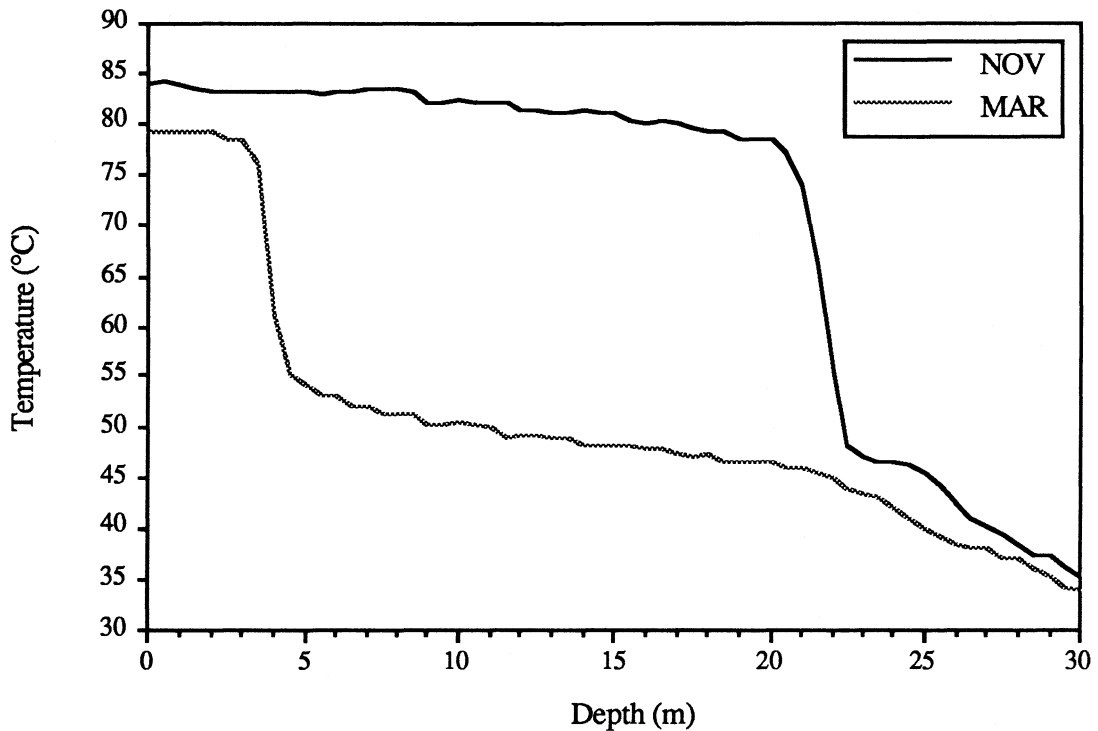


Figure 3.3: Lyckebo Cavern Profiles for March 1 and November 1, 1987

Measured thermal energy balances on the Lyckebo cavern for two annual cycles are summarized in Table 3.2 (Brunström, 1987a).

Table 3.2: Annual Energy Balances for the Lyckebo Cavern (in GW-h)

	<u>1984-85</u>	<u>1985-86</u>
Solar Energy Injected - Collectors	1.24	1.27
- Simulated	7.72	7.38
Supplementary Energy Injected	3.02	2.00
Energy Extracted	7.91	8.10
Ground Losses	3.14	3.01
Change in Internal Energy	+ 0.93	- 0.46

3.2 Available Data

Table 3.3 lists the type of data obtained from Älvkarleby Laboratory for the Lyckebo system. Figure 3.4 shows the locations for the measurement of energy flows and heat exchanger temperature data. Hourly energy flows indicated at points 1, 2, 3, and 4 were calculated by the Älvkarleby Laboratory using measured flowstream temperatures and volumetric flowrates (Brunström, 1988). Mass flow data used in the TRNSYS SST component were back-calculated from the energy flow data and temperature measurements at points 5, 6, 7, and 8 by assuming no heat losses from the heat exchangers. A daily cavern temperature profile, averaged from measurements by 60 thermocouples placed every 0.5 m along the cavern depth, was also given in the data.

Table 3.3: Available Lyckebo Data

<u>Variable</u>	<u>Label, Figure 3.4</u>
Date	
Hour	
Energy flow (MW) , solar injection	1
" , electric boiler injection	2
" , total injection	3
" , extraction to district heating	4
Temperature (°C) , cold side injection heat exchanger	5
" , hot side injection heat exchanger	6
" , cold side extraction heat exchanger	7
" , hot side extraction heat exchanger	8

Temperature Profile (°C) : daily average of continuous measurement at every 0.5 m depth

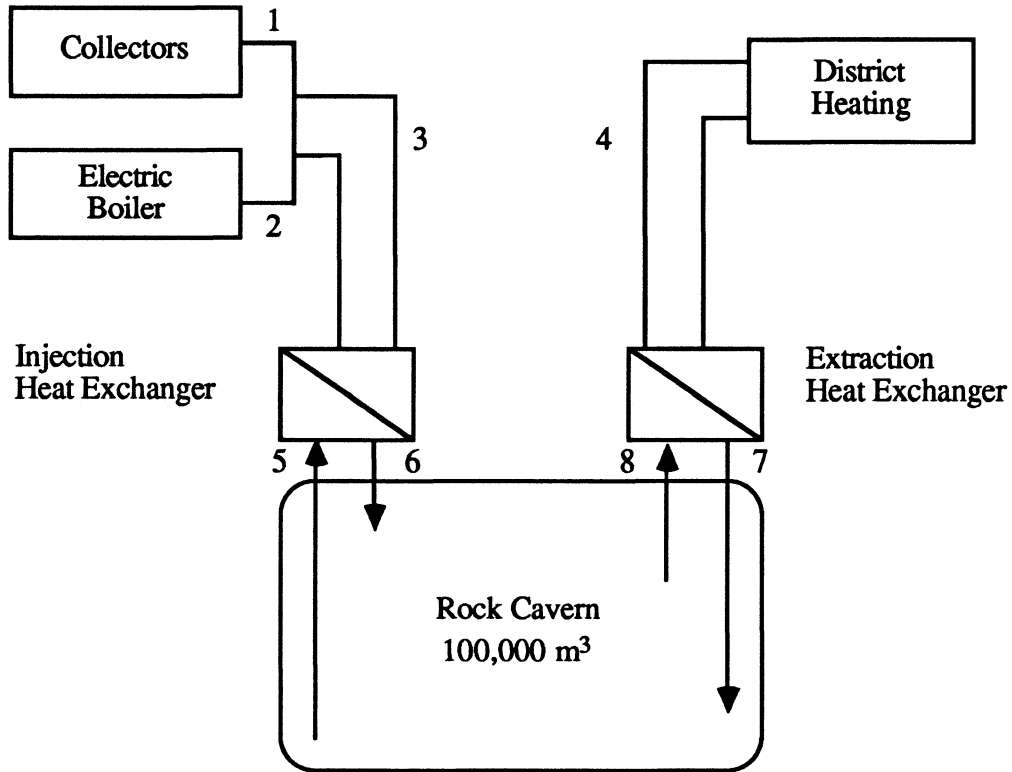


Figure 3.4 Schematic of Lyckebo Heating Plant Showing Locations for Data Measurement

An energy balance on the Lyckebo system over any time period is given by $\Delta E_S = E_{in} - E_{out} - E_{env}$. Hourly values of E_{in} and E_{out} , given in the data, can be integrated (added) to determine values for any time period. The change in internal energy of the cavern ΔE_S was found from the given daily temperature profile data from day i to day j using

$$\Delta E_{S,j-i} = V_S \rho C_p (\bar{T}_j - \bar{T}_i) \quad (3.1)$$

where

\bar{T}_i = average cavern temperature at end of day i (°C)

V_s = volume of store (m³)

The heat losses from the store over a period, E_{env} , could be thus be found by subtraction. Table 3.4 gives monthly summaries of the storage volume energy flows from the Lyckebo operational data for the 12 months preceding December, 1987. Approximately 31% of the energy injected in the cavern during this period appears as losses to the surrounding rock. Cavern losses were not found for 1985 and 1986 because week-long or larger blocks of data were missing for these two years.

The SST validation simulation spanned five years, from the time when the Lyckebo CSHPSS system became operational in April, 1983 through November, 1987. Three years of hourly operational data were obtained covering the years 1985, 1986, and 11 months of 1987. As discussed in Section 2.1.5, it was necessary to approximate the thermal diffusion in the ground surrounding the storage volume for the period of April 1983 through the beginning of 1985. The sinusoidal pre-heating cycle (Figure 2.8) was used in lieu of data for this period.

Missing data was replaced with hours from surrounding days. Data for 1987 was nearly complete, while 11% was missing for 1986 and 19% was missing for 1985.

Table 3.4: Lyckebo Operational Data Monthly Energy Balance for 1987 Simulation Year

<u>Day</u>	<u>Date</u>	<u>Avg Temp</u>	<u>ΔE_s (TJ)</u>	<u>E_{in} (TJ)</u>	<u>E_{out} (TJ)</u>	<u>E_{env} (TJ)</u>
334	30-Nov-86	69.94	-----	-----	-----	-----
365	31-Dec-86	69.47	-0.20	4.96	3.25	1.91
031	31-Jan-87	57.65	-4.95	0.00	4.91	0.04
059	28-Feb-87	50.17	-3.13	0.10	3.53	-0.30
090	31-Mar-87	49.19	-0.41	3.28	3.68	0.01
120	30-Apr-87	53.66	1.87	5.06	2.44	0.75
151	31-May-87	58.07	1.85	4.82	1.87	1.10
181	30-Jun-87	57.97	-0.04	2.15	1.28	0.91
212	31-Jul-87	65.62	3.21	5.66	0.81	1.64
243	31-Aug-87	65.47	-0.06	2.57	1.12	1.51
273	30-Sep-87	66.92	0.61	3.34	1.39	1.34
304	31-Oct-87	69.67	1.15	4.76	1.73	1.88
334	30-Nov-87	<u>73.93</u>	<u>1.79</u>	<u>6.25</u>	<u>2.11</u>	<u>2.35</u>
Avg:		61.49	Total: 1.67	42.95	28.12	13.15

3.3 Description of Validation Simulation

The objective for the validation of the TRNSYS SST component was to match predicted cavern temperature profiles and losses to those of the data. Simulation and actual average temperatures on the last day of the month were compared, rather than average monthly temperatures, as a stringent test of SST predictive capabilities. Ground loss comparisons were also used to validate the SST model; however, data for the storage volume injected and extracted energies were not used for the entire simulation, making loss comparisons unreliable for the start of the simulation.

The validation simulation made use of nearly all the available data. Figure 3.5 shows the chronology of data use in the validation simulation. April 1, 1985 was chosen as the start of the data input, rather than the first day of available data, January 1. Hourly massflow and temperature data were used to drive the model. The measured storage volume profile for March 31, 1985 was entered as a starting cavern temperature profile

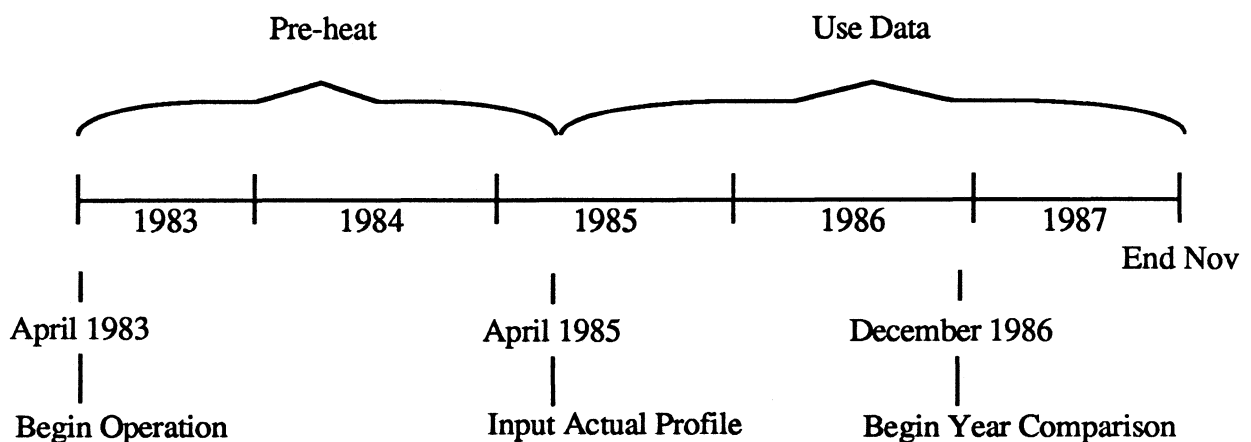


Figure 3.5 Chronology of Lyckebo Data Use for SST Model Validation

after the 2 years of pre-heating. The 2 m transition zone for this date began at a depth of 4 m, indicating near depletion of the store.

Experience with seasonal storage simulations has shown that it is best to begin an annual cycle when the store is starting the charging phase in April rather than during the winter discharging phase; the available data for January through March 1985 was therefore not used. In this manner, the effect of errors in storage volume and ground temperature profiles are minimized, as it is easier to predict conditions at the low point of an annual cycle. If the initial storage volume temperature profile is unknown, it can be assumed that the store is depleted on April 1 and is near a fully mixed state. A single value for the storage temperature can then be given. Storage volume losses during winter months are better predicted having a previous history in the ground temperature profile. An error in the initial temperature profile of the surrounding ground may thus affect the quantity of energy available for extraction to the load during winter discharge for simulations starting at the beginning of a calendar year.

Because the system is experiencing transient rather than steady state losses throughout the 5 year simulation (known from measured loss data), only results for the final year of the simulation were compared to the data values. The simulated temperature profile of the surrounding ground following the two years of pre-heat would be undoubtedly different than the actual profile. This initial incorrect ground profile would in turn produce inaccurate simulation heat losses and temperature profiles, with the amount of error decreasing with time. By continuing the hourly simulation for several years with actual data, inaccuracies in the ground profile would "self-correct". It is therefore the 12 months from December 1986 to November 1987 (further referred to as

the "1987 Simulation Year") which comprise the comparison between the Lyckebo operational data and its prediction by use of the SST model.

3.4 Lyckebo Cavern Thermosiphon

An additional difficulty in the validation simulation of the Lyckebo CSHPSS system is the presence of a convective heat flow through a crack system in the cavern. The phenomenon was reported by Brunström (1987b) of the Älvkarleby Laboratory. Heat losses from the cavern were measured to be as much as 50% greater than design predictions, with the increase due to this mechanism. Figure 3.6 depicts the location of the cracks which presumably lead to a tunnel used during construction of the cavern. No net loss of water from the cavern has been observed.

The cracks act as a thermosiphon, drawing hot water from near the top of the storage volume and returning cold water to the bottom with density differences as the driving force. The ground surrounding the bypass tunnel will remain cooler than that of the storage volume for many annual cycles. Thus, the warm water entering the tunnel cools and sinks, creating the thermosiphon.

Älvkarleby Laboratory estimated that the annual mean flowrate in the crack system was $2 \text{ m}^3/\text{hr}$. This value was found from the difference between measured and computer calculated annual conductive heat losses for three cycles and a 50°C average temperature difference in the store. Brunström chose one month when the store was fully charged (September 15 to October 15, 1985) for further study. The thermosiphon flowrate was

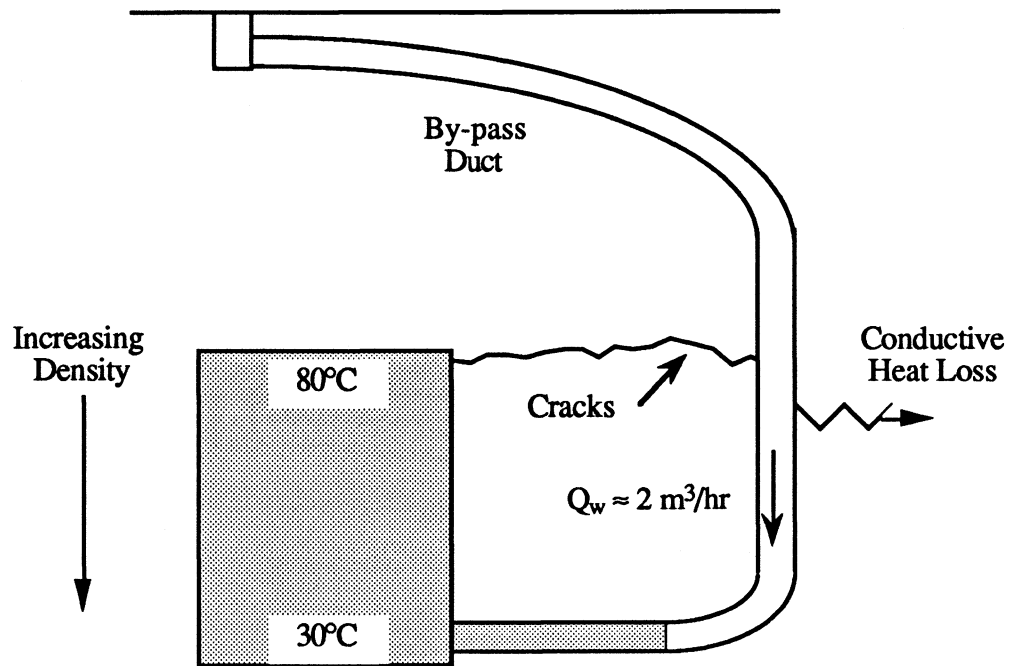


Figure 3.6: Crack System in Lyckebo Cavern Acts as a Thermosiphon

then estimated to be 4 m³/hr at this time, again by completing an energy balance. A simulation with the SST model and known energy flows for this period was performed. The Brunström simulation included a model for the thermosiphon heat flow which assumed water leaves from the top of the cavern and returns to the bottom storage volume node at a temperature of 28°C at this higher flowrate. Results gave a storage temperature profile in agreement with the measured profile.

A simple model of the Lyckebo cavern thermosiphon heat losses based on the Älvkarleby report was developed for use in the present TRNSYS SST validation simulations. The thermosiphon flowrate was estimated as a linear function of the density differences in storage volume temperature profile. The return thermosiphon flow is inserted into the storage volume profile as in Section 2.2.2. Heat conduction from the

thermosiphon flowstream to the surrounding ground was not modelled.

The average density of the water in the cavern, $\bar{\rho}$, was found by integrating the density of the liquid over the height of the storage volume (recall that the storage volume nodes in the SST model are equi-volume but not necessarily the same height), such that

$$\bar{\rho} = \frac{\int_{\text{bottom}}^{\text{top}} \rho_x dx}{\int_{\text{bottom}}^{\text{top}} dx} \cong \frac{\sum_{jj=1}^N \rho_{jj} h_{jj}}{H_s} \quad (3.2)$$

where

$$\begin{aligned} \rho_{jj} &= \text{density of a storage volume node} && (\text{kg/m}^3) \\ h_{jj} &= \text{height of a storage volume node} && (\text{m}) \\ H_s &= \text{height of storage volume} \end{aligned}$$

The density of water, ρ , was generated from a third order polynomial curve fit of data (CRC, 1973) between 20 and 100 °C.

The thermosiphon flowrate was scaled to the actual average density of the water in the cavern for the 1987 simulation year (December 1986 through November 1987). Initially, a value of 4 m³/hr was chosen as a maximum flowrate occurring at minimum density. A flowrate of 2 m³/hr was estimated by Brunström to be an approximately average value. The minimum flowrate at maximum density was undetermined. This is shown in Figure 3.7 where a linear correlation between the scale on the left hand side and

that on the right hand side was assumed. Then, changes in thermosiphon flowrate - density scaling were made in subsequent simulations by choosing minimum flowrates while keeping the maximum value near $4 \text{ m}^3/\text{hr}$.

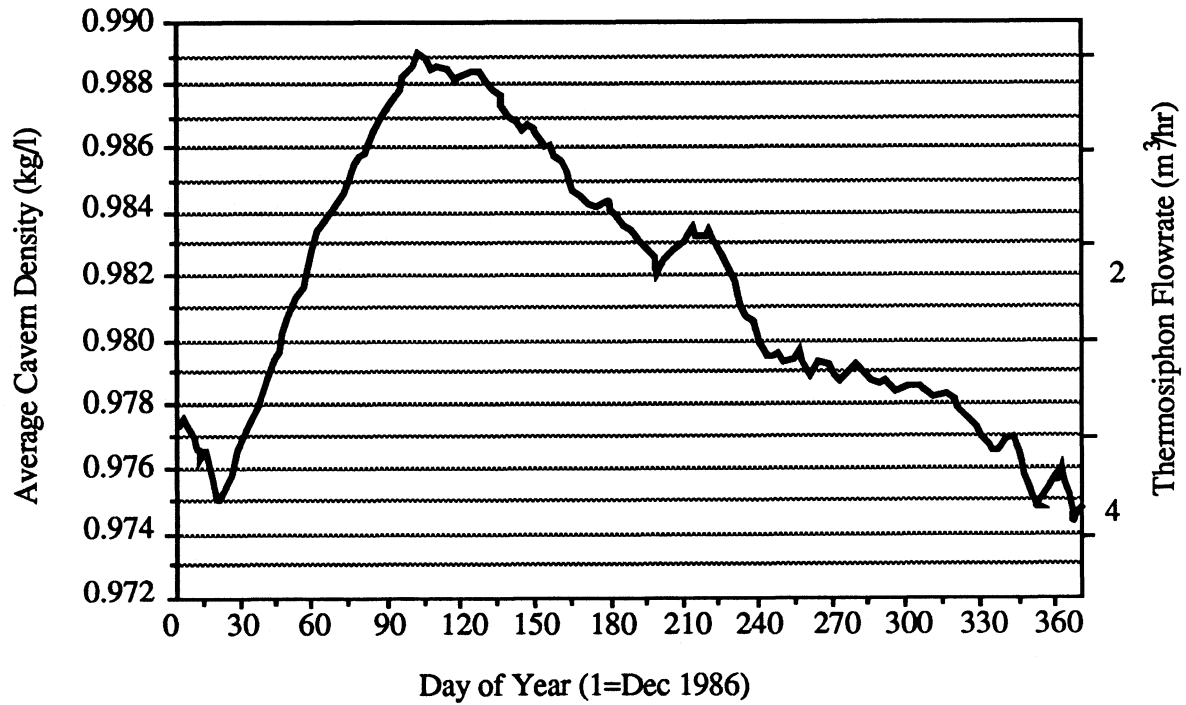


Figure 3.7: Daily Average Density of Water in Cavern vs. Day of Simulation

Thermosiphon heat losses, E_{loss} , were then found by

$$E_{\text{loss}} = \dot{m} C_p (T_{\text{top}} - 28^\circ\text{C}) \quad (3.3),$$

where

\dot{m} = flowrate of the thermosiphon,

and added to the conductive storage heat losses, E_{env} , of the SST program.

3.5 Simulation Procedure

The section summarizes the steps taken in preparation for the execution of the validation simulations using the Lyckebo operational data.

Several changes in the SST code were made in order to use the data. The subroutine which simulated the cavern thermosiphon was added. Code allowing the input of an initial storage temperature profile was added. A grid using the toroidal shape and measurements of the Lyckebo cavern (Wallentun, 1986) was entered using the grid pre-processor program, rather than using the default shape of a vertical cylinder (a brief discussion of differences in simulation results for the two shapes follows). Computer code was added which would allow variable extraction (section 2.2.4), rather than fixed extraction from the bottom, on the collector side of the storage volume and was nearly identical in logic to that of the load side. Data temperatures of storage extraction to the load and to the collector were used as SST "demand" temperatures. This addition resulted in simulation injected and extracted energies exactly matching those of the data.

Variations on the maximum and minimum of the "pre-heat" sinusoid amplitude were made, using the initial thermosiphon flowrate suggested by Figure 3.7. Values of 70 °C and 40 °C were chosen as the parameters which gave results most consistent with Table 3.4 . Then, variations in thermosiphon flowrate - density scaling were made.

Table 3.5 lists the SST parameters used in the TRNSYS validation simulation. A value of 60 storage volume nodes was chosen to match since temperature measurements of the cavern were taken every 0.5 meter along the 30 meter cavern depth.

Table 3.5: TRNSYS SST Parameters Used In Validation Simulation

<u>Variable</u>	<u>Use</u>	<u>Value</u>	
VOLST	Tank volume	100,000	(m ³)
HEIGHT	Tank height	30	(m)
THISO	Thickness insulation	0	(m)
FRIST	Relative weight of insulation	(Top)	1
FRISS	" " " "	(Sides)	1
FRISB	" " " "	(Bottom)	1
RISLAM	Thermal conductivity of insulation	0.04	(W/m-°C)
DEPTH	Distance between ground & top of tank	30	(m)
TSTIN	Initial temp in storage volume	**	
CWATER	Volumetric heat cap. of fluid	4.19E6	(J/m ³ -°C)
WFLOWX	Max flowrate (If RLSTO>0)	1	(m ³ /Day-VOLST)
RLSTO	Char. length of dispersion term	1	(m)
DISPER	Darcy power	1	
RLAMST	Thermal cond. of storage volume	0.67	(W/m-°C)
CSTO	Volumetric heat cap for storage	4.19E6	(J/m ³ -°C)
TIMO3	Duration of simulation	1	(Years)
IPRE	No. of pre-heat cycles	2	
TCMAX	Max pre-heat store temp	70	(°C)
TAIR	Ground surface temp during pre-heat	1	(°C)
TSTART	Initial ground surface temp	6.5	(°C)
TGRAD	Gradient of TSTART (us. negative)	0	(°C/m)
NEQ	Number of storage nodes	60	
ILAY	No. ground layers w/ diff thermal props	1	
RLAML	Thermal conductivity in a layer	3.5	(W/m-°C)
CL	Volumetric heat cap in a layer	2.2E6	(J/m ³ -°C)
THL	Thickness of a layer	1000	(m)

**Actual Lyckebo cavern profile of 3/31/85 entered

3.6 Simulation Results

Two type of simulations were performed to validate the SST model, one with storage buffers and one without buffers. Although the methods presented to circumvent the aforementioned difficulties in performing validation simulations (the cavern thermosiphon and no data for an initial ground temperature profile) could not be expected to yield an exact match with data cavern profiles and measured heat losses, it was found that very good agreement was still obtained. Differences between actual and predicted ground losses were approximately the same for the two types of simulations.

3.6.1 Results Without Use of Buffers

A preliminary simulation was performed using the simulation procedure outlined in the previous section and without the use of storage volume buffers. Results for this simulation are presented in Table 3.6. The Lyckebo actual data average temperatures for the last day of the month and the measured monthly heat losses are repeated from Table 3.4. The difference between last day average temperatures and monthly heat losses for the simulation results and actual data are also listed.

The simulation results generally are in agreement with the actual values. The mean absolute difference in predicted and actual values of last day of the month average storage temperatures is 1 °C, with differences of nearly 3 °C for January and 2 °C for July. Calculated monthly losses were generally within 0.33 TJ of measured values, with the

predicted annual loss within 9% of the measured value.

Table 3.6: Preliminary Results for Validation Simulation

<u>Date</u>	<u>Average Temperature (°C)</u>			<u>Monthly Loss (TJ)</u>		
	<u>Actual</u>	<u>Simulation</u>	<u>Difference</u>	<u>Actual</u>	<u>Simulation</u>	<u>Difference</u>
31-Dec-86	69.47	69.30	0.17	1.91	1.58	0.33
31-Jan-87	57.65	60.40	-2.75	0.04	0.48	-0.44
28-Feb-87	50.17	50.47	-0.30	-0.30	-0.17	-0.13
31-Mar-87	49.19	48.66	0.53	0.01	0.09	-0.07
30-Apr-87	53.66	51.86	1.80	0.75	0.68	0.06
31-May-87	58.07	56.54	1.53	1.10	0.97	0.13
30-Jun-87	57.97	59.11	-1.14	0.91	0.92	-0.01
31-Jul-87	65.62	63.64	1.98	1.64	1.43	0.21
31-Aug-87	65.47	66.87	-1.40	1.51	1.41	0.10
30-Sep-87	66.92	67.82	-0.90	1.34	1.33	0.01
31-Oct-87	69.67	70.38	-0.71	1.88	1.55	0.33
30-Nov-87	73.93	74.89	-0.96	2.35	1.76	0.59
Average:	61.49	61.66	-0.17			
Annual Total:				13.15	12.00	1.15

Figures 3.8a and 3.8b show actual data and preliminary simulation temperature profiles of the Lyckebo cavern for June and September 1987. The two curves are in excellent agreement for June, but the simulation profile for September shows numerical dispersion in comparison to the actual temperature profile. Here the term "numerical dispersion" refers to the slope of the simulation curve which is much less steep than the nearly vertical slope of a well defined transition zone shown by the actual cavern profile. Because the performance of the collector and load subsystems is fixed via use of operational data, this dispersion can be contributed solely to the numerical method of the model rather than changes in the cavern temperature profile.

Predicted ground losses from the storage volume consisted of two parts, those from pure conduction into the rock and those due to the cavern thermosiphon. Conduction losses predicted by the SST model were added to those predicted by the linear correlation of thermosiphon flowrate and daily integrated average density to give the monthly ground losses shown in Table 3.6. The contribution of each loss type to the total monthly loss during the simulation year is given in Table 3.7. Thermosiphon losses consisted of nearly half the simulation total losses on annual basis.

Figure 3.9 shows the thermosiphon correlation used in the simulation. The maximum and minimum of the correlation were obtained by trial and error. The maximum flowrate at minimum integrated average density is approximately $5 \text{ m}^3/\text{hr}$, rather than a value of $4 \text{ m}^3/\text{hr}$ suggested by the original study. The simulation results were more sensitive to the choice of maximum than minimum flowrate, which corroborates with a high contribution of thermosiphon losses observed during periods of

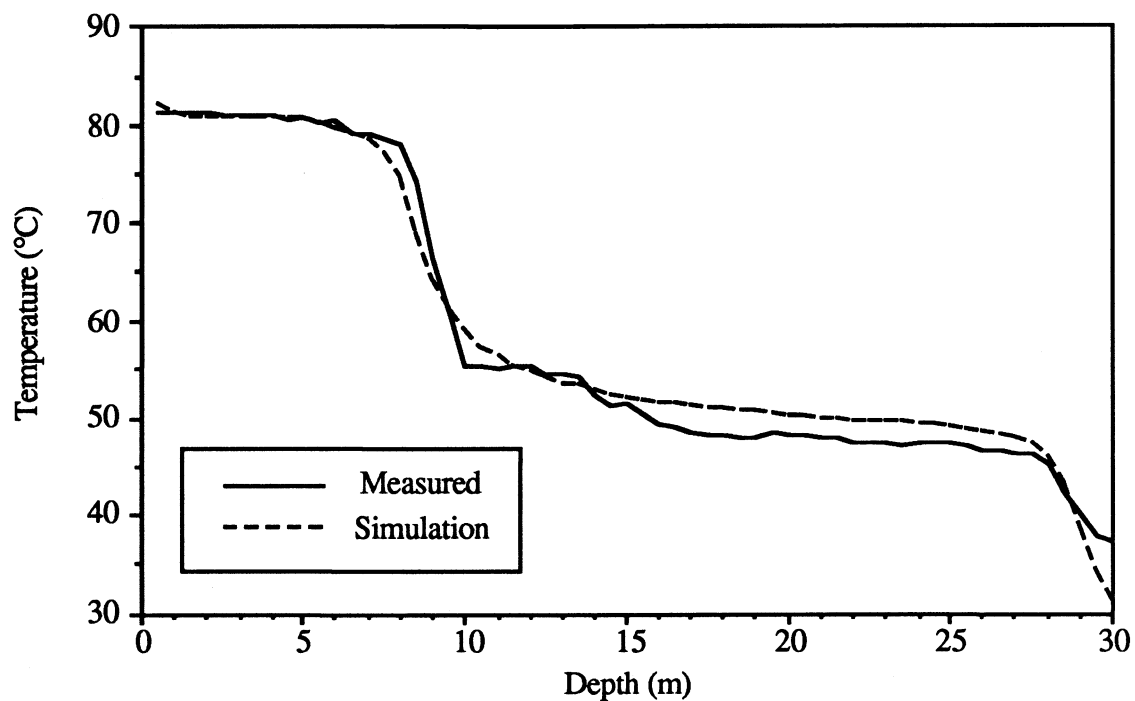


Figure 3.8a: Measured and Simulation (without Buffers) June 1987 Storage Profiles

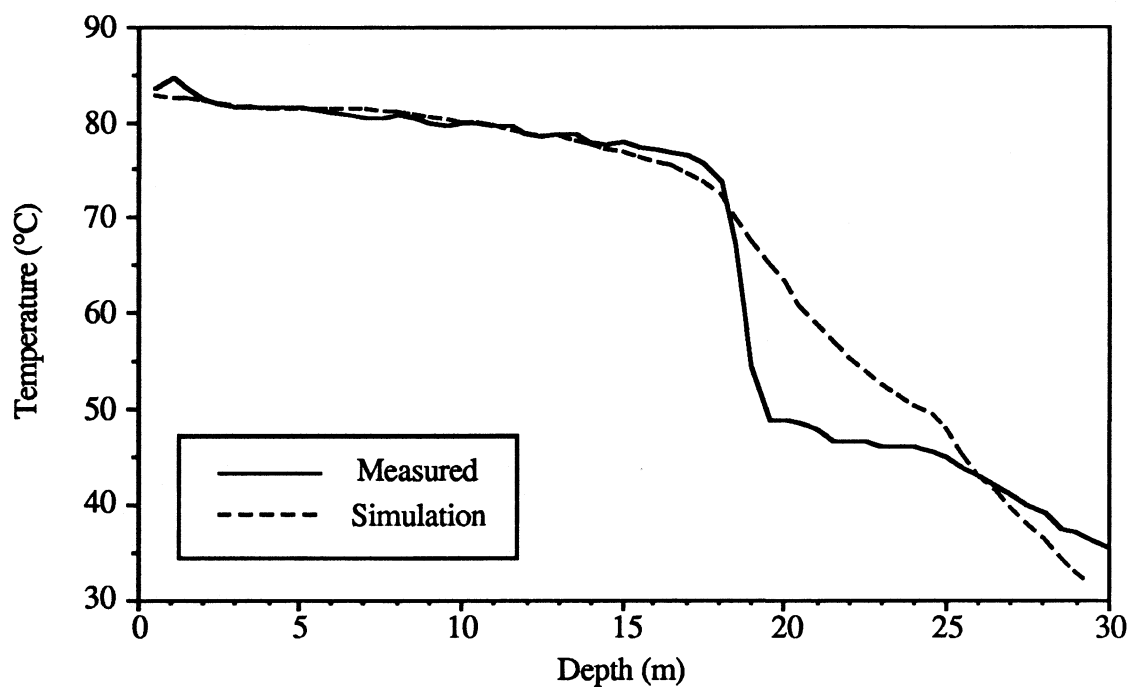


Figure 3.8b: Measured and Simulation (without Buffers) Sept. 1987 Storage Profiles

Table 3.7: Thermosiphon Losses as Percent of Total Ground Losses (in kJ)

<u>Conductive</u>	<u>Thermosiphon</u>	<u>Total</u>	<u>% Thermosiphon</u>
7.60E+08	8.20E+08	1.58E+09	51.9
4.55E+07	4.38E+08	4.84E+08	90.6
-3.04E+08	1.34E+08	-1.71E+08	(-78.2)
2.85E+07	5.77E+07	8.62E+07	66.9
5.63E+08	1.21E+08	6.84E+08	17.7
6.94E+08	2.77E+08	9.71E+08	28.5
5.63E+08	3.58E+08	9.21E+08	38.8
9.02E+08	5.28E+08	1.43E+09	36.9
7.53E+08	6.56E+08	1.41E+09	46.6
6.76E+08	6.51E+08	1.33E+09	49.1
7.88E+08	7.65E+08	1.55E+09	49.3
8.80E+08	8.83E+08	1.76E+09	50.1
6.35E+09	5.69E+09	1.20E+10	47.3

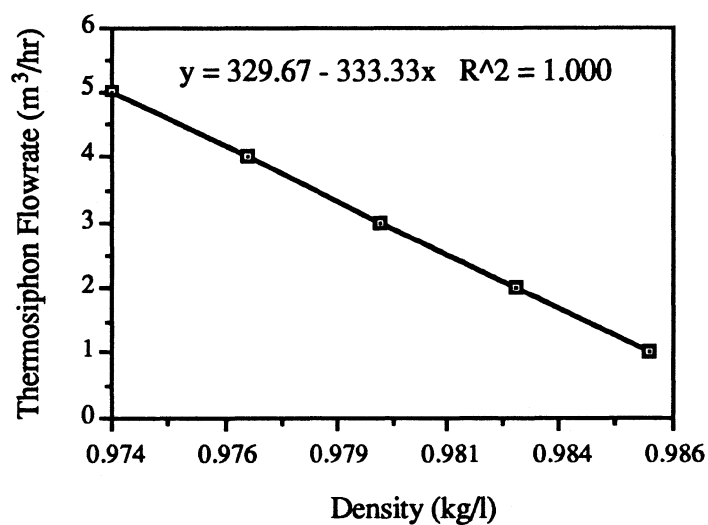


Figure 3.9: Thermosiphon Flowrate vs. Density

high energy injection into the Lyckebo cavern.

The same simulation was repeated for an automatically generated cylindrical storage volume. Thus, the 18 m of rock separating the inner boundary of the storage volume and axis of revolution was not modelled. Resultant ground losses were less than those for the simulation with the toroidal storage volume and found to be 11.4 TJ annually. Accordingly, the annual average storage temperature was 3.3 °C warmer than both the actual and previously predicted values.

3.6.2 Results with Use of Buffers

A second simulation of the Lyckebo system was performed using buffers. The buffer system, discussed in section 2.4, was added to counter the appearance of numerical dispersion. The buffers used in this simulation were injected into the storage volume when completely full, rather than being purged after 24 hours. In this manner, the temperature profile was updated by a net shift (plug flow), rather than cell volume mixing, and the maximum effect of a buffer system was observed. The effect of buffer size (e.g., full, 24 hour, etc.) and number of nodes on numerical dispersion is discussed in Section 3.8.

Figures 3.10a and 3.10b show the resultant profiles for the full buffer simulation during the same months of 1987. Indeed, the shape of the simulation curves more closely match the actual data profiles. However, the simulation temperature profiles fall below the actual curves near the top of the cavern and above the actual near the bottom of

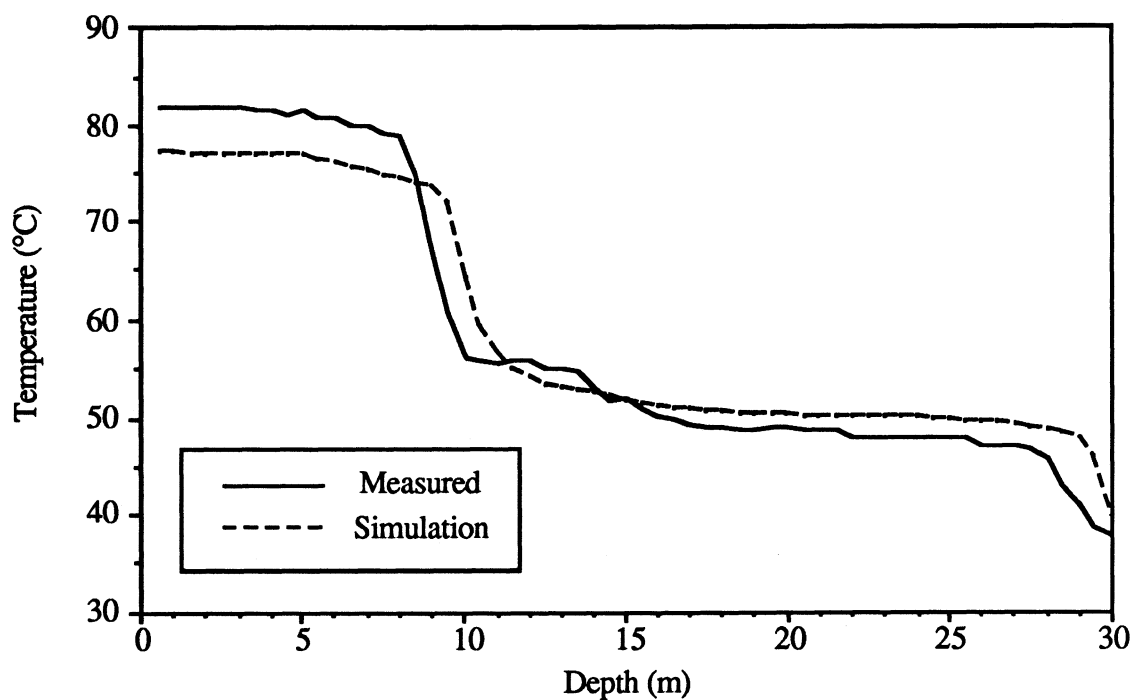


Figure 3.10a: Measured and Simulation (with Buffers) June 1987 Storage Profiles

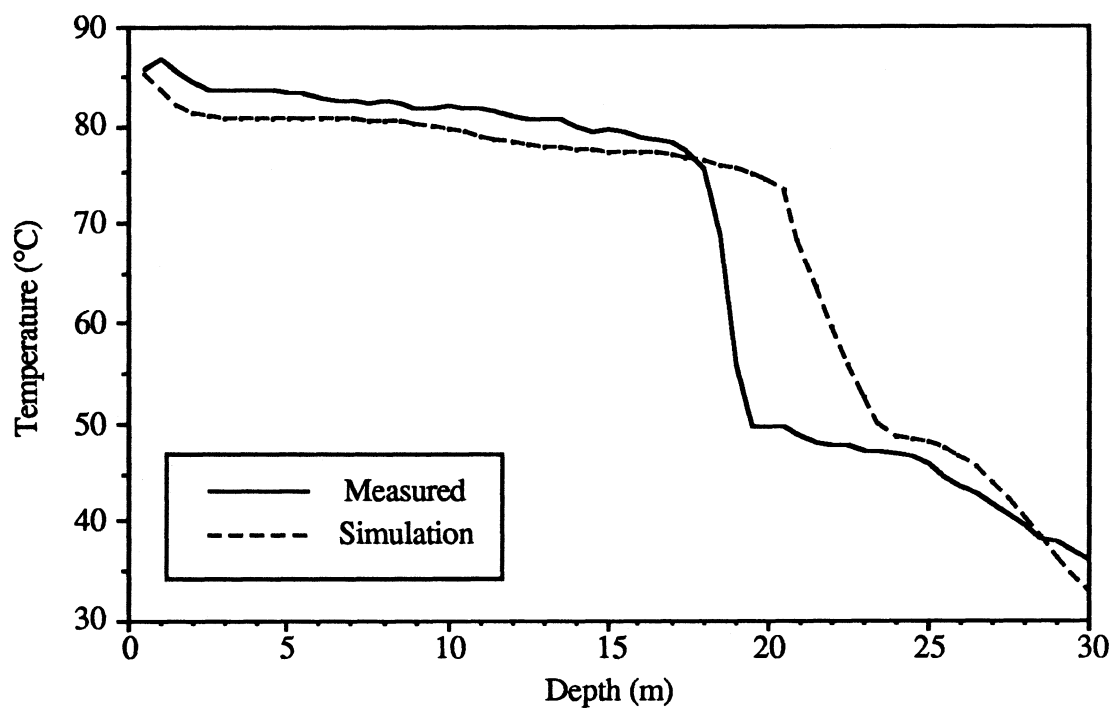


Figure 3.10b: Measured and Simulation (with Buffers) Sept. 1987 Storage Profiles

the cavern. This is a result of the temperature averaging of the incoming flowstreams within the buffer (equation 2.13).

The simulation results, shown in Table 3.8, do not match the measured losses and average temperatures as well as the previous simulation. The predicted values in monthly losses are generally slightly less than those of the previous simulation. Presumably, this is because the water injected from the heat source was at a lower average buffer temperature, resulting in a cooler layer at the top of the store. Again, the mean absolute difference in values for last day of the month average storage temperatures is 1 °C. Three months, all occurring at the end of the simulation are warmer than the actual average temperatures by 2.2 to 3.5 °C. The storage losses are underpredicted for these same months, indicating low thermosiphon losses, rather than conductive losses.

A change in the thermosiphon model likely caused the high temperatures in the store and low ground losses at the end of the full buffer simulation. The thermosiphon model was modified such that it also functioned as a buffer to avoid any "cell volume mixing". The flow through the thermosiphon was calculated every hourly timestep. When the volume of the thermosiphon flow over time was equal to that of a node, extraction of hot water from the top of the cavern and injection of cold water into the bottom of the cavern occurred. At a maximum flowrate of 5 m³/hr, movement of water in the thermosiphon model took place every 14 days. Large amounts of energy were continuously supplied by the electric boiler during these same months. The storage temperature profile on the last day of these months were likely between movements of a thermosiphon plug. Thus, the simulated temperature profiles which were compared to the data did not reflect all thermosiphon losses.

Table 3.8: Full Buffer Results for Validation Simulation

<u>Date</u>	<u>Average Temperature (°C)</u>			<u>Monthly Loss (TJ)</u>		
	<u>Actual</u>	<u>Simulation</u>	<u>Difference</u>	<u>Actual</u>	<u>Simulation</u>	<u>Difference</u>
31-Dec-86	69.47	70.45	-0.98	1.91	1.71	0.20
31-Jan-87	57.65	57.49	0.16	0.04	0.60	-0.56
28-Feb-87	50.17	49.17	1.00	-0.3	-0.05	-0.25
31-Mar-87	49.19	48.52	0.67	0.01	-0.22	0.23
30-Apr-87	53.66	53.19	0.47	0.75	0.74	0.01
31-May-87	58.07	57.89	0.18	1.1	0.99	0.11
30-Jun-87	57.97	57.83	0.14	0.91	0.81	0.10
31-Jul-87	65.62	66.40	-0.78	1.64	1.34	0.30
31-Aug-87	65.47	66.34	-0.87	1.51	1.35	0.16
30-Sep-87	66.92	69.14	-2.22	1.34	1.27	0.07
31-Oct-87	69.67	72.27	-2.60	1.88	1.53	0.35
30-Nov-87	73.93	77.40	-3.47	2.35	1.76	0.59
Average:	61.49	62.17	-0.68			
Totals:				13.15	11.83	1.32

3.7 Equivalent Conductivity Of Thermosiphon

Simulations without the use of the thermosiphon model were performed to find a value of thermal conductivity for the rock surrounding the Lyckebo cavern which would yield annual ground losses equivalent to those of the data. The purpose of these simulations was to determine reasonable values of rock conductivity could account for the observed ground losses. Measured values of annual ground losses were determined as the difference between the measured energy injected into and extracted from the cavern and the annual change in internal energy of the store. The measured value of rock conductivity ranges from 3.1 to 3.5 W/m-°C (Wallentun, 1986). The value used in the previous simulations is 3.5 W/m-°C.

Values of rock conductivity between 5.0 and 10.0 W/m-°C were examined. The 2 years of pre-heat were performed using these higher conductivities, while the SST grid was held constant (conductivity is one of the parameters which determines the grid when automatic generation is used). Other parameters and procedures were the same as in the validation simulations. The predicted annual ground losses with conductivities in this range are shown in Figure 3.11. The ground losses of Figure 3.11 can be compared to the measured value for the 1987 simulation year (December 1986 through November 1987) of 13.15 TJ (Table 3.4). A simple comparison of annual conductivities, however, is not a good predictor of an equivalent conductivity as explained below.

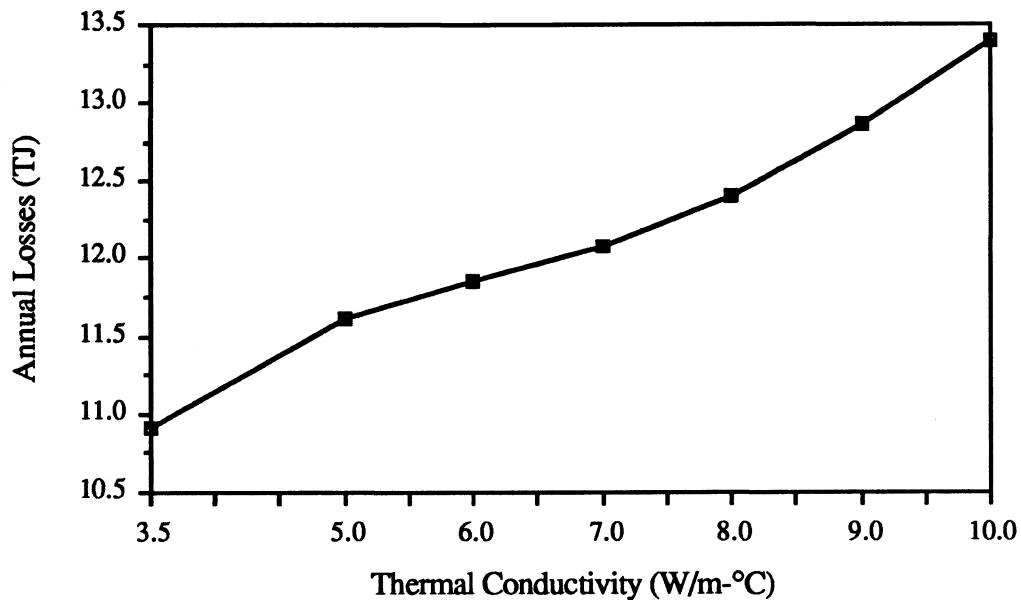


Figure 3.11: Predicted 1987 Annual Losses at Higher Rock Conductivities

Because the storage forcing functions used to drive the SST model (recorded injection and extraction temperatures and massflows of the Lyckebo operational data) were held constant, there is a narrow range of thermal conductivities (greater than 3.5 W/m-°C) which yield a storage volume energy balance when the thermosiphon subroutine is not used. With the actual value of rock conductivity and no thermosiphon, the simulation storage profiles become too warm or too cold for the load and collector "demand" temperatures of the operational data (Section 3.5) to be met. Although thermal conductivities of 8 through 10 W/m-°C yielded annual loss predictions which were increasingly closer to the actual value, all three failed to satisfy a storage volume energy balance; these values had energy balance closure errors during the end of annual cycles (i.e., the month of March) of 15, 23, and 30%, respectively. (Conversely, an error of 11% was observed during the month of November using a thermal conductivity of 3.5

W/m-°C for the no thermosiphon simulation.) The closure for simulations using thermal conductivities of 5 to 7 W/m-°C was within 1% for all months.

An equivalent conductivity was further selected from the range of possible values by examining the resultant storage volume last day temperature profiles (by inspection) and average temperatures for the 1987 simulation year. A thermal conductivity of 6.0 W/m-°C resulted in profiles in which the temperatures near the bottom of the cavern were too hot and average temperatures which were about 2 °C above the actual values. Conversely, a thermal conductivity of 8.0 W/m-°C resulted in storage profiles in which the temperatures at the top of the cavern were too cold and average temperatures were about 2 °C below the actual values. A value of 7.0 W/m-°C appeared to give correct stratification of storage volume temperature profiles and average temperatures which matched actual values well (with the exception of the last month of the simulation).

Figure 3.12 shows measured values of monthly cavern losses for 1987 and those predicted with a thermal conductivity of 7.0 W/m-°C. Also plotted are the monthly ground losses predicted using the thermosiphon loss model in the validation simulation (without buffers) of Section 3.6.1. It is seen that both simulations failed to predict the high losses experienced at the end of the simulation during which time the electric boiler is run continuously (Figure 3.2b).

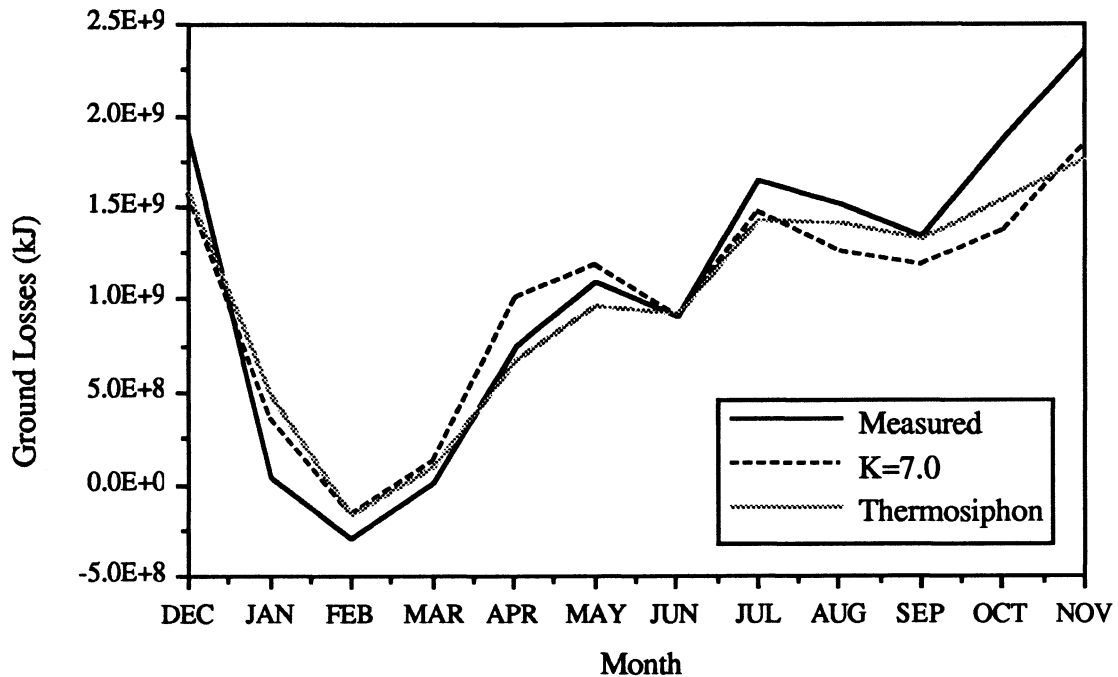


Figure 3.12: Monthly 1987 Measured Losses for Lyckebo Cavern and Simulated Losses with $k=7.0$ and for Thermosiphon Loss Model

Similar plots (not shown) of monthly losses at conductivity values of 8 through 10 $\text{W/m}^\circ\text{C}$ were examined. Even though the resultant annual loss predictions were closer to the measured value, monthly loss predictions using these thermal conductivity values were clearly wrong. Monthly losses during March through July were greater than both the measured values and those predicted using 7 $\text{W/m}^\circ\text{C}$. Simulations using conductivities of 8 through 10 $\text{W/m}^\circ\text{C}$ predicted more energy gains during winter months than both the measured values and those predicted using 7 $\text{W/m}^\circ\text{C}$. Losses predicted near the end of the simulation using conductivities of 8 through 10 $\text{W/m}^\circ\text{C}$ were even lower than those predicted using 7 $\text{W/m}^\circ\text{C}$, as the last day average store temperature were 2 to 6 $^\circ\text{C}$ less than that of the 7 $\text{W/m}^\circ\text{C}$ rock.

3.8 Effect Of Buffer Size And Number Of Nodes

The effects of both buffer size and the number of nodes on simulation results were investigated. Two sets of simulations were performed. The first set of simulations used buffers which were injected into the storage volume when full (resulting in plug flow), after 24 hours, and without the use of buffers and were compared for three storage volumes which differed in number of nodes. The second set of simulations investigated only the effect of varying the number of nodes, without the use of buffers.

Increasing the number of storage volume nodes results in increased thermal stratification and increased system efficiency, until some point where increasing the number of nodes has no effect. The simulations presented here used only input data to drive the SST model, rather than a full system simulation which models the collectors and the load. Any changes in solar collector and load subsystems performance due to changes in store temperatures are therefore not included. The storage volume temperature profile and ground losses are thus the only variables of consideration in investigating the effects of stratification and buffer size.

The use of hourly data as SST "demand" temperatures made the use of full buffers possible. Full buffers were found to be not compatible with full system TRNSYS simulations (iterating with collector and load subsystem components) in which the concept of variable extraction outlet is used. If the temperature profile of the storage volume is not held constant during the period in which a buffer is filling, then the storage volume energy balance will not be satisfied. Each of the two full buffers is injected into

the storage volume when completely filled, rather than simultaneous injection, changing the temperature profile before the other is injected. As a buffer is injected, the water leaving the store must have the same temperature as that on which variable extraction calculations at previous timesteps were based. The storage volume extraction temperature determines either the subsystem flowrate or the return temperature of the flow stream. These variables in turn determine the volume and temperature of the buffer contents.

A set of three simulations similar to the Lyckebo validation simulation were performed to investigate the effect of use of full, 24 hour and no buffers for a set number of nodes. Simulations using 10, 30 and 60 nodes were investigated. Parameters identical to those from Table 3.5 were used for all nine simulations (three buffer types each at 3 levels of stratification) with the exception that each simulation was given the same initial storage temperature profile. In this manner, all simulations exhibited the same storage volume and ground temperature profiles after two pre-heat cycles. Data was input starting April, 1985 as in the validation simulation. These simulations did not include the cavern thermosiphon model.

Differences in full, 24 hour and no buffer storage volume temperature profiles are clearly seen after 4 months of simulation in Figures 3.13a and 3.13b for 10 and 30 nodes. In the 10 node simulation, temperatures are slightly warmer near the top of the store for the 24 hour buffer than for the full buffer. The appearance of the 24 hour buffer simulation profile is also improved over that with no buffer. Increasing the number of nodes to 30 brings changes the appearance of the temperature profiles for all three buffer sizes by somewhat sharpening the transition between hot and cold temperatures. The 24 hour buffer profile also becomes closer to that of the full buffer. Increasing the number

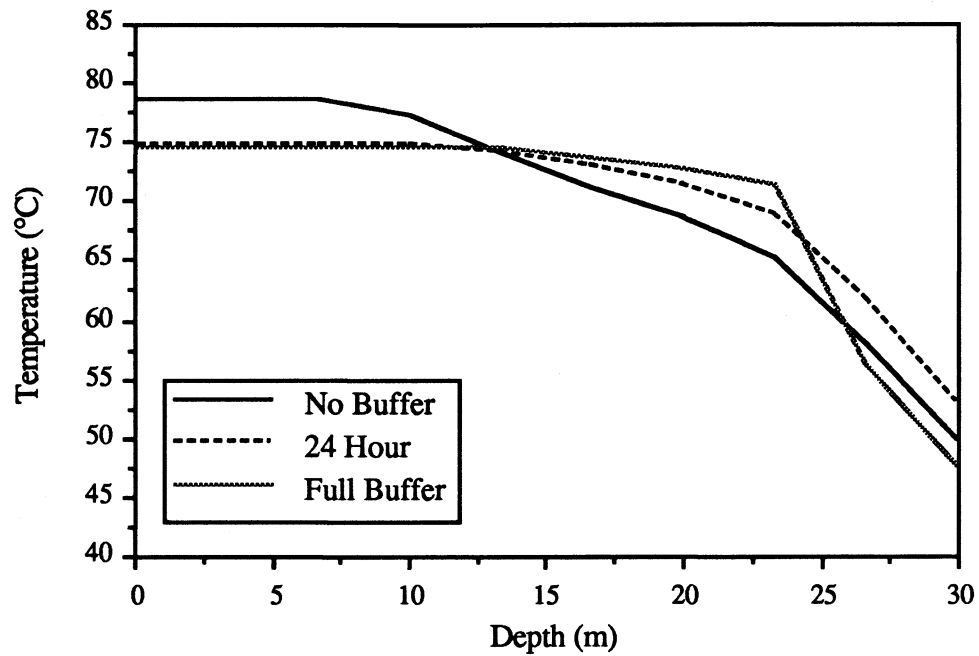


Figure 3.13a: 10 Node Profiles After 4 Months for No, 24 Hour and Full Buffers

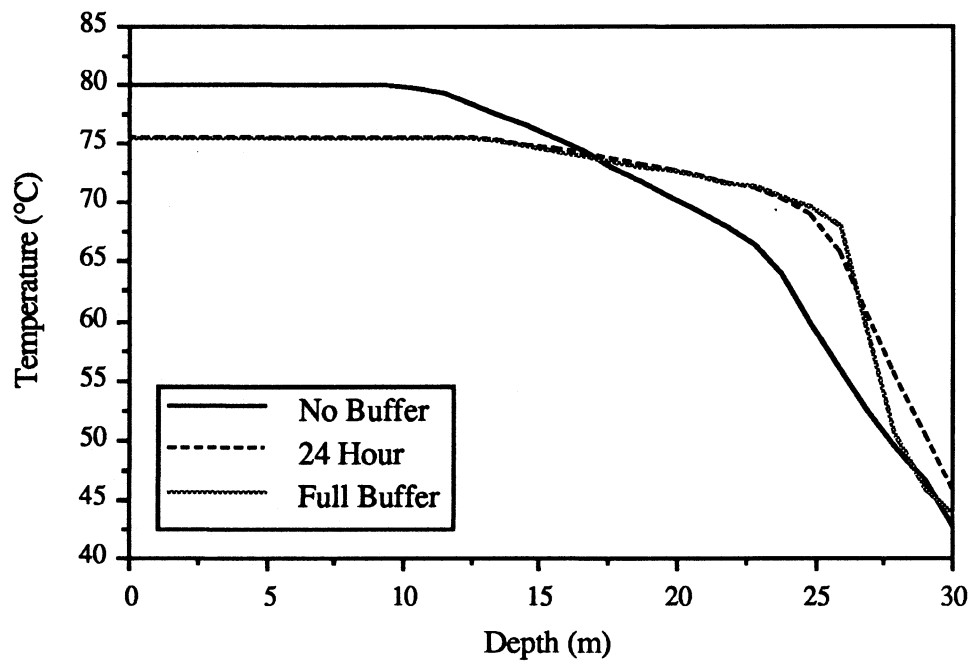


Figure 3.13b: 30 Node Profiles After 4 Months for No, 24 Hour and Full Buffers

of nodes to 60 (not shown) further sharpens the hot and cold transitions. Full buffers and those purged after 24 hours gave nearly identical results for the Lyckebo 100,000 m³ storage volume when 60 nodes were used.

These comparisons illustrate the two types of temperature flowstream mixing represented in these simulations: temperature averaging inside buffers and "cell volume mixing" within the store. Increasing the buffer size increases the retention time of the buffer contents and the amount of buffer temperature averaging. Increasing the number of nodes decreases cell volume mixing. 24 hour buffers can serve as a compromise between these two mixing effects when a small number of nodes is used.

While data hourly storage volume injection temperatures (shown in Figure 3.2d) are nearly constant for the load, they do fluctuate for the relatively constant heat sources, particularly for turn-on and turn-off hours. Temperature averaging within the buffers would not be seen in full system simulations which operate with constant collector outlet temperature and constant load return temperature during the period in which the buffers are filling.

Annual heat losses decreased slightly as the buffer size or number of nodes was increased. The maximum difference in annual heat losses among these simulations was 5%. Thus, the choices of buffer size and number of nodes by themselves (i.e., without consideration of subsystem performance) makes little difference in the prediction of annual storage losses.

A set of three simulations similar to the Lyckebo validation simulation without the use of buffers were performed to investigate the effect of increasing the number of nodes. The simulations used 10, 30 and 100 nodes. Parameters identical to those from Table 3.5 were used for all three simulations with the exception that an initial, fully mixed storage temperature of 40 °C was specified. Again, the simulations exhibited the same storage and ground profiles after two pre-heat cycles and did not include the cavern thermosiphon model.

Major differences in the shape of storage volume temperature profiles were seen using different numbers of nodes. Profiles for last day of August (after 5 months data input into the simulations) are shown in Figure 3.14a. The highly stratified temperature profiles of the Lyckebo cavern (Figure 3.3) showed a hot layer and a cool layer of water, separated by a sharp transition zone. It is seen that the storage temperature profile for the 10 node simulation has a shape which little resembles the highly stratified profiles. Because buffers were not used, flowstreams were injected into the storage volume hourly. The Lyckebo load stream flows at an approximate rate of 50 m³/hr and the intermittent heat source stream flows at an approximate rate of 100 m³/hr. Cell volume mixing (equation 2.11) therefore occurs at every timestep for the 10 node storage volume. The profile for the 30 node simulation has a shape which better defines hot and cool regions of the storage volume, but the transition between the two is not sharp. At the SST limit of 100 nodes, however, the features of the highly stratified temperature profiles are seen, along with details in the hot and cool portions of the curve which were not visible in the 30 node profile.

At the limit of 100 nodes, cell volume mixing is at a minimum. The numerical

model behaves most closely to the plug flow model at this limit. A given flow will more quickly fill a storage volume cell over time as the size of the cell decreases with an increasing number of nodes. Given the energy flows of the Lyckebo data, 60 nodes were insufficient to prevent cell volume mixing and the associated numerical dispersion for the no buffer simulation of Section 3.6.1.

Monthly values of ground losses for 10, 30 and 100 nodes are plotted in Figure 3.14b. Because the ground temperature profile after two years of pre-heat were identical at the start of each simulation, the differences in monthly losses occur only as a result of differing storage volume profiles. The least stratified profile of 10 nodes shows larger extremes in loss fluctuations than do the more stratified profiles of 30 and 100 nodes. The monthly average storage volume temperatures (not shown) were nearly the same for all three simulations. The total annual ground losses for the 10 and 100 node simulations differed by approximately 5%.

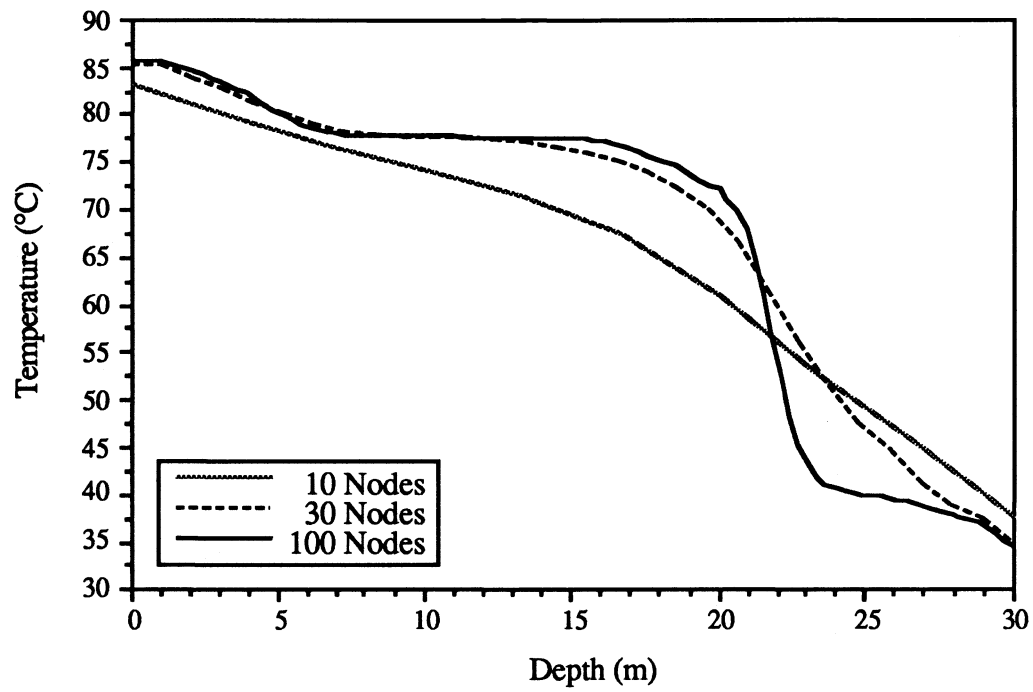


Figure 3.14a: Storage Profiles after 5 Months Simulation for 10, 30, and 100 Nodes

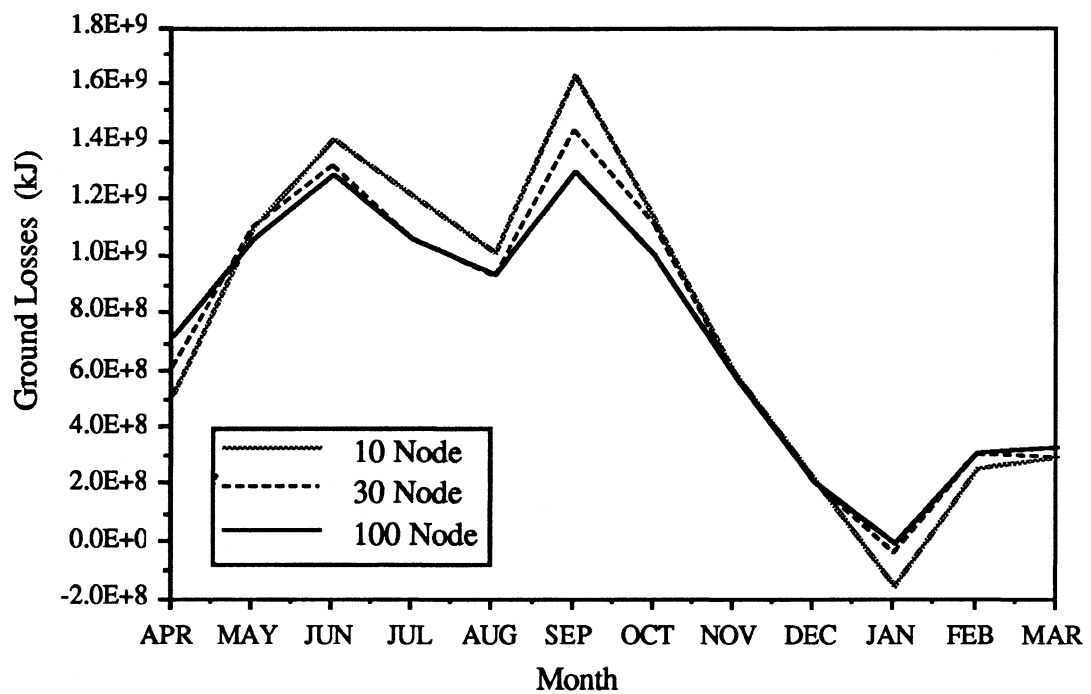


Figure 3.14b: Monthly Ground Losses for 10, 30, and 100 Nodes

Chapter 4

Comparison of TRNSYS and MINSUN CSHPSS Simulations

This chapter presents the result of computer simulations of Central Solar Heating Plants with Seasonal Storage (CSHPSS) performed using both the TRNSYS and MINSUN computer programs. Both programs include a storage volume component based on the Lund University Seasonal Storage Tank (Lund-SST). Other TRNSYS components were adapted to perform similarly to those of MINSUN. A comparison of each program's simulations indicated the differences between the two programs.

The procedure of the comparisons included a careful examination of each program's component models and control strategies through a series of test simulations. Two types of testing were performed: simulations which focused on the SST model and simulations which investigated individual subsystems. Differences in the programs are discussed in detail with specific examples as they arise in the series of test simulations.

Two full CSHPSS system simulations were also performed. The first was a simulation of the Lyckebo system with a 100,000 m³ uninsulated rock cavern. It used a high temperature distribution system with no heat pump. Parameters were based on a MINSUN optimization simulation. The second comparison simulated a smaller 15,000 m³ pit storage system which is proposed for construction in Franklin, Massachusetts. This system uses a low temperature distribution system with a heat pump.

4.1 Program Descriptions

The MINSUN program was developed under the International Energy Agency Subtask VII. It was written specifically for the simulation and optimization of CSHPSS systems. MINSUN contains simplifying assumptions and less detailed component models than TRNSYS. These simplifications allow the user to run many simulations quickly. The program is also used as a predictive tool. MINSUN works with a daily timestep, pre-processing hourly weather data to yield daily useful collected energy values and building loads.

In contrast, the TRNSYS program has a large library of components, making it very flexible for detailed analyses of many types of thermal systems. Although the TRNSYS timestep may be varied, the TRNSYS version is most commonly used with an hourly timestep. The TRNSYS modified SST differs from the current MINSUN version according to Table 2.1. Most importantly, it lets the user vary the number of storage volume nodes and makes use of non-cylindrical storage geometries like that of the Lyckebo CSHPSS.

When the TRNSYS SST 24-hour buffer strategy is in use, the timestep for the storage volume becomes daily, rather than hourly, similar to that of MINSUN. Then, the volume (from both the collector and load flowstreams) injected into the store at the end of the day is an accumulated daily total for both programs. All TRNSYS simulations in the SST and subsystem test comparisons used 24-hour buffers.

4.2 Previous Comparison Study

Only one other comparison of the two programs is known to the author (Krischel, 1985 and 1986). The TRNSYS results were used as a validation of the MINSUN program, although the component models and control strategies of each were different. The thermal performance of various storage unit/ collector combinations with and without heat pumps were investigated. Several configurations were presented additionally using TRNSYS that were not available with the MINSUN program.

The Krischel study used the TRNSYS and MINSUN components that existed at that time, without modification. The Lund SST model was implemented in the MINSUN program. The available TRNSYS tank model did not include calculations of the surrounding ground. Instead, a single UA loss coefficient was employed (Krischel, 1988). The TRNSYS version also lacked variable extraction capabilities.

Yearly solar fractions in the Krischel study were found to be 15% higher in MINSUN simulations than in TRNSYS simulations for non-heat pump systems and 10% higher in MINSUN simulations for heat pump systems. The monthly energy from the collector array for the first type of simulation was shown to be always greater in the MINSUN system, by as much as 20%. The MINSUN strategy for interpolation of daily useful energy from a Q_u vs. T_i table has since been modified (Section 4.5.1). The MINSUN simulations resulted in lower predicted system loads than TRNSYS for some months.

It was observed that the MINSUN simulations produced a more stratified storage

volume temperature profiles than TRNSYS, contributing to better system performance. Although Krischel attributes this difference to the presence of variable extraction in the SST, it should be noted that differences in modelling of storage volume losses between the two programs would affect the relative levels of stratification. The stratified temperature profile of the surrounding ground in the SST model helps maintain stratification and supplies energy to the store during winter months. TRNSYS tank losses were based on a single hourly ambient temperature over the entire tank surface, encouraging destratification of the tank fluid.

4.3 Description of Test Simulations

The comparison of the two simulation programs consisted of six simulations which tested losses and stratification of the SST model and the operation of the collector and load subsystems of each program. These comparisons were necessary to further understanding of the MINSUN program. Although documentation of the MINSUN models was available (Chant, 1985), many details of the program operation were not known. TRNSYS collector and load models were modified as details of MINSUN subsystem calculations became known so that the programs had similar models (e.g., pipe and heat pump models).

Figure 4.1 shows the default system configuration for the MINSUN program which was used in the comparison. (Because an auxiliary energy source was not explicitly modelled, it does not appear in the figure.) A TRNSYS simulation is generally more detailed, and might further include heat exchangers between the storage volume,

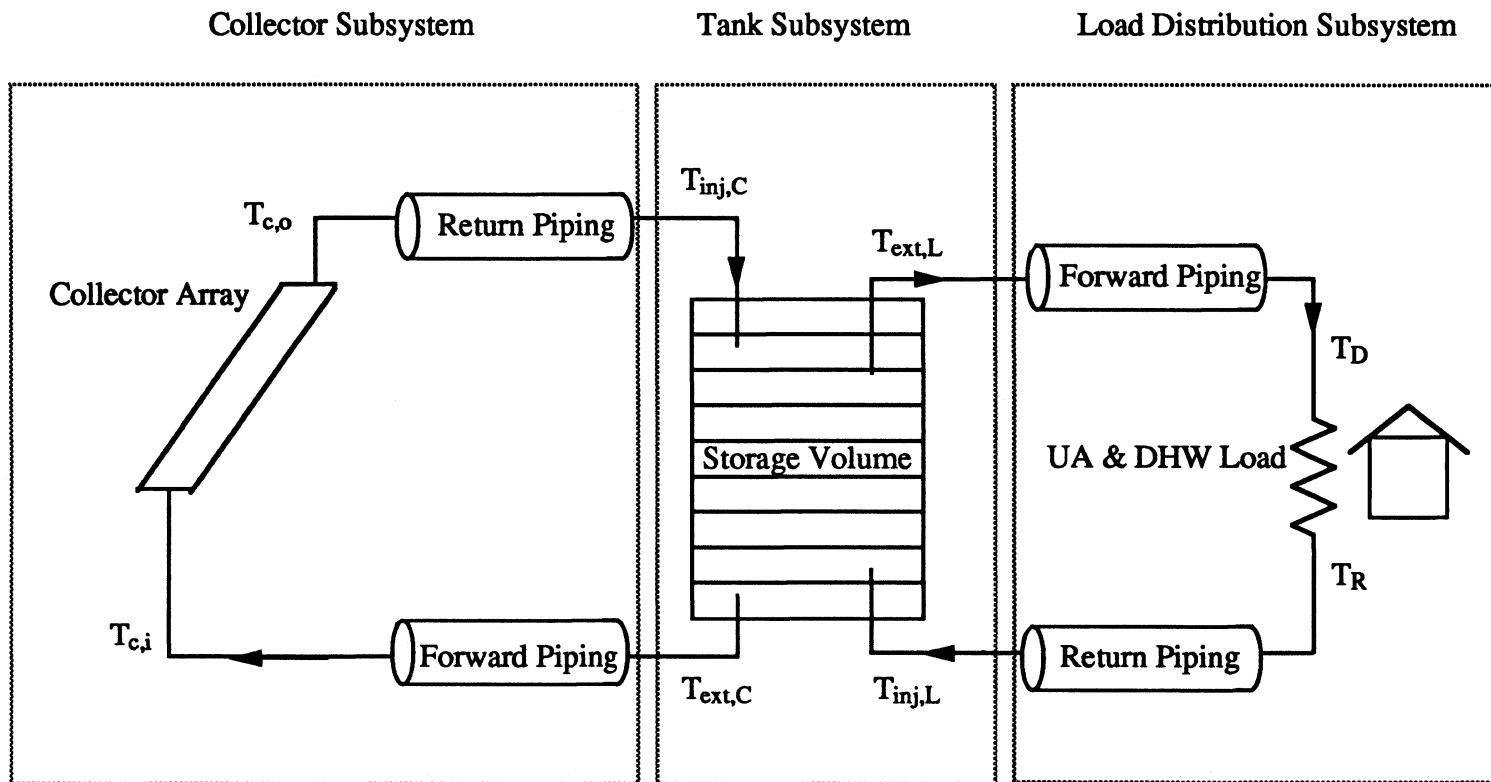


Figure 4.1: Schematic of Agreed Configuration for TRNSYS vs. MINSUN Comparison

buffer tanks, controllers, hydronics, and other components which would add to the reality of a simulation.

Table 4.1 gives a short description of the six test simulations. Copenhagen TMY weather data and a set of parameters which were agreed upon by the author and her collaborator, D. Breger (a U.S. participant in IEA Task VII), were used for each program. The parameters in Appendix F were generally used with changes noted in Table 4.1.

Comparison testing of the SST model were performed in simulations 1.A through 1.B.iii. Losses were compared by giving the SST a constant high temperature with no injection or extraction in simulation 1A. Three aspects of stratification in the SST model with a highly insulated storage volume were next compared in simulations 1.B.i through 1.B.iii: injection of energy, extraction of energy, and both injection and extraction. Testing of the build up of stratification in an initially fully mixed storage volume was accomplished by the injection of constant collector energy at a constant collector outlet temperature with no load present. Stratification resulting from the extraction of a constant load was examined at a constant load return temperature with no injected energy. A comparison of storage volume temperature profiles resulting from simultaneous energy injection and extraction was accomplished with both constant collector and load daily total energies and constant return temperatures.

Table 4.1: Schedule of TRNSYS vs. MINSUN Test Simulations

ID	Test Objective	Method	Results
1.A	Compare losses of SST model	90 °C initial store temperature Infinite store heat capacity	Identical
	Compare stratification of SST with no losses: (insulated store)		
1.B.i	Injection only at constant temperature MINSUN: repeated day TRNSYS: Use MINSUN temperatures and daily energy	90 °C outlet temperature Constant collector (heat source) energy	Identical
1.B.ii	Extraction only at constant temperature MINSUN: repeated day TRNSYS: Use MINSUN temperatures and daily energy	45 °C load return temperature Constant load	Identical
1.B.iii	Constant injection and extraction	Combine two previous simulations	Very slight difference
2	Compare collector subsystem	Various collector inlet (initial store) temps Insulated Store Copenhagen TMY data	Section 4.5
3	Compare load distribution subsystem	90 °C initial store temperature 80 and 60 °C load demand temps Insulated Store	Section 4.5

A repetition of the data for April 15 was chosen for the constant injection and extraction energies test simulations. Because differences were found in the values of useful collected and load energies predicted by MINSUN and TRNSYS, a simple heat source and load source were substituted for use in the TRNSYS simulations for these tests by taking the total MINSUN energies divided into hourly fractions and supplying constant source outlet temperatures. This change served to minimize differences in the collector and load subsystems, allowing observation of differences in the SST model.

Subsystems of each program were tested with the full Copenhagen TMY data in test simulations 2 and 3. Several comparison simulations of the collector subsystem were run using the same initial conditions with the exception of initial store temperatures (ergo several collector inlet temperatures). Similarly, several comparison simulations of the load distribution subsystems were run with the same initial storage volume temperatures and load return temperatures while changing the load demand temperatures. Descriptions of the subsystems in each program are presented in Section 4.5 along with the results of the subsystem comparison simulations.

4.4 Results of SST Test Simulations

The basis of comparison for results of SST test simulations (1.A through 1.B.iii of Table 4.1) consisted both of monthly integrated energies and storage volume profiles on the last day of the month. It was found that the performance of TRNSYS and MINSUN SST models were nearly identical when the model was driven with the same energy

flows. The compared monthly values of storage volume losses for test simulation 1A were identical. Likewise, the end of month storage volume temperature profiles were identical for the warm-up and cool-down stratification comparisons of test simulations 1.B.i and 1.B.ii. A slight difference in storage node temperatures, ranging from 0 to 0.2 °C, was observed after 15 days of simulation when heat source injection and load source extraction were combined. (The period of comparison was relatively short because the store quickly became uniformly hot with the chosen parameters.)

The difference in profiles for test simulation 1.B.iii is attributed to differences in the design of the two codes as to when ground losses are calculated relative to when the daily collector and load accumulated volumes are injected into the store, as outlined in Table 4.2. Ground losses are updated twice during the MINSUN SST daily timestep, once after the collector flowstream is injected into the store and again after the load flowstream is injected.

Table 4.2: TRNSYS vs. MINSUN SST Design of Daily Updates

TRNSYS SST (with Buffers)	MINSUN SST
Hourly: Inject Return Flow into Buffers "Extract" Forward Flow Daily: Inject Buffers into Store Update Losses to Ground	Daily: Inject from Collector Update Losses to Ground Extract to Load Update Losses to Ground
Temperature of Extraction Nodes - remain constant over 24 hours, except if buffer becomes filled - are not affected by losses	Temperature of Extraction Nodes - are affected by losses

The MINSUN loss strategy becomes important in understanding the program's load distribution subsystem. Because MINSUN uses the storage volume profile at the beginning of the daily timestep in the calculation of load flowrates, there is often a slight difference between the amount of energy extracted from the store to meet the load and the load itself. This difference then is shown as load auxiliary energy. The TRNSYS SST avoids this error by satisfying the collector and load extraction requirements on an hourly basis before updating losses for the 24 hour period.

4.5 Results of Subsystem Test Simulations

In this section, descriptions of the subsystems in each program are presented, along with mostly qualitative results of the subsystem comparison simulations. These simulations were integral to the understanding of MINSUN subsystem calculations and control strategies. The use of the same parameters as in the Lyckebo comparison simulation served to exaggerate absolute differences found between the two programs, which became more subtle with the smaller system studied in Section 4.7.

It was found through the subsystem test simulations that a fundamental difference in the structure of the MINSUN and TRNSYS computer programs is the ease with which calculations may be followed. Component subroutines in TRNSYS are modular, independent programs linked by a main program. The control strategies of TRNSYS components are either self-contained or directed by other component subroutines. Unlike MINSUN, TRNSYS may require iteration between component subroutines during a timestep to converge calculations. The MINSUN main program participates in

component calculations, sometimes placing calculation criterion before calling subroutines. The main program may change units or groupings of values entered into the MINSUN parameter listing before passing them. Because its program hierarchy is complex, understanding the structure of the MINSUN program subsystems turned out to be a matter of deduction.

4.5.1 Collector Subsystems

The TRNSYS Type 1 collector model used in this investigation determines collected useful energy on a hourly basis, with the presence of flow through the subsystem determined by an on/off temperature-based differential controller. The operational strategy for the constant temperature outlet collector used in these simulations is outlined in Table 4.3. The user may specify either the same or different values for the minimum temperature at which the controller turns on the collector and the desired outlet temperature. Parameters were chosen for performance similar to that of the Lyckebo system (Section 3.1). Values of 60 °C controller turn-on and 90 °C desired outlet temperature were used in test simulation 2 and the Lyckebo comparison simulation. A stagnation temperature of 60 °C therefore triggers the collector to turn on, but the outlet temperature would fall below this value in the presence of flow, turning the collector off until the "on" outlet temperature is above this value. As insolation increases, an outlet temperature of 90 °C is obtained by varying the collector flowrate between specified minimum and maximum values. If the collector turn-on and desired outlet temperatures are specified as the same value, then, for high values (e.g. 90 °C), early morning and late evening hours may not be included in the total daily useful collected energy.

Table 4.3: TRNSYS Collector Strategy for Constant Temperature Outlet

User specifies: desired outlet temperature, T_o
 minimum and maximum collector flowrate
 minimum acceptable T_o at minimum flowrate

Hourly calculations: $Q_u = A_C F_R [S - U_L (T_i - T_a)]$

- 1) Controller turns on collector if stagnation temperature is \geq minimum acceptable T_o .
- 2) Find Q_u and multiply by array factor.
- 3) Find T_o given T_i
- 4) If T_o is not same as desired, estimate new flowrate from

$$Q_u = \dot{m} C_p (T_o - T_i) .$$

- 5) Find new Q_u and iterate new flowrate between minimum and maximum until either desired T_o or T_o at minimum flowrate is reached.
 - 6) Controller turns collector off if T_o at minimum flowrate falls below minimum acceptable T_o .
-

Additionally, an array factor (Section 2.3), equal to 0.88 for test simulation 2 and the Lyckebo simulation, is multiplied to the value of Q_u before the outlet temperature is determined.

The MINSUN program determines useful collected energy on a daily basis, with the assumption that the collector is in operation for all hours with horizontal radiation I_H greater than 50 kJ/hr-m^2 . The program first determines total daily useful energy from hourly values based on a given set of collector inlet temperatures (typically 10, 30, 50, 70 and 90°C). It then constructs a table of the useful energy collected and number of hours of operation versus the set of collector inlet temperatures for each day of the simulation. Table 4.4 shows the Q_u vs. T_i table with an example of the type of output from the MINSUN radiation pre-processing routine "UMSORT". (This output was actually generated using TRNSYS.) This table can then be used in a number of subsequent simulations for the same location. Values of useful energy are multiplied by the specified array factor before their entry onto the table.

The MINSUN strategy for interpolation of the UMSORT Q_u vs. T_i table is outlined in Table 4.5. Because $F_R U_L$ is held constant in MINSUN, the daily useful energy is a linear function of the collector inlet temperature (for linear efficiency flat plate collectors). The actual collector inlet temperature is known from the storage profile during the simulation. The useful energy and hours of operation for each day are then interpolated from the table between values generated from the given set of collector inlet temperatures. A daily collector flowrate or collector outlet temperature can then be calculated, since Q_u and T_i are known. The normal (minimum) collector flowrate is assumed for outlet

Table 4.4: "UMSORT" Example Output

Collector Inlet:	10 °C		30°C		50 °C		70 °C		90 °C	
DAY	Qu/A (kJ/m2)	HRS	Qu/A	HRS	Qu/A	HRS	Qu/A	HRS	Qu/A(Est.)	HRS
1	6.917E+03	12	4.073E+03	9	1.974E+03	5	1.237E+03	2	0.E+00	0
2	8.826E+03	12	5.813E+03	9	3.479E+03	8	1.656E+03	5	3.E+02	2
3	1.706E+03	10	1.083E+02	2	0.000E+00	0	0.000E+00	0	0.E+00	0
4	4.181E+03	11	2.252E+03	5	1.226E+03	3	6.795E+02	1	0.E+00	0
5	6.625E+03	12	3.712E+03	8	1.630E+03	6	4.618E+02	2	0.E+00	0
6	5.514E+03	12	2.188E+03	11	7.247E+02	3	3.209E+02	1	0.E+00	0
7	1.203E+04	11	9.125E+03	9	6.719E+03	8	4.417E+03	8	3.E+03	6
8	2.206E+03	11	3.018E+02	2	0.000E+00	0	0.000E+00	0	0.E+00	0
9	1.434E+04	12	1.127E+04	10	8.438E+03	9	5.913E+03	8	3.E+03	5
10	8.153E+03	10	5.698E+03	8	3.896E+03	4	2.958E+03	3	1.E+03	1
.										
.										
.										

Table 4.5: MINSUN Collector Strategy for Constant Temperature Outlet

User specifies: upper and lower limit of collector outlet temperature, T_{Max}
 (T_{Max} is also a function of the maximum storage temperature)
 minimum and maximum collector flowrate

Hourly calculations (prior to simulation): $Q_u = A_C F_R [S - U_L (T_i - T_a)]$

Build UMSORT table of daily Q_u vs. T_i for one year of data.

- 1) Assume values of T_i (10, 30, 50, 70 and 90 C).
- 2) Assume constant critical radiation value of 50 kJ/hr-m² (no radiation).
- 3) Find hourly Q_u independent of flowrate (assume constant F_R).
- 4) Sum hourly Q_u for each day.

Daily calculations (during simulation):

- 1) Given T_i , value of daily Q_u is interpolated from table for each day.
- 2) Find T_o at minimum flowrate.
- 3) If $T_o > T_{Max}$, find new flowrate at $T_o = T_{Max}$ from

$$Q_u = \dot{m} C_p (T_o - T_i) .$$

- 4) Any T_o at minimum flowrate is accepted.

Above method predicts higher annual Q_u than TRNSYS:

Collector dynamics and stagnation temperature are not considered:

- Actual T_o may fall below resultant T_o , even at minimum MINSUN flowrate.
- Morning and evening hours may be erroneously included in daily Q_u .

Interpolation of table modified so independent variable = $(T_i + T_o) / 2$, decreasing Q_u .

temperatures up to the maximum allowable value. If the outlet temperature is above the maximum allowable at the given daily Q_u and minimum flowrate, then a new, higher flowrate is calculated at the maximum allowable collector outlet temperature. Thus, at the minimum flowrate, the daily collector outlet temperature may be very low (e.g., 30°C for test simulation 2) in comparison to the desired outlet temperature (e.g., 90°C) with the criterion that the collectors are operated for all hours where I_H is greater than 50 kJ/m². It was found that the direct interpolation of the UMSORT table overpredicted the daily useful collected energy of existing systems (Breger, 1989). A modification was made to this process by Task VII users where the average of the collector inlet and outlet temperatures $[(T_i + T_o)/2]$ was used as the independent variable for the table interpolation, effectively increasing the amount of collector losses per day.

Table 4.6 shows the assumptions of the MINSUN program collector subsystem and whether they were implemented into the TRNSYS components. MINSUN calculates a single collector flowrate for each day, while the TRNSYS collector flowrate is calculated on an hourly basis. Although the TRNSYS Type 1 model would normally reduce the amount of energy collected when the collector flowrate is not equal to the test flowrate, this feature was overridden for these comparisons since the MINSUN program holds F_{RUL} constant. [A flowrate of 0.005 l/s-m² reduced from a test flowrate of 0.015 l/s-m² would yield about a 3% reduction in Q_u with the given collector parameters using the calculation method of Duffie (1980).] The usual correction of F_R for collectors in series is presumably taken into account by the presence of the "array factor". MINSUN produces a single daily outlet temperature, whereas the TRNSYS "constant temperature outlet" collector probably will not yield the same value of T_o for every hour of operation.

Table 4.6: List of MINSUN Collector Subsystem Assumptions

<u>Item</u>	<u>Implemented in TRNSYS models during comparison?</u>
Variable collector flowrate	yes
Single daily flowrate	no
Qu independent of flowrate (constant $F_R U_L$)	yes
Number of collectors in series = 1	yes
Lack of controller based on outlet temperature	no
Single daily outlet temperature	no

Because MINSUN does not use a collector controller, all hours of radiation above 50 kJ/hr-m² will be included in the MINSUN daily total radiation, including hours during which the TRNSYS collectors may not be in operation.

Hourly values of direct normal radiation I_{dn} and horizontal radiation I_H were used in both programs to compute the tilted surface radiation components. The hourly beam radiation on a horizontal surface I_b is found by

$$I_b = I_{dn} \cdot \cos(\theta_z) \quad (4.1)$$

where

$$\theta_z = \text{solar zenith angle}$$

The diffuse radiation is then found by subtraction of I_b from I_H . When direct normal

radiation readings are not available, a diffuse fraction correlation is necessary. The MINSUN program makes use of the Boes diffuse fraction correlation; the correlation, which appears in the UMSORT program, seems somewhat different (i.e., limits on k_T and linear slope) than that published in the literature (Erbs, 1984). The TRNSYS program allows the user to choose from several diffuse fraction correlations.

Appendix D shows an hourly account of Run 2 results of the radiation components calculated by both programs and final total Q_u values for April 15th Copenhagen TMY data. The calculated beam and diffuse tilted surface radiation components are different, resulting in the total daily MINSUN tilted surface radiation I_T slightly greater than TRNSYS (which includes an hour of radiation which is below the MINSUN critical radiation level). This was traced to different methods in computing the solar hour angle (ω , a component of θ_z), where the MINSUN program is 7.5° ahead of TRNSYS. The total daily useful energy collected on this particular day is summarized in Table 4.7. After the array factors and the MINSUN modified interpolation scheme are applied, the MINSUN total daily useful energy becomes less than that of TRNSYS because of an increase in the quantity $F_R U_L (T_i - T_a)$. Because the TRNSYS model accounts for collector operational control, its total daily useful energy is further reduced as hours which cannot produce the minimum collector outlet temperature are excluded. Using the previously specified controller temperatures and a minimum flowrate of 0.001 l/s-m^2 , the total TRNSYS collected energy less collector losses for this day is 16060 kJ/m^2 versus 11638 kJ/m^2 for MINSUN. The relative amounts of collected useful energy for each program will vary over time. Again, it is noted that the number of hours of collector operation may differ for the two programs on any given day.

Table 4.7: Summary of April 15 Total Qu/A (kJ/m²) Calculation Results

	<u>TRNSYS</u>	<u>MINSUN</u>
Daily Qu/A	19333	19511
After interpolation		13226
After array factor	17013	11638
After operational control	16060	

4.5.2 Load Distribution Subsystems

The total system load for the load distribution subsystem depicted in Figure 4.1 consisted of a houseload plus the losses experienced in the forward and return piping. The houseload was made up of a UA load with constant DHW load and internal gain for 550 houses. The DHW load was 22% of the total annual system load.

Simulation testing of the load subsystems showed minor differences between the two computer programs. Table 4.8 lists load distribution system assumptions made by the MINSUN program and whether they were implemented in TRNSYS simulations. The assumption of parallel auxiliary energy mode¹ is used exclusively in MINSUN simulations; the implication that energy is extractable from the store even when the load demand temperature cannot be met may not be appropriate for the Lyckebo system because the boiler supplies energy directly to the Lyckebo cavern as needed, maintaining

¹Parallel auxiliary energy makes up that part of the load which cannot be extracted from a flowstream of capacitance rate $\dot{m}C_p$ and temperature T_i , regardless of system configuration. This is in contrast to series auxiliary energy which supplies the entire load when the flow stream cannot meet the entire load.

high distribution temperatures. The differences in modelling the load subsystems gave MINSUN somewhat lower loads than TRNSYS. The strategy used in MINSUN for load calculations is outlined in Table 4.9 with subsystem temperatures as depicted in Figure 4.1.

Although the same weather data and calculations for house loads were used in the two programs, MINSUN predicts somewhat lower UA loads for warm days during the space heating season. Hours in which the ambient temperature is above the threshold ambient temperature (above which the heating degree days are zero) were still credited with an internal gain, effectively reducing the constant DHW load. Example daily houseload calculations with values produced by TRNSYS and the "UMSORT" program are shown in Appendix E

Table 4.8: List of MINSUN Load Subsystem Assumptions

<u>Item</u>	<u>Implemented in TRNSYS models during comparison?</u>
Parallel Auxiliary Mode	yes
Space heating season	yes
UA Load = 0 for $T_a \geq 10^\circ\text{C}$	yes
Forward pipe inlet temperature is same as outlet	no
Daily variable demand temperature from storage	no

The same pipe model is used in the two programs, yet different values of the losses experienced in the load forward piping are found as a result of different calculation strategies. MINSUN first calculates the forward pipe loss and resultant temperature drop ΔT in the pipe with the assumption that the pipe inlet temperature is equal to the load demand temperature T_D . The load flowrate is determined from the calculated houseload and the specified house model inlet and outlet temperatures. Next, the program determines the storage volume extraction temperature above the demand temperature which is required to meet the pipe losses, equal to $T_D + \Delta T$ of the forward pipe. The same load demand temperature is used at the MINSUN load inlet, ahead of the forward piping. The TRNSYS subsystem produces a straightforward reduction in the temperature of the load flowstream from piping losses and the house load. The inlet temperature of the forward piping is equal to the load extraction temperature in a TRNSYS simulation.

It was necessary to select one of two options in the determination of a TRNSYS load extraction temperature. One choice was to set the TRNSYS extraction temperature to the MINSUN value of $T_D + \Delta T$ (of the forward pipe) for an average day during each heating season, resulting in higher TRNSYS forward pipe losses. A second choice was to set the TRNSYS extraction temperature to the load demand temperature T_D , which gave both programs the same temperature at the inlet of the forward pipe. This choice yielded higher load flowrates in TRNSYS, which, because of the inverse exponential relation of the load flowrate to the temperature drop across the forward pipe length (equation 2.16), had a small effect in increasing the piping temperature drop.

Table 4.9: MINSUN Load Calculations

$$\text{Houseload} = Q_L = [UA(T_s - T_{\text{mod}}) - Q_{\text{gain}}]^* + Q_{\text{DHW}} \quad * \text{ heating season only}$$

1) Determine Load Subsystem flowrate \dot{m}_L based on House Load Q_L and user defined house demand and return temperatures, T_D and T_R .

$$\dot{m}_L = Q_L / C_p (T_D - T_R)$$

2) Determine Forward Pipe Loss Q_{LF} . T_D is used as pipe inlet, not store extraction temperature $T_{\text{ext,L}}$.

$$\Delta T_{o,1} = \Delta T_{i,1} (1 - \exp \{-UA/\dot{m}C_p\})$$

$$\Delta T_{i,1} = T_D - T_\infty$$

$$Q_{LF} = \dot{m}_L C_p \Delta T_{o,1}$$

3) Determine extraction temperature required from store, $T_{\text{ext,L}}$

$$T_{\text{ext,L}} = T_D + \Delta T_{o,1}$$

4) Determine Return Pipe Loss Q_{LR} and temperature returning to store, $T_{\text{inj,L}}$.

$$\Delta T_{o,2} = \Delta T_{i,2} (1 - \exp \{-UA/\dot{m}C_p\})$$

$$\Delta T_{i,2} = T_R - T_\infty$$

$$Q_{L2} = \dot{m}_L C_p \Delta T_{o,2}$$

$$T_{\text{inj,L}} = T_R - \Delta T_{o,2}$$

Single, constant values of load extraction temperatures for the space heating and for the non-space heating seasons were chosen for use in the full TRNSYS simulations; these were set to the load demand temperatures, T_D , of MINSUN. Thus, the temperature delivered to the houseload in TRNSYS simulations is less than T_D by an amount equal to the temperature drop ΔT across the forward piping.

Simulations for test 3 were run with both 80 and 60 °C load demand temperatures. The MINSUN storage volume extraction temperature varied from 81 to 85 °C for $T_D = 80$ °C. Although both programs used a value of 80 °C as the inlet temperature of the forward piping, the TRNSYS forward pipe losses were somewhat higher. Differences in forward pipe losses between the two programs lessened with the lower load demand temperature. Since the forward piping losses are approximately 5% of the total load (more when there is no space heating), the impact of the differences in pipe losses for the two programs tends to be minor.

4.6 MINSUN and TRNSYS Results for Lyckebo Simulation

A full simulation of the Lyckebo CSHPSS system was performed. The TRNSYS deck used in this simulation appears in Appendix F. The parameters listed in Appendix F are nearly identical to those used in the MINSUN simulation of Lyckebo.

Results of this simulation are not comparable with the simulations of Chapter 3 which used Lyckebo operational data. Dissimilarities between the two simulations

include a generated, cylindrical storage volume for this study rather than a toroidal storage volume, 10 storage volume nodes rather than 60, and a comparison simulation heat source consisting of the Lyckebo theoretical value of 28,800 m² of collectors. The actual Lyckebo system uses an electric boiler and 15% of the above collector area. The presence of the thermosiphon system in the Lyckebo cavern further precludes a comparison between the actual and simulated systems.

The MINSUN simulation of the Lyckebo plant from which these parameters were taken (Wallentun, 1987) was an economic optimization, based on 1986 energy prices in Sweden. The simulation was part of planning for expansion of the collector area. The collector area of 28,800 m² used in the simulations produces a 100% solar energy fraction for the system. Building a CSHPSS plant to supply 100% of the predicted energy needs for all years is very expensive, as it must be designed to accommodate years of low insolation or high heating loads. The study found a solar energy fraction of 80 - 85% to be optimal, which would reduce the necessary collector area to 25,000 m².

The differences found between the results for the TRNSYS and MINSUN Lyckebo simulations are consistent with the differences in each program's models and calculation strategies found in the test simulations. A comparison of the average storage volume temperatures on the last day of the month for the 1 year simulation (Figure 4.2) shows that TRNSYS predicts warmer temperatures throughout the annual cycle. These temperatures ensue from the larger values of useful collected energy (Q_u) in the TRNSYS simulation (Figure 4.3a). The differences in Q_u diminish after the fifth month of simulation as the TRNSYS collector losses increase with increasing storage volume temperatures. Storage volume losses (Figure 4.3b) are generally greater for the

TRNSYS simulation. Although the same pipe and house load models were employed in the two programs, small differences in the total system loads (Figure 4.3c) are seen as a result of the manner in which the pipe loss and UA load calculations were performed (Section 4.5.2). The auxiliary energy required by each simulation is shown in Figure 4.3d. The annual auxiliary energy requirement was found to be 4.4 TJ for the MINSUN simulation and 1.4 TJ for the TRNSYS simulation.

The differing values of useful collected energy for the two systems is mostly a result of two factors: the daily (modified) interpolation scheme of MINSUN and operational control of TRNSYS collectors. The first of these factors seems to have a greater role in the observed differences than the second and was an intentional adjustment based on experience and observation rather than having a theoretical basis. Therefore, the determination of which program is "more correct" is rather subjective.

The full TRNSYS simulation required 5:00 minutes of CPU time on a MicroVAX II computer. Because the MINSUN program pre-processes hourly data in the calculation of both daily useful collected energy and daily system loads, the CPU time of 8 seconds on a VAX 8600 reflects only the time necessary to make storage volume calculations for 365 daily timesteps. (The VAX 8600 is ca. 5 times faster than the MicroVax II computer.)

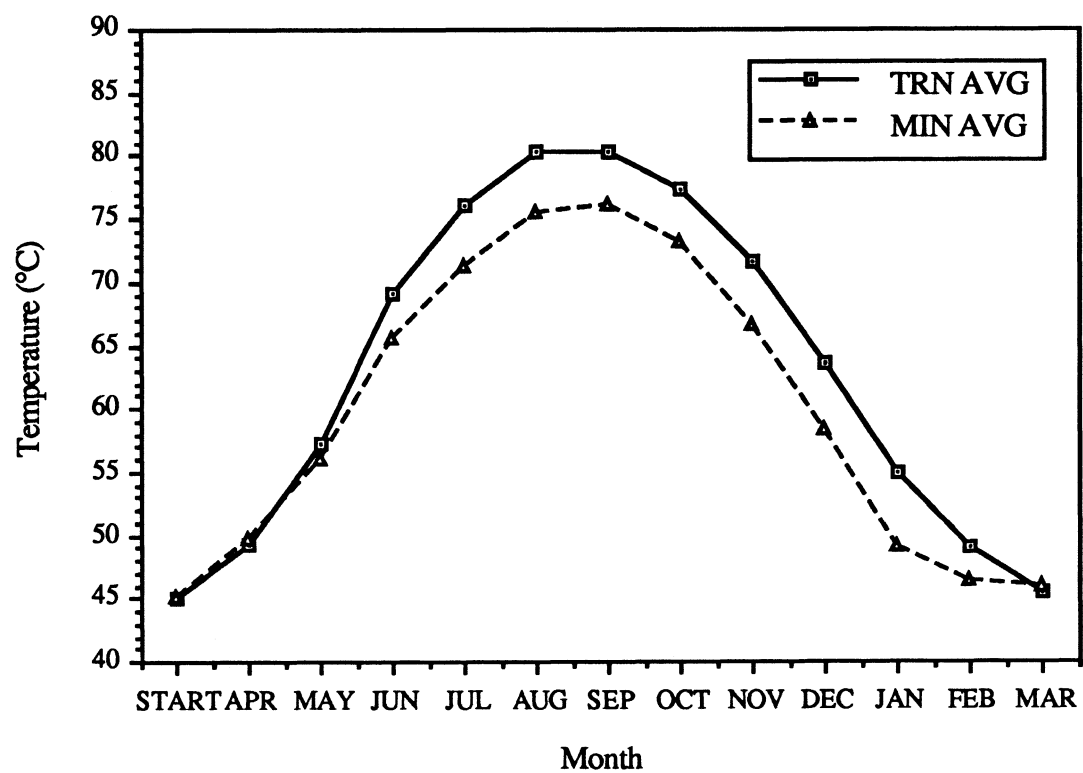


Figure 4.2: Comparison of Lyckebo Cavern Average Storage Temperatures
on Last Day of Month

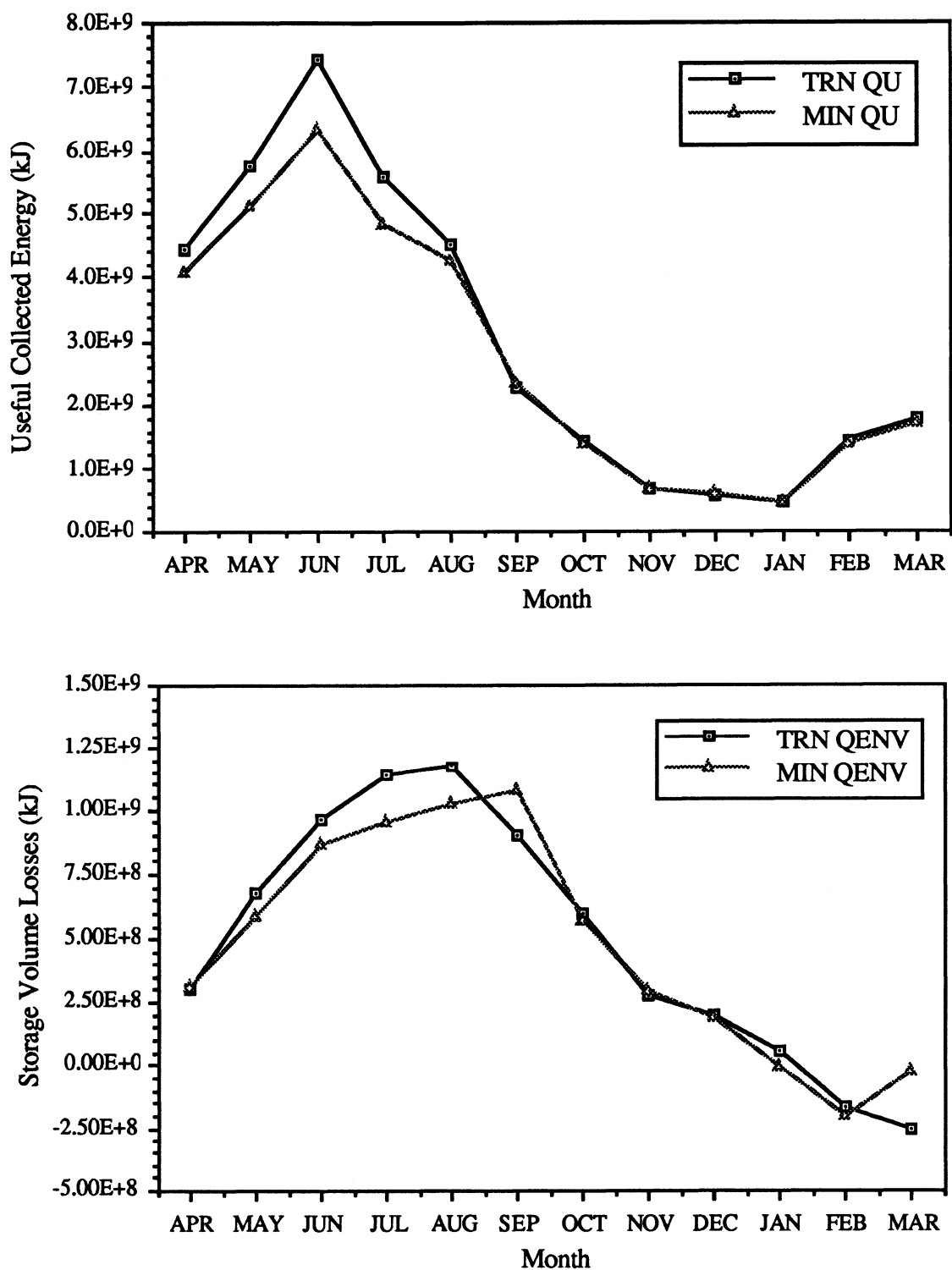


Figure 4.3 a,b: Comparison of Useful Collected and Storage Volume Loss Energies

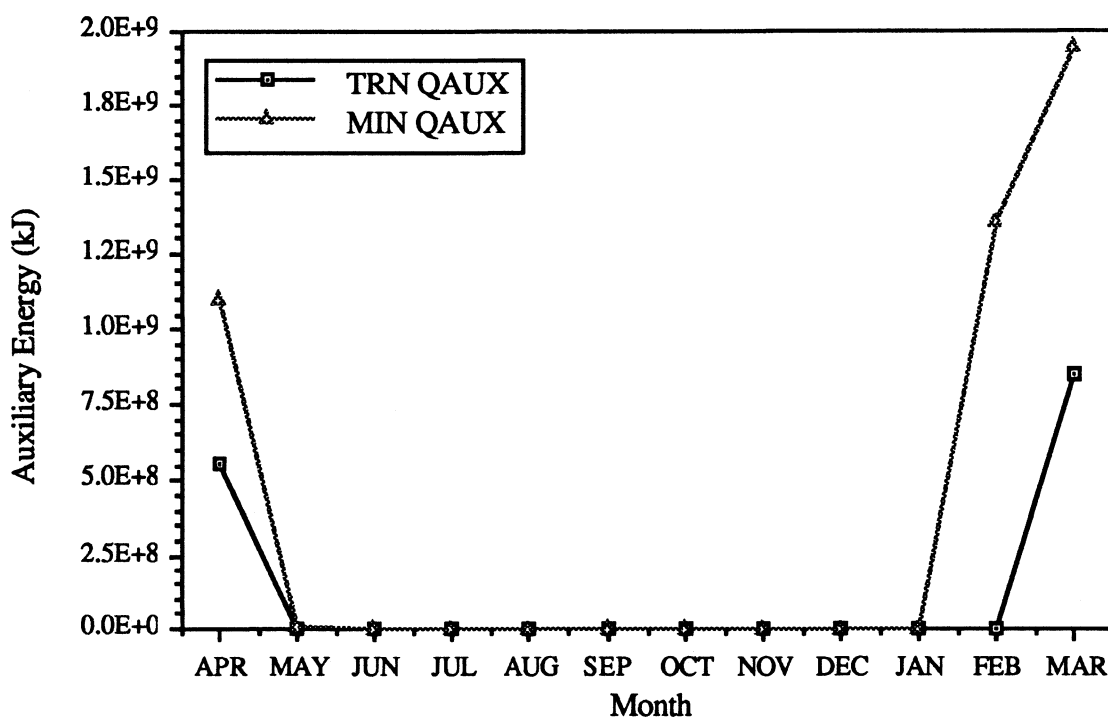
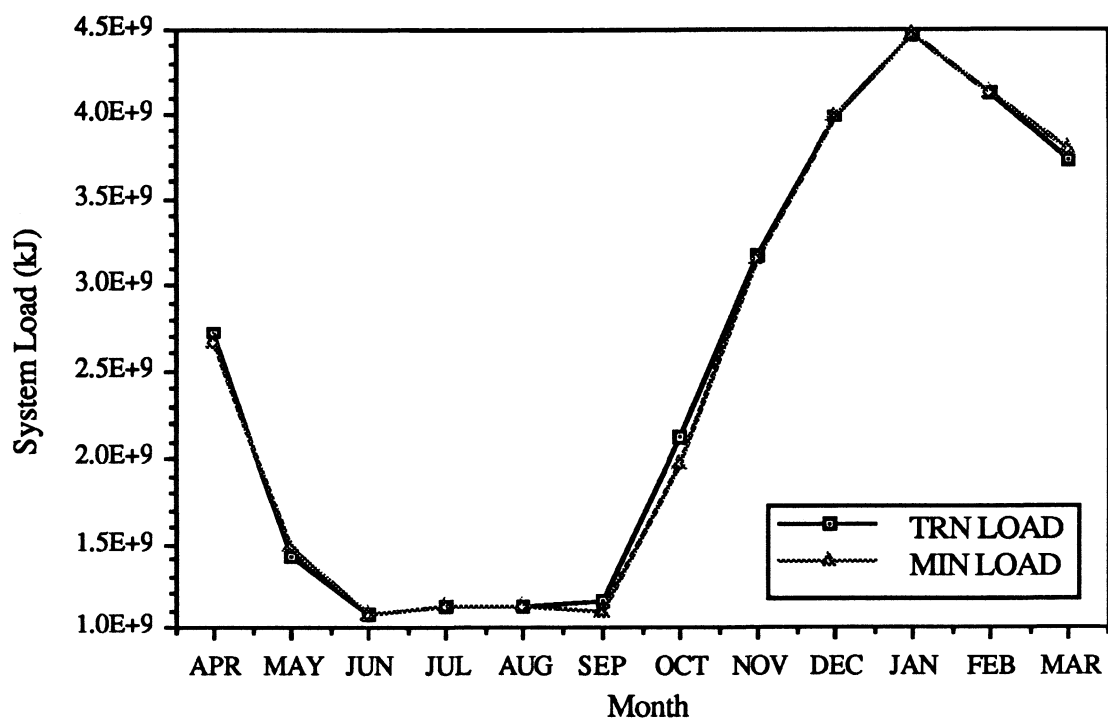


Figure 4.3 c,d: Comparison of Load and Auxiliary Energies

4.7 MINSUN and TRNSYS Results of Franklin System Simulation

A full simulation of the proposed CSHPSS system at the Tri-County Regional Vocational Technical School in Franklin, Massachusetts was performed. This is a much smaller system than Lyckebo, with an insulated "pit" storage volume of 15,000 m³ and collector area of 3500 m². The TRNSYS deck used in this simulation appears in Appendix G.

The MINSUN simulation from which these parameters were taken (Breger, 1988) was a site design study in which the storage volume and collector area were determined by optimization of both solar energy cost and solar fraction. The range of collector areas and storage volumes investigated were 1000 to 5000 m² and 5000 to 30,000 m³. The study found that at the minimum unit solar energy costs an optimal value solar fraction value equal to 0.77 was determined, where the energy taken from the store is supplied both to a heat pump and directly to the load.

Figure 4.4 shows the default MINSUN configuration of a heat pump system which was used in the comparison simulation. (An auxiliary energy source, used when neither the store or heat pump can meet the load, was not explicitly modelled and is not shown). The heat pump is bypassed when the storage volume is warm enough to supply the load directly. Otherwise, the load loop is separate from the store (Figure 2.9) with water entering the heat pump condenser at the outlet temperature of the return pipe and leaving the condenser either at the load demand temperature T_D (TRNSYS) or slightly warmer at $T_D + \Delta T$ of the forward pipe (MINSUN). (As in Section 4.5.2, the TRNSYS load model delivers $T_D - \Delta T$ to the load.)

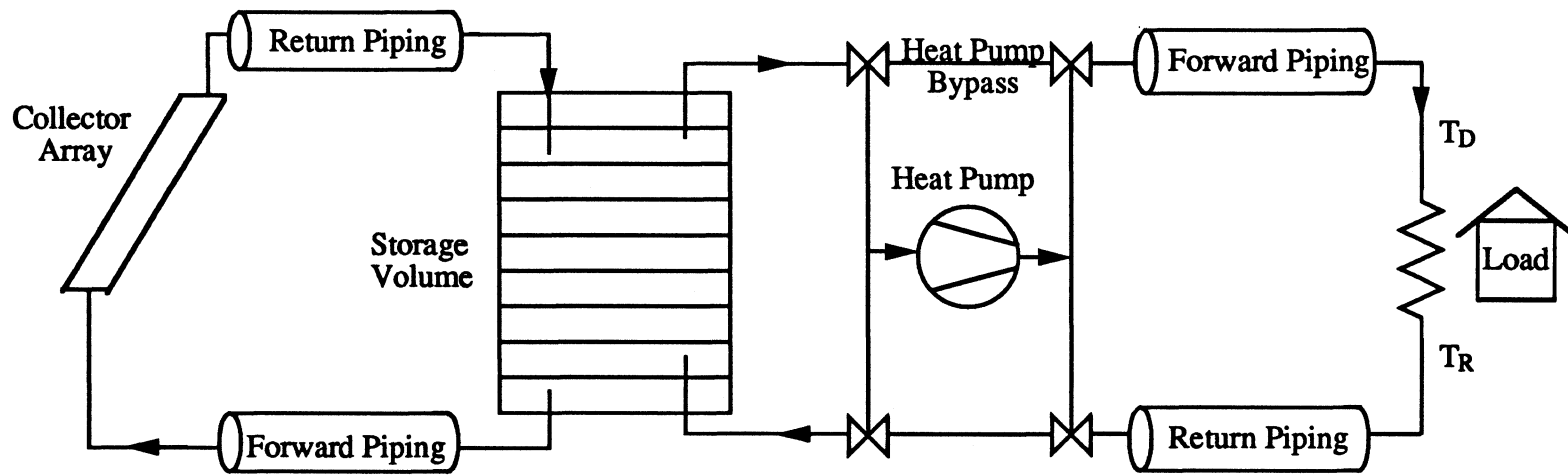


Figure 4.4: Schematic of Configuration for Franklin School Comparison

The strategy employed for the operation of the heat pump differed somewhat between the two programs. The specified constant flowrate through the evaporator over 24 hours required a volume greater than that contained in one of the 10 storage volume nodes. In MINSUN, the two nodes which are used to meet the total daily flow are that with the lowest utilizable temperature and the node directly above it. The program changes the temperatures of these two storage volume nodes to an average temperature before supplying energy to the evaporator. When the TRNSYS hourly timestep is used, the flowrate is satisfied with the volume contained in one node and, therefore, no temperature averaging is done.

The TRNSYS SST model used in this simulation did not make use of the 24 hour buffers due to the strategies employed in the operation of the collector array and the heat pump. Collectors were operated at a constant flowrate rather than the approximately constant outlet temperature of the Lyckebo simulation. Because the collector outlet temperature ranged from 20 to 90 °C, the effect of temperature averaging within a collector buffer was undesirable. Use of the 24 hour buffers would have required the same storage volume node averaging of temperatures found in the operation of the MINSUN heat pump. This averaging would have interfered with the 24 hour "frozen profile" in the storage volume which takes place with buffer use (Section 3.6).

Table 4.10 summarizes the annual energy values and performance parameters for each program. The TRNSYS simulation required more auxiliary energy than MINSUN, with the majority occurring during the last month of the simulation (Figure 4.6c). TRNSYS required less input energy into the heat pump compressor, however, making

the total non-solar energy (auxiliary + compressor) required to meet the load nearly equal for the two simulations. The solar fraction of energy supplied to the load, F , was defined as the remainder of the energy required to meet the load:

$$F = 1 - (Q_{\text{aux}} + Q_{\text{compressor}}) / Q_{\text{Load}} \quad (4.2)$$

Thus, values of solar fraction, are equal for the two programs. An overall heat pump COP (discussed below) was calculated using total annual values of condenser and compressor energies .

Table 4.10: Annual Summaries of Franklin School System Performance

	<u>TRNSYS</u>	<u>MINSUN</u>
Qu	7.22E9	7.16E9
System Load (kJ)	8.37E9	8.25E9
Load Auxiliary Energy (kJ)	0.77E9	0.43E9
Compressor Input Energy (kJ)	1.47E9	1.77E9
Total Non-Solar Energy Consumed (kJ)	2.24E9	2.20E9
Solar Fraction	0.73	0.73
Condenser Energy (kJ)	6.45E9	6.84E9
Overall COP of Heat Pump	4.38	3.86

A comparison of average storage temperatures on last day of each month during the

Franklin School simulations (Figure 4.5) shows the two systems nearly equal, with TRNSYS average temperatures falling below those of MINSUN near the end of the simulation. Monthly system loads (Figure 4.6a) and useful collected energy (Figure 4.6b) were nearly the same for the two programs. As expected, ground losses follow the pattern of storage temperatures (Figure 4.6c). Although storage temperatures were nearly equal for the two programs, the TRNSYS version of the heat pump model obtained a higher overall COP. This is probably a result of the temperature averaging of the MINSUN heat pump, as last day of the month temperature profiles showed TRNSYS profiles with greater temperature extremes.

The TRNSYS simulation bypasses the heat pump more than MINSUN. Figure 4.7a shows the TRNSYS and MINSUN condenser energies along with monthly load values for reference. The energy delivered by the condenser is equal to the system load in the heat pump model except when either the store meets the load directly, or auxiliary energy is necessary. (Auxiliary energies are shown in Figure 4.6d.) Figure 4.7b compares the energy direct from the store to the load. The load is met by the store directly during the entire months of August, September and October and part of November in the TRNSYS simulation. Because the criterion for direct supply is a warmer temperature in MINSUN, the program alternately uses the heat pump and direct store supply of energy to meet the load during the same period. The MINSUN temperature drop in the forward pipe was 8 °C with only a DHW load present; the temperature in the store after collector flowstream injection was therefore required to be at least $T_D + \Delta T$, or 78 °C, for direct store supply.

The performance of the heat pump is described by Figures 4.8 which shows the

monthly compressor energies consumed. Operation is more efficient for the TRNSYS simulation where monthly values of compressor energy are less. An overall heat pump COP (equation 2.21) of 4.38 was found for the TRNSYS simulation, while the MINSUN COP is 3.86. As the storage volume becomes too cool during the late winter months to supply energy to the evaporator at a return temperature above the specified value of 20 °C, the required compressor energy decreases and the load is met by auxiliary energy.

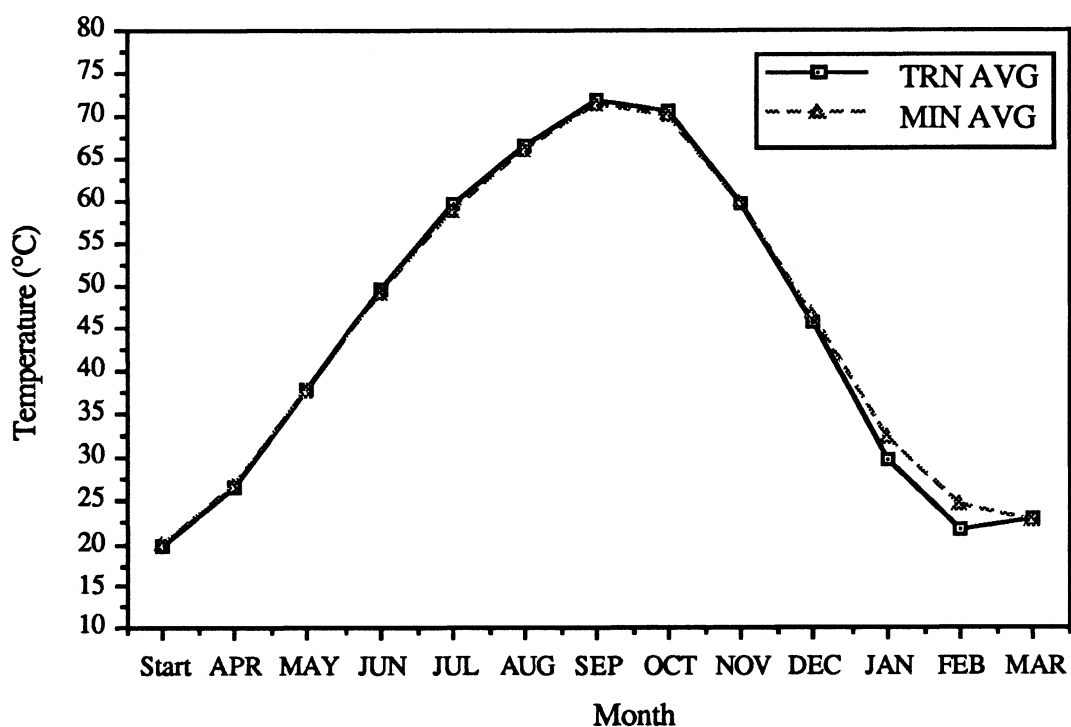


Figure 4.5: Comparison of Franklin School Average Storage Temperatures on Last Day of Month

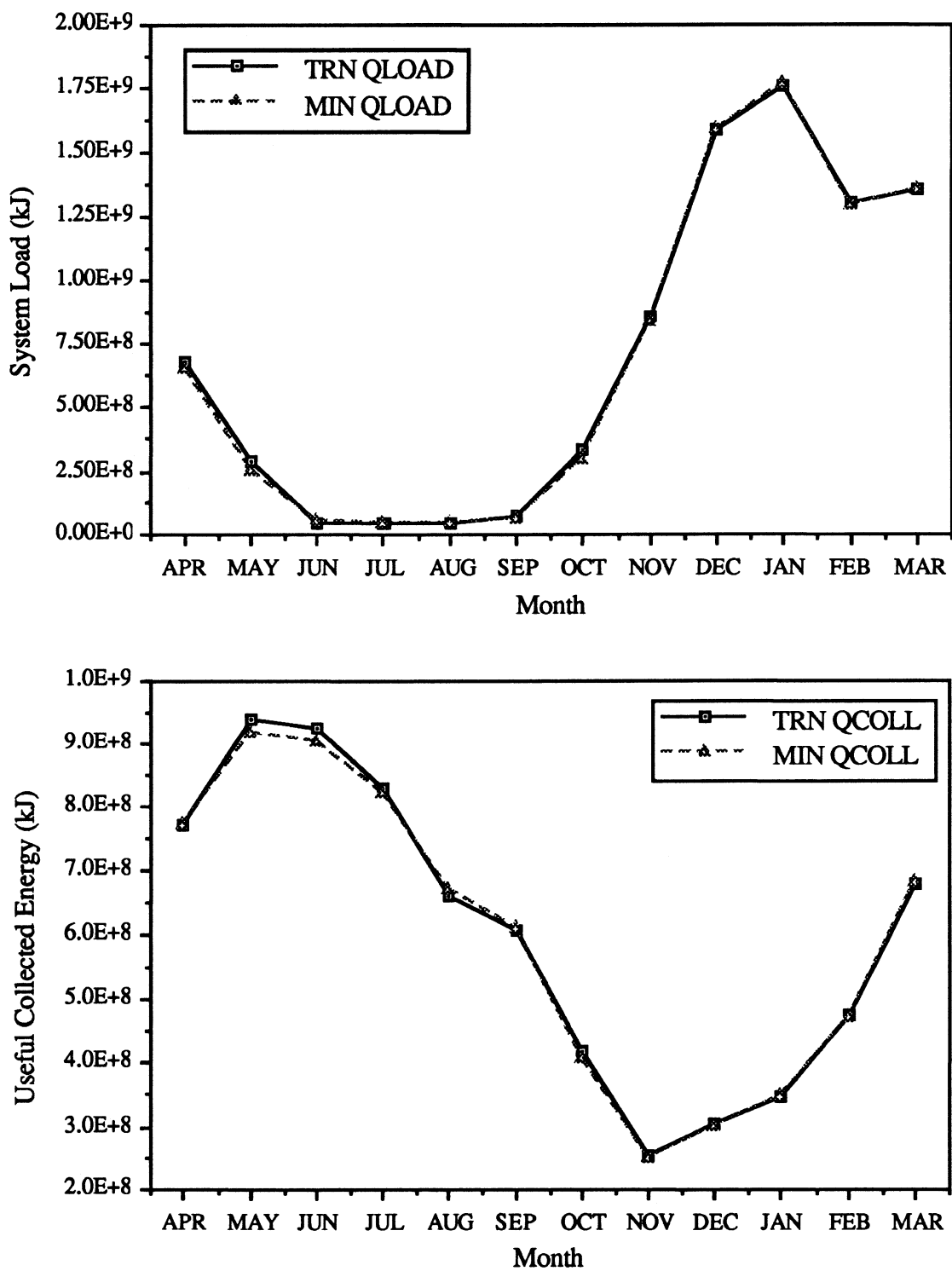


Figure 4.6 a,b: Monthly System Load and Qu for Franklin System

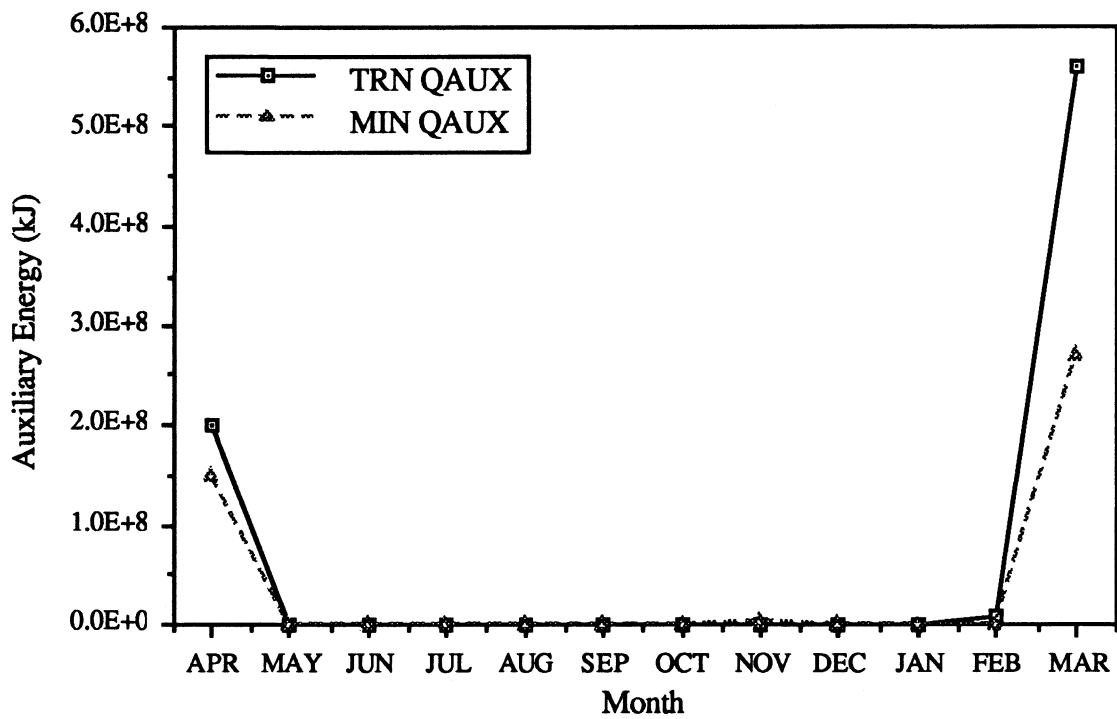
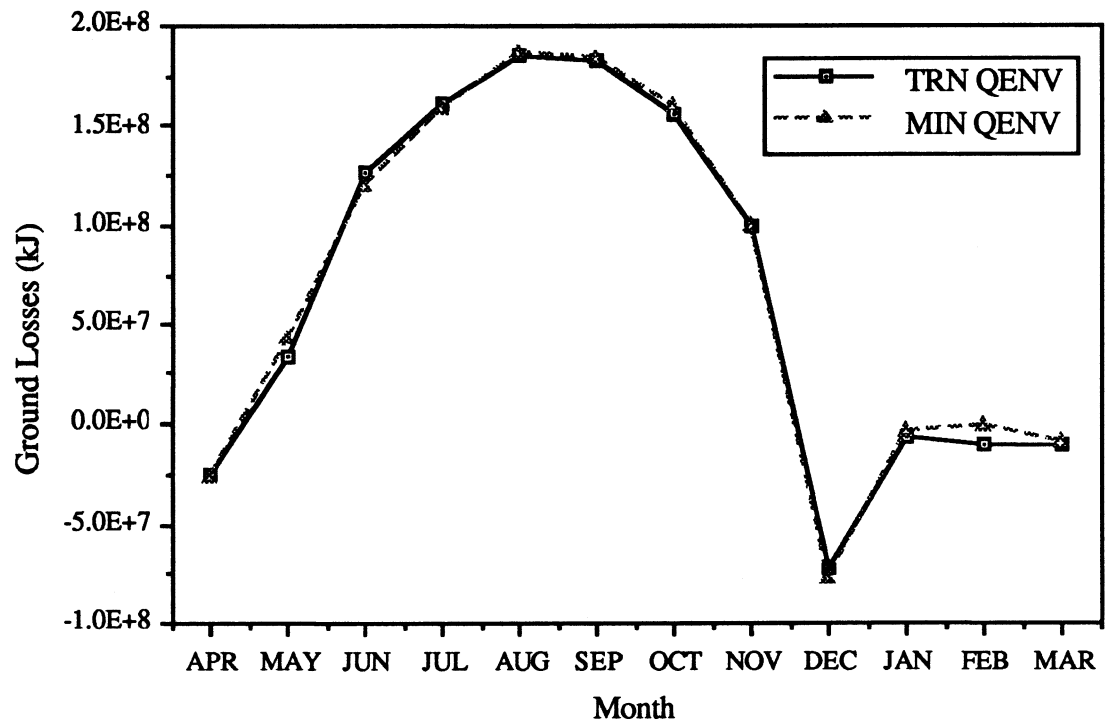


Figure 4.6 c,d: Monthly Ground Losses and Auxiliary Energies for Franklin System

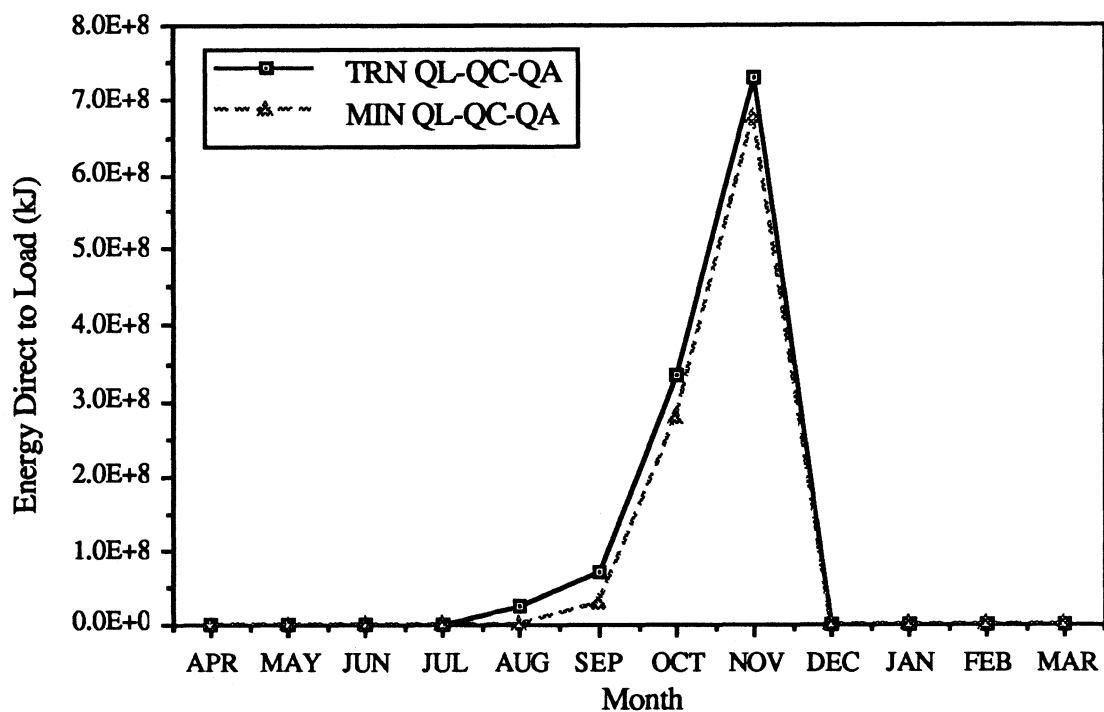
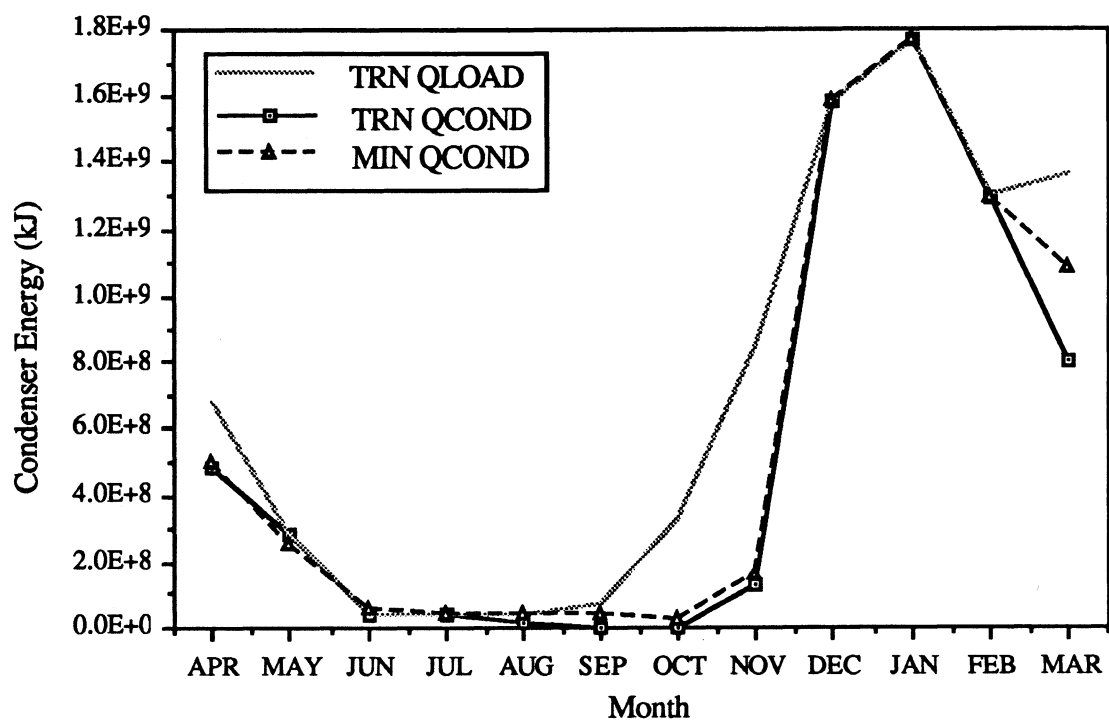


Figure 4.7a,b: Heat Pump Condenser and Direct to Load Energies

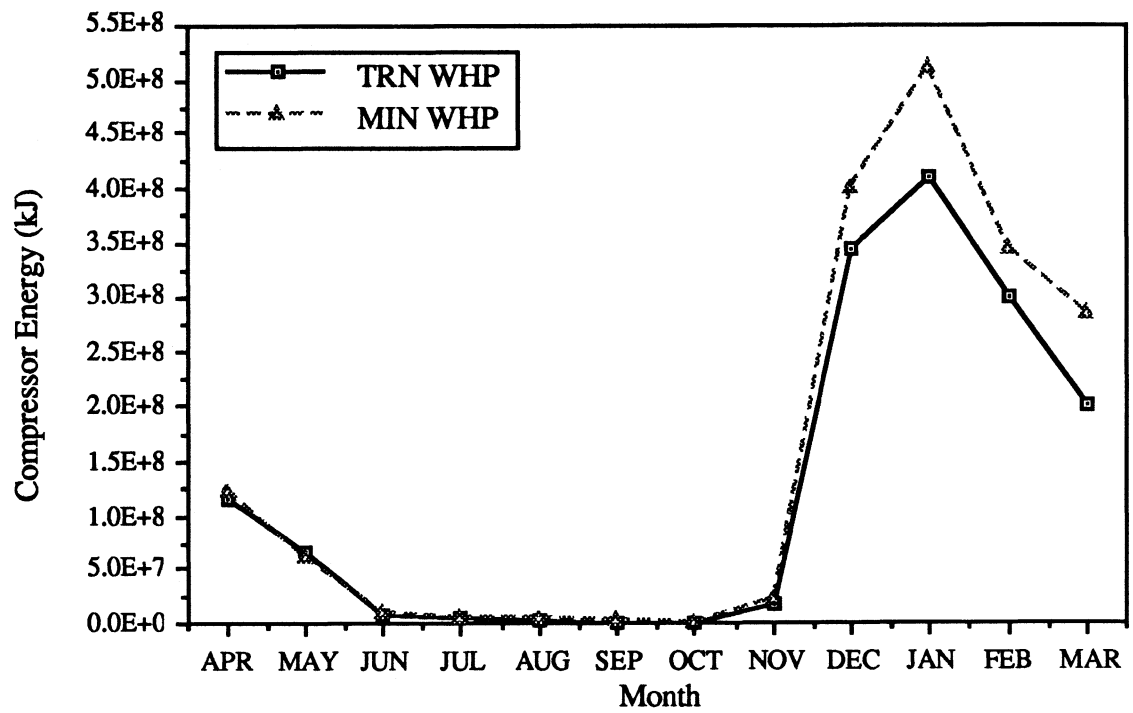


Figure 4.8: Monthly Heat Pump Compressor Energies

Chapter 5

Discussion and Conclusions

This chapter summarizes the results of the simulations performed in this study and gives the findings of the work.

5.1 Validation of the SST Model

Method

The validation simulation of the Lund SST model was subject to the limitations of the Lyckebo operational data and difficulties of the system. Unknown initial conditions were approximated. The performance of model was unchecked for first 3-1/2 years of simulation, from April 1983 to November 1986 because data was unavailable or missing.

Errors in prediction of monthly cavern losses were greatest for periods of high energy injection. These errors can be directly attributed to the presence of the cavern thermosiphon. If these prediction errors are included in the thermosiphon cavern losses for the 1987 simulation year, then the contribution of the thermosiphon to the total annual losses is greater than half. A more sophisticated model of the crack system may not be warranted, as the stability of the size of the crack throughout the simulation is unknown.

Given the difficulties in modelling, monthly heat losses and cavern temperatures were predicted more closely than anticipated. The model generally performed well in following the storage profile temperatures of the actual system.

Shape of Storage Volume Profile: Predicted vs. Actual

When hourly flows are passed through the SST model, the shape of the predicted storage volume temperature profile showed less sharp transitions between the hot and cold layers as activity in the store increased during the annual cycle. Predicted thermosiphon losses increase with average storage temperature, contributing to numerical dispersion at every timestep. It is difficult to quantify the extent of dispersion solely attributable to either of the thermosiphon or SST models. This numerical dispersion is a function of the flow through a given cell volume over time, rather than the size of storage volume or the number of nodes by themselves. Numerical dispersion is problematic in that the decrease in stratification associated with it will affect system performance. However, the performance of the load and collector subsystems was held constant for the validation simulations by use of the Lyckebo data, allowing a fair comparison of the use of buffers and increased number of nodes as solutions to numerical dispersion.

The use of buffers saves some computation time and is warranted only for constant return temperature from both the collector and load. The 24 hour buffer system gives the SST storage volume an effective timestep of one day, similar to that of the MINSUN program. Both of these methods of attaining a daily timestep help alleviate some of the numerical dispersion by increasing the volume injected into the store, but neither provide the minimum dispersion found with use of the full buffer model (i.e., similar to the plug flow model of Figure 2.2). The inaccurate representation of non-constant store inlet

temperatures found with the use of buffers appears to be a poor tradeoff to the observed reduction in numerical dispersion. Savings in the computational time required seems to be an unimportant consideration in the modelling of CSHPSS for two reasons: the savings in CPU time for storage volume calculations are likely small when the time necessary for finite difference calculations in the ground is considered, and accurate modelling of flowstream temperatures, resulting in good predictions of system performance, must take precedence.

Increasing the number of nodes in the storage volume will decrease numerical dispersion. However, 60 nodes for the validation simulation were apparently insufficient to completely alleviate dispersion using Lyckebo data and parameters. The load flowstream of the Lyckebo system required ca. 1.4 days to fill one of the 60 nodes while the collector flowstream required from 0.8 to 2 days. The recommendation which can be drawn from the present studies is to adjust the number of nodes to the expected flowrate over a timestep; the number of storage volume nodes should be chosen such that the volume contained in a storage cell is somewhat greater than the volume injected or extracted over a timestep. A large number of nodes is therefore recommended for use with hourly TRNSYS timesteps.

The importance of the shape of storage profile for prediction of annual losses was shown to be small when subsystem performance was held constant. The affect of storage profile shape (i.e., presence of numerical dispersion) on subsystem performance is beyond the scope of the present study.

Equivalent Conductivity

The equivalent conductivity of rock surrounding Lyckebo cavern is approximately 7 W/m-°C. Predicted monthly losses were lower than measured during periods of high injection again indicating a sensitivity to the presence of the cavern thermosiphon.

Justification of Complexity of Model

The SST model is quite adaptable to suit many different control strategies and shapes of both insulated and non-insulated storage volumes. The concept of variable extraction was introduced; it models the operation and performance of a CSHPSS system more closely than the control methods of previous models. There is some discussion in the literature (Dalenbäck, 1987a) as to whether variable extraction itself has a performance advantage in that the highest temperature water at the top of the store is "saved" and the time at which additional heat must be supplied to the store is postponed. The adaptation of the model into TRNSYS allows the computational simulation of many configurations instead of the specific configurations assumed by MINSUN. The many "custom" options enable the user to isolate effects of particular system design features such as control strategy.

Future CSHPSS systems will probably use less complicated designs than the continuously variable extraction/injection system at Lyckebo for reasons of reliability and first cost (Dalenbäck, 1987a and b). The newer designs may include injection and extraction at several fixed depths. The resultant offset in solar fraction between a few thermostat controlled subsystem-to-storage connections and continuously variable is predicted to be from 0.05 to 0.15 units, depending on the size of the storage volume to

collector area ratio and temperature employed in the load distribution system (Lund, 1987).

5.2 Comparison of TRNSYS and MINSUN

The new TRNSYS version of the Lund-SST model performs identically to that of the MINSUN version when each is driven with the same energy flows. A minor exception is found in the design of the two codes when ground losses are calculated relative to the injection of collector and load accumulated volumes. Because nearly all details of the MINSUN models were incorporated into TRNSYS complete system simulations, it was expected that the two programs gave similar results.

The greatest modelling differences in the two programs were found in the collector subsystem. While program differences in the amount of useful energy collected is dependent on both location and system size, the use of the MINSUN modified interpolation scheme and presence of collector operational control in TRNSYS were indicated as the two major sources of differences in Q_u . These sources of differences in Q_u were better compared by eliminating the usual TRNSYS corrections for F_R and series collectors. Differences in performance of the collector subsystem due to the MINSUN transformation of hourly collector useful energies and temperatures into daily values are not easily quantified.

The TRNSYS load subsystem components were written to perform similarly to those of MINSUN and performed nearly identically. Minor exceptions were found in

setting the house heating load to zero for warm hours during the space heating season and in the temperature found at the inlet of the forward piping.

The incorporation of MINSUN assumptions into the TRNSYS models used in this study were not meant as as theoretical validation or general agreement with those assumptions. The MINSUN method of predicting *daily* values of Q_u and subsystem outlet temperatures may not be justifiable for many CSHPSS systems. Instantaneous values of collector outlet temperatures cannot be accurately represented by a single daily, especially if the collector flowrate is not modulated. Although the Lyckebo CSHPSS system is a good example of where the MINSUN assumptions of constant load inlet and outlet temperatures are valid, this type of control strategy is not universal. Use of the MINSUN daily timestep has indeed greatly reduced the necessary computational time of a simulation, but accuracy and flexibility in the prediction of flowstream temperatures has been sacrificed. Detailed analyses based in reality (i.e., TRNSYS) would allow a better examination of collector components and control strategies. Sources of useful energy reduction could be determined and would be preferable to gross adjustments of Q_u by the array factor and modified Q_u versus T_i interpolation scheme used in MINSUN.

Because TRNSYS has none of the optimization capabilities of MINSUN, it may be beneficial to use the two programs in a complementary manner. MINSUN is useful in the gross selection of the many options available for CSHPSS systems. Once a general system is chosen, the accurate modelling of components (e.g., use of a realistic heat pump model rather than the Carnot heat pump model used in this study) available with TRNSYS is mandated when the extreme cost of seasonal storage systems is considered.

5.3 Future work

Following the probable operational control designs of future pit and cavern seasonal storage systems, another useful feature which could be easily adapted into SST model is fixed extraction and injection at specified depths.

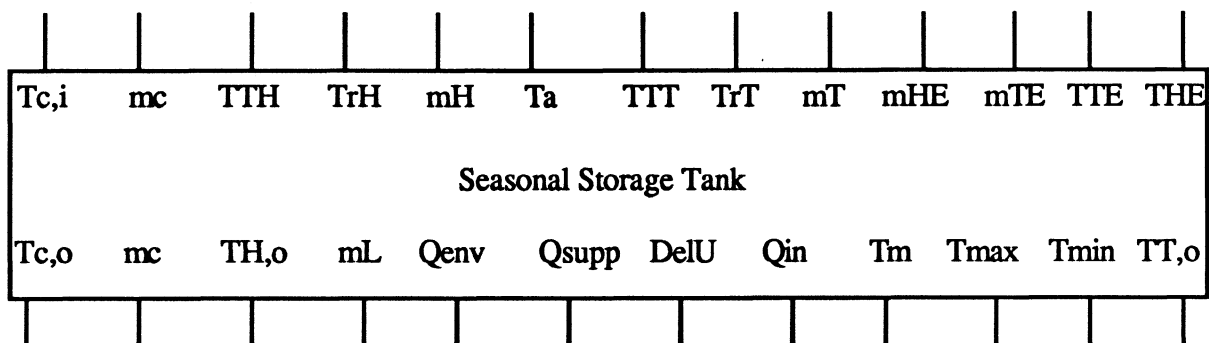
The Lund models for seasonal storage in aquifers (Lund-AST) and ducts (Lund-DST) were made available and are similar in form to the SST model. These and similar models should be reviewed and developed for use in TRNSYS to complete the program's seasonal storage modelling capabilities.

Future studies should include the use of TRNSYS seasonal storage system models for feasibility studies of future U.S. CSHPSS projects. It would also be most interesting to follow the development and monitoring of the proposed Kungälv CSHPSS facility in Sweden, which will have a storage volume of 400,000 m³ and serve 5,000 residences.

Appendix A: Flow Diagram of TRNSYS SST

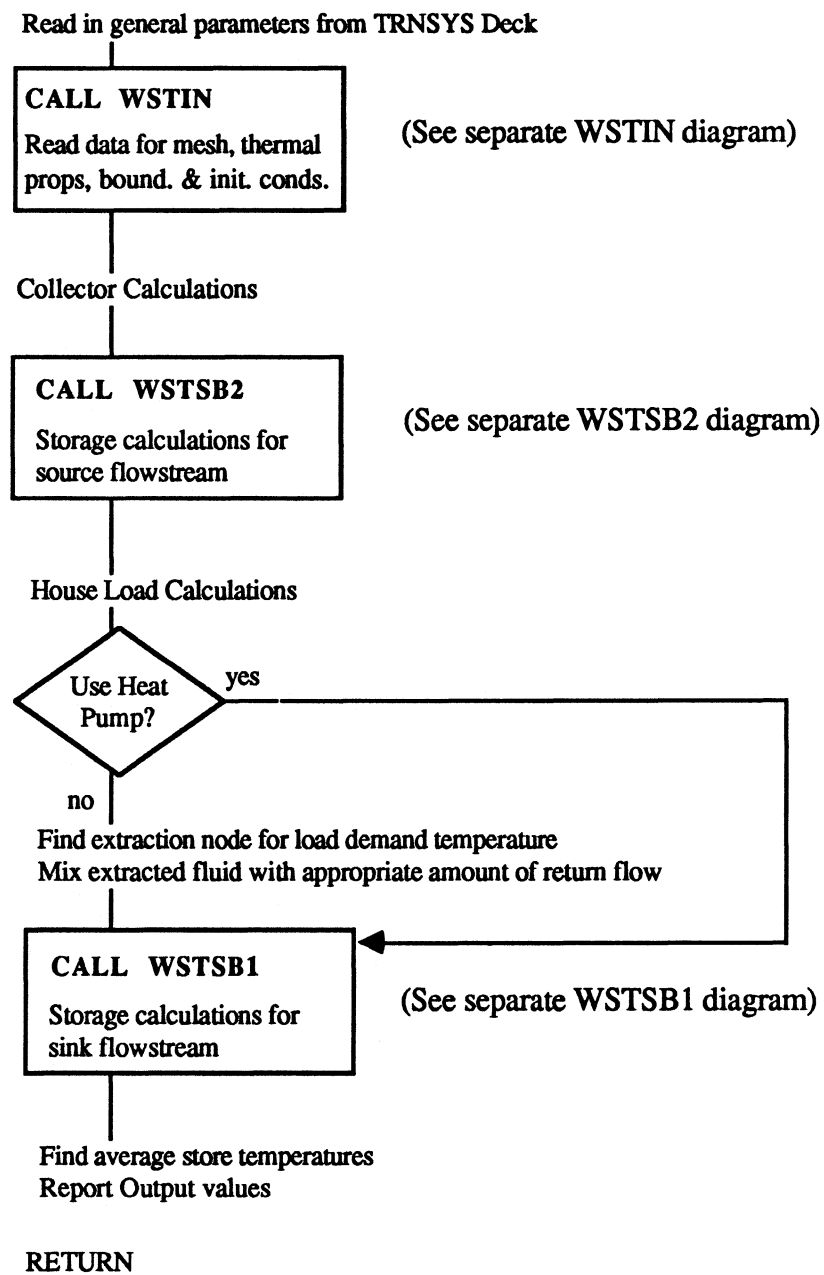
- including schematic of inputs and outputs for TRNSYS components

SST Component Inputs and Outputs

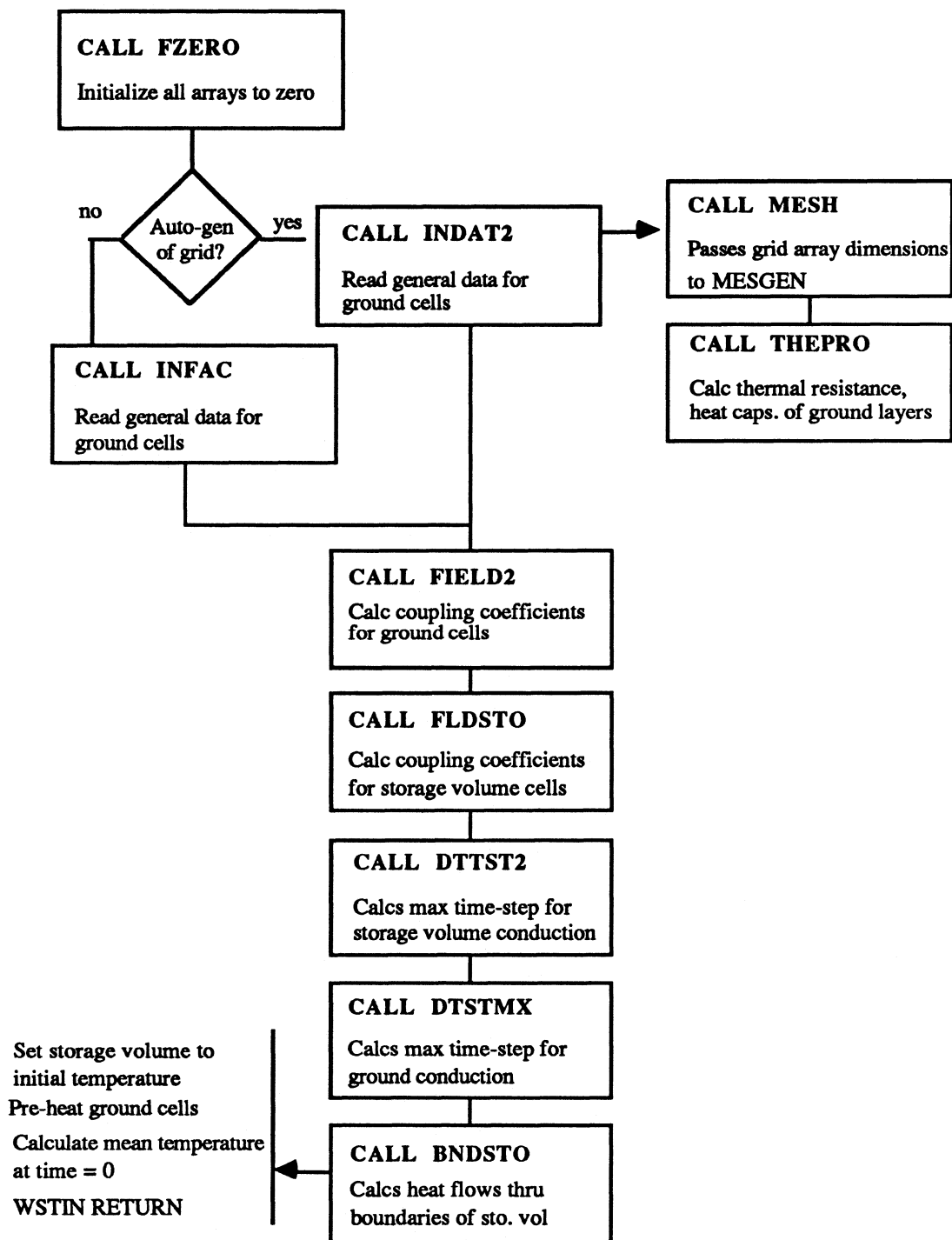


<u>I/O</u>	<u>Symbol</u>	<u>Description</u>
XIN(1)	Tc,i	Temperature of Store Inlet from Heat Source (°C)
XIN(2)	mc	Mass flowrate of Inlet from Heat Source (kg/hr)
XIN(3)	TTH	House Load Demand Temperature (°C)
XIN(4)	TrH	House Load Return Temperature (°C)
XIN(5)	mH	Mass flowrate of House Load Return (kg/hr)
XIN(6)	Ta	Ambient Temperature (°C)
XIN(7)	TTT	Tap Load Demand Temperature (°C)
XIN(8)	TrT	Tap Load Return Temperature (°C)
XIN(9)	mT	Mass flowrate of Tap Load Return (kg/hr)
XIN(10)	mHE	House Load Flowrate thru Heat Pump Evaporator (kg/hr)
XIN(11)	mTE	Tap Load Flowrate thru Heat Pump Evaporator (kg/hr)
XIN(12)	TTE	Temp. of Tap Load thru Heat Pump Evaporator (°C)
XIN(13)	THE	Temp. of House Load thru Heat Pump Evaporator (°C)
OUT(1)	Tc,o	Temperature of Store Outlet to Heat Source (°C)
OUT(2)	mc	Mass flowrate of Outlet to Heat Source (kg/hr)
OUT(3)	TH,o	Extraction Temperature to House Load (°C)
OUT(4)	mL	Flow thru Store (less bypass) (kg/hr)
OUT(5)	mL,tot	Total Flow to Load (kg/hr)
OUT(6)	Qenv	Rate of Ground Losses (kJ/hr)
OUT(7)	Qsupp	Rate of Extracted Energy (kJ/hr)
OUT(8)	DelU	Change in Internal Energy (kJ)
OUT(9)	Qin	Rate of Injected Energy (kJ)
OUT(10)	Tm	Average Temperature of Store (°C)
OUT(11)	Tmax	Maximum Temperature of Store (°C)
OUT(12)	Tmin	Minimum Temperature of Store (°C)
OUT(13)	TT,o	Extraction Temperature to Tap Load (°C)

TRNSYS VERSION OF LUND-SST MODEL



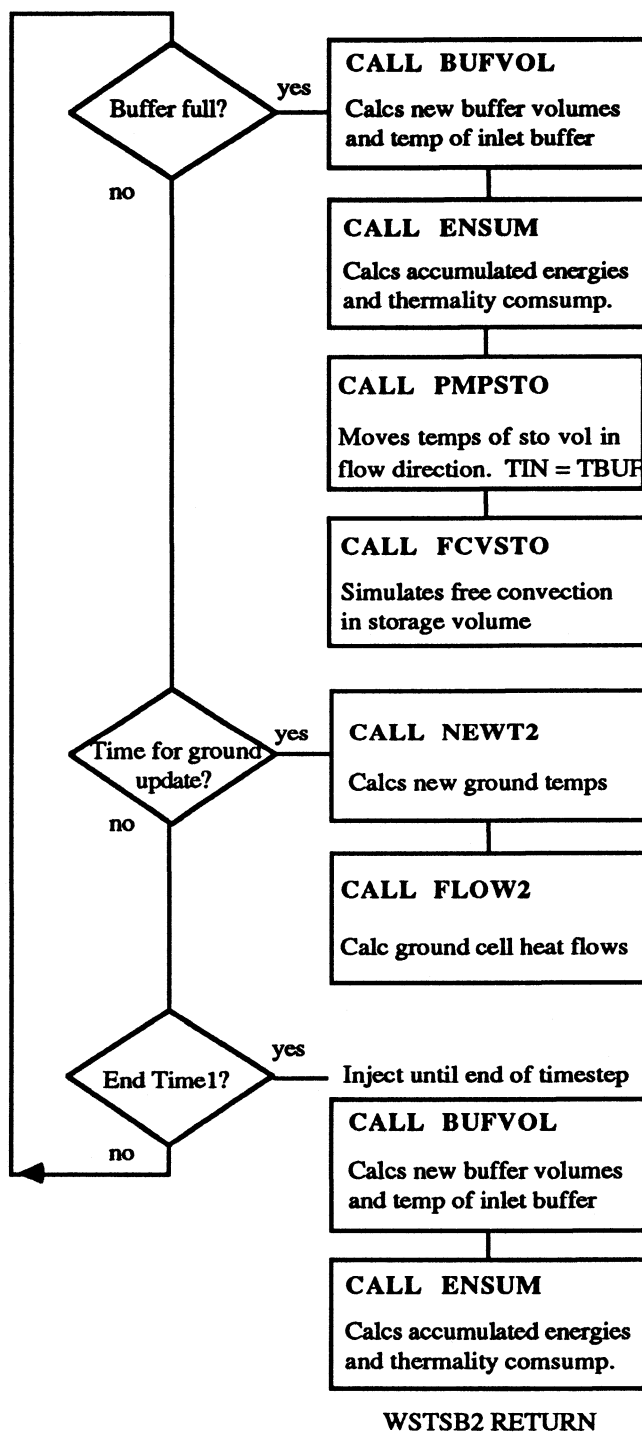
SUBROUTINE WSTIN



SUBROUTINE WSTSB2

Save arrays if first call of timestep

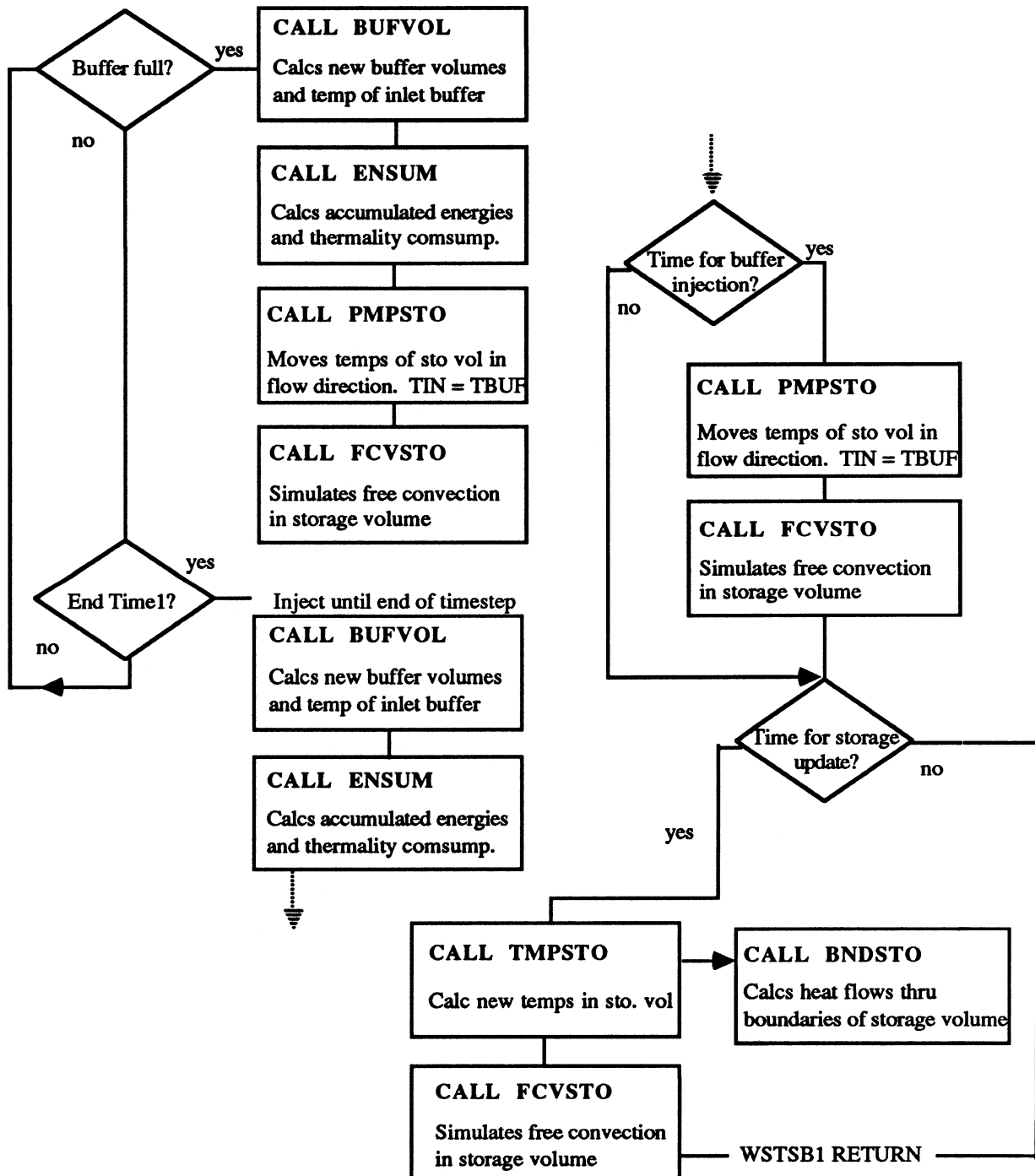
Calc time required for updates = Time1



Subroutine WSTSB1

Save arrays if first call of timestep

Calc time required for updates = Time1



Appendix B Grid Pre-Processor Program

- including new TRNSYS SST subroutine INFAC which acts as an interface between the Pre-Processor and the SST

```
*****
*   GRID PRE-PROCESSOR PROGRAM FOR TRNSYS-SST   *
*   BASED ON LUND UNIVERSITY SST SUBROUTINES   *
*   D. Kozlowski, Solar Energy Laboratory, 17 Jan 89   *
*****
```

```
C*-- Program writes to FORTRAN LUN 20. Subroutine INFAC of SST
C*-- reads LUN 20 and passes variables through COMMON. Run only
C*-- if user-defined grid is needed, if 24 hour buffer or fixed
C*-- extraction is desired, or if changes to LUN 20 are needed.
C*-- The TRNSYS - SST PARAMETERS are superseded by the results of
C*-- this program.
```

```
DIMENSION IMN(20),IMX(20),JMN(20),JMX(20),T(20,30)
DIMENSION RLAM(20,30),CIN(20,30),RISOR(20,30),RISOZ(20,30)
DIMENSION R(20),RM(20),Z(20),ZM(20),ZSTO(101),ZMSTO(101)
DATA IDIM,JDIM,JJDIM/20,30,101/
```

```
96  FORMAT(10I8)
98  FORMAT(10G12.6)
```

```
WRITE(*,*) '***SST*** GIVE DATA FOR BUFFER & EXTRACTION OPTIONS'
WRITE(*,*) 'Give 1 if you want any of these options'
WRITE(*,*) 'Give 0 otherwise; default value = 0'
READ(*,96) I1
WRITE(*,96) I1
IF(I1.EQ.0) GOTO 100
WRITE(*,*) 'Give 1 if you want 24-Hour Buffers'
WRITE(*,*) 'Give 0 otherwise; default value = 0'
READ(*,96) LB24
WRITE(*,96) LB24
WRITE(20,96) LB24
```

```
WRITE(*,*) 'Give 1 if you want fixed extraction; this means '
WRITE(*,*) 'EXTRACT to load from TOP of store (collector side '
WRITE(*,*) 'already fixed at bottom). Also recall the return flow'
WRITE(*,*) 'mixing is assumed in use to meet demand temperature'
WRITE(*,*) 'Give 0 otherwise; default value = 0'
READ(*,96) LTOP
WRITE(*,96) LTOP
WRITE(20,96) LTOP
```

```
WRITE(*,*) 'Give 1 if you want fixed injection; this means INJECT'
WRITE(*,*) 'from collector at TOP of store and from load '
WRITE(*,*) 'at BOTTOM of store '
WRITE(*,*) 'Give 0 otherwise; default value = 0'
READ(*,96) LBOT
WRITE(*,96) LBOT
```

```

WRITE(20,96) LBOT

100 WRITE(*,*) '***SST*** GIVE DATA FOR GRID'
    WRITE(*,*) 'Give 1 if you want automatic mesh generation'
    WRITE(*,*) 'Give 0 otherwise'
    READ(*,96) MAUT
    WRITE(*,96) MAUT
    WRITE(20,96) MAUT
    IF(MAUT.EQ.0) GOTO 99

    WRITE(*,*) 'Give IMAX,JMAX,LCOORD (LCOORD= 2 =radial coordinates)'
    READ(*,96) IMAX,JMAX,LCOORD
    WRITE(*,96) IMAX,JMAX,LCOORD
    WRITE(20,96) IMAX,JMAX,LCOORD

    IMAX1=IMAX+1
    JMAX1=JMAX+1
    IF(IMAX1.LE.IDIM.AND.JMAX1.LE.JDIM) GO TO 47
    WRITE(16,3) IDIM,JDIM
    3 FORMAT(2X,' ***WST*** INPUT ERROR MAX ALLOWED DIMENSIONS ARE',
    *2I3,/, ' ***WST*** INPUT FOR GLOBAL PROBLEM')
    IND=IND+1
47  CONTINUE

    WRITE(*,*) 'Give the number of rectangular subregions'
    READ(*,96) NA
    WRITE(*,96) NA
    WRITE(20,96) NA

    WRITE(*,*) 'Give for each subregion I-MIN,J-MIN,I-MAX,J-MAX (RET)'
    DO 130 IA=1,NA
    READ(*,96) IMN(IA),JMN(IA),IMX(IA),JMX(IA)
    WRITE(*,96) IMN(IA),JMN(IA),IMX(IA),JMX(IA)
130 WRITE(20,96) IMN(IA),JMN(IA),IMX(IA),JMX(IA)

    WRITE(*,*) 'Give the cell-structure for the R-direction (m)'
    CALL COORD(R,RM,L)
    IF(R(2).EQ.0.) R(2)=1.E-10*R(3)
    RM(1)=R(2)
    IF(L.EQ.IMAX) GO TO 30
    WRITE(16,25) L,IMAX
25  FORMAT(1X,2I5,' ***WST*** ERROR IN R - INPUT GLOBAL PROBLEM')
    STOP
30  CONTINUE

    DO 131 I=1,IMAX1

```

```
131 WRITE(20,98) R(I),RM(I)
```

```

WRITE(*,*)' Give the cell-structure for the Z-direction (m)'
CALL COORD(Z,ZM,L)
IF(L.EQ.JMAX) GO TO 400
WRITE(16,35) L,JMAX
35 FORMAT(1X,2I5,' ***WST*** ERROR IN Z - INPUT GLOBAL PROBLEM')
STOP
400 CONTINUE
DO 132 J=1,JMAX1
132 WRITE(20,98) Z(J),ZM(J)

```

```

WRITE(*,*)' Give 1 if you want ground parameters (TSTART,TGRAD,'
WRITE(*,*)' ILAY, RLAML, CL, THL) read from TRNSYS deck '
WRITE(*,*)' Give 0 otherwise'
READ(*,96) IDFLT
WRITE(*,96) IDFLT
WRITE(20,96) IDFLT

```

```
IF(IDFLT.EQ.1)GOTO 55
```

```

WRITE(*,*)' Give the heat conductivities (W/(M*DEG C)) and'
WRITE(*,*)' the heat capacitivities (J/(M3*DEG C)) (REAL,REAL)'
CALL SOIL2(RLAM,CIN,IDIM,JDIM)

```

```

IM1=IDIM/10
M1 = 0
IF(IM1*10 .NE. IDIM) M1=IM1*10 + 1
DO 50 J=1,JDIM
DO 40 L1=1,IM1
40 WRITE(20,98) (RLAM(I,J),I=(L1-1)*10+1,L1*10)

IF(M1 .NE. 0) WRITE(20,98) (RLAM(I,J),I=M1,IDIM)
50 CONTINUE

```

```

DO 51 J=1,JDIM
DO 41 L1=1,IM1
41 WRITE(20,98) (CIN(I,J),I=(L1-1)*10+1,L1*10)

```

```

IF(M1 .NE. 0)WRITE(20,98) (CIN(I,J),I=M1,IDIM)
51 CONTINUE

```

```

WRITE(*,*)' Give the insulations between each pair of cells'
WRITE(*,*)' I-1 and I ((M2*DEG C)/W)'

```

```

CALL INPUT2(RISOR,IDIM,JDIM)
DO 52 J=1,JDIM
DO 42 L1=1,IM1
42 WRITE(20,98) (RISOR(I,J),I=(L1-1)*10+1,L1*10)

IF(M1 .NE. 0) WRITE(20,98) (RISOR(I,J),I=M1,IDIM)
52 CONTINUE

WRITE(*,*)' Give the insulations between each pair of cells'
WRITE(*,*)' J-1 and J ((M2*DEG C)/W)'
CALL INPUT2(RISOZ,IDIM,JDIM)
DO 53 J=1,JDIM
DO 43 L1=1,IM1
43 WRITE(20,98) (RISOZ(I,J),I=(L1-1)*10+1,L1*10)

IF(M1 .NE. 0) WRITE(20,98) (RISOZ(I,J),I=M1,IDIM)
53 CONTINUE

WRITE(*,*)' Give initial ground temperatures including the '
WRITE(*,*)' boundary values (DEG C)'
CALL INPUT2(T,IDIM,JDIM,LQST,LPRT)
DO 54 J=1,JDIM
DO 44 L1=1,IM1
44 WRITE(20,98) (T(I,J),I=(L1-1)*10+1,L1*10)

IF(M1 .NE. 0) WRITE(20,98) (T(I,J),I=M1,IDIM)
54 CONTINUE
WRITE(*,*)' The INFAC subroutine will print out the ground '
WRITE(*,*)' parameters you have entered.'
55 CONTINUE

WRITE(*,*)' ***SST*** GIVE DATA FOR HEAT STORAGE VOLUME'

WRITE(*,*)' Give ISTOMN,JSTMIN,JSTMAX, and the number of '
WRITE(*,*)' radii in the storage volume '
READ(*,96) ISTOMN,JSTMIN,JSTMAX,NR
WRITE(*,96) ISTOMN,JSTMIN,JSTMAX,NR
WRITE(20,96) ISTOMN,JSTMIN,JSTMAX,NR

WRITE(*,*)' Give I,J for each ground cell inside boundary '
WRITE(*,*)' of storage volume which corresponds to lower, outer'
WRITE(*,*)' corner of each radii (RET)'
J2=JSTMIN-1

```

```

DO 70 N=1,NR
J1=J2+1
READ(*,96) I2,J2
WRITE(*,96) I2,J2
WRITE(20,96) I2,J2
70 CONTINUE

IF(J2.NE.JSTMAX) WRITE(*,61) I2,J2,JSTMAX
61 FORMAT(' ***SST*** INPUT ERRORS IN STORAGE VOLUME COORDINATES',
' 318)

WRITE(*,*) ' Give JJMAX'
READ(*,96) JJMAX
WRITE(*,96) JJMAX
WRITE(20,96) JJMAX
IF(JJMAX+1.GT.JJDIM.OR.JJMAX.LT.3) WRITE(*,401) JJDIM
401 FORMAT(2X,' ***SST*** INPUT ERROR. MAX ALLOWED DIMENSION IS',
' 14,' AND SMALLEST ACCEPTED VALUE IS 3')

WRITE(*,*) ' Give the cell-structure for the Z-direction '
WRITE(*,*) ' in the storage volume (m)'
CALL COORD(ZSTO,ZMSTO,L)
JJ2=JJMAX+1
DO 20 JJ=1,JJ2
ZSTO(JJ)=ZSTO(JJ+1)
20 ZMSTO(JJ)=ZMSTO(JJ+1)

ZSTO(JJMAX+1)=Z(JSTMAX+1)
ZMSTO(JJ2)=ZSTO(JJMAX+1)

DO 21 JJ=1,JJ2
21 WRITE(20,98) ZSTO(JJ),ZMSTO(JJ)

IF(L.NE.JJMAX+1) WRITE(*,250) L,JJMAX
250 FORMAT(' ***SST*** ERROR IN ZSTO - INPUT',2I5)

99 WRITE(*,*) 'END INDAT1 PROGRAM'

END

SUBROUTINE COORD(B,BM,L)
INTEGER NA(101)
REAL A(101),B(101),BM(101)

```

```

DO 99 I=1,101
A(I)=0.
B(I)=0.
BM(I)=0.
99  NA(I)=0

```

```

55 FORMAT(G12.6)
56 FORMAT(I8)
57 FORMAT(6(I8,G12.6))

```

```

WRITE(*,*)' Give the position of the first boundary (m)'
READ(*,55) B(2)
WRITE(*,55) B(2)

```

```

WRITE(*,*)' Give the number of size-groups along the axis = "N"'
READ(*,56) NANT
WRITE(*,56) NANT

```

```

WRITE(*,*)' Give for each size-group the number of cells '
WRITE(*,*)' (INTEGER), and the size (m) (REAL W/ DECIMAL POINT)'
WRITE(*,*)' After 6 sets, RETURN; repeat until "N" is reached'
READ(*,57) (NA(I),A(I),I=1,NANT)
WRITE(*,57) (NA(I),A(I),I=1,NANT)

```

```

L=2
DO 10 J=1,NANT
NE=NA(J)
DO 5 I=1,NE
L=L+1
B(L)=B(L-1)+A(J)
BM(L-1)=(B(L)+B(L-1))/2.
5 CONTINUE
10 CONTINUE

```

```

B(1)=B(2)
BM(1)=B(1)
BM(L)=B(L)
L=L-1
RETURN
END

```

```

SUBROUTINE SOIL2(A1,A2,IDIM,JDIM)
DIMENSION A1(IDIM,JDIM),A2(IDIM,JDIM)

```

```

55 FORMAT(2G12.6)
56 FORMAT(I8)

```


57 FORMAT(4I8,2G12.6)

58 FORMAT(2I8,2G12.6)

```

WRITE(*,*)'Give the general values (REAL VALUE W/ DECIMAL POINT)'
READ(*,55) C1,C2
WRITE(*,55) C1,C2
DO 10 I=1,IDIM
DO 10 J=1,JDIM
A1(I,J)=C1
A2(I,J)=C2
10 CONTINUE

```

```

WRITE(*,*)' Give ITYP = 1, 5 (IF BLOCKS), OR 7 (IF SINGLE CELLS)'
READ(*,56) ITYP
WRITE(*,56) ITYP

```

```

IF(MOD(ITYP,5).NE.0) GO TO 30
WRITE(*,*)' Give the number of blocks'
READ(*,56) IBLOCK
WRITE(*,56) IBLOCK

```

```

WRITE(*,*)' Give for each block I-MIN,J-MIN,I-MAX,J-MAX '
WRITE(*,*)' (INTEGER VALUES), and Actual values of parameters'
WRITE(*,*)' (REAL WITH DECIMAL POINT)'
DO 20 IBL=1,IBLOCK
READ(*,57) IMN,JMN,IMX,JMX,C1,C2
WRITE(*,57) IMN,JMN,IMX,JMX,C1,C2
DO 20 I=IMN,IMX
DO 20 J=JMN,JMX
A1(I,J)=C1
A2(I,J)=C2
20 CONTINUE

```

```

30 IF(MOD(ITYP,7).NE.0) GO TO 50
WRITE(*,*)' Give the number of single cells'
READ(*,56) NUMEX
WRITE(*,56) NUMEX

```

```

WRITE(*,*)' Give for each single cell I,J, Actual values'
DO 40 NUM=1,NUMEX
READ(*,58) I,J,C1,C2
WRITE(*,58) I,J,C1,C2
A1(I,J)=C1
A2(I,J)=C2
40 CONTINUE

```

50 CONTINUE

RETURN
END

SUBROUTINE INPUT2(A, IDIM, JDIM)
DIMENSION A(IDIM, JDIM)
55 FORMAT(G12.6)
56 FORMAT(I8)
57 FORMAT(4I8, G12.6)
58 FORMAT(2I8, G12.6)

WRITE(*, *) ' Give the general value (REAL WITH DECIMAL POINT)'
READ(*, 55) C
WRITE(*, 55) C
DO 10 I=1, IDIM
DO 10 J=1, JDIM
A(I, J)=C
10 CONTINUE

WRITE(*, *) ' Give ITYP = 1(SINGLE VALUE), 5(BLOCKS), 7(SINGLE CELLS)
C, or 35(5&7)'
READ(*, 56) ITYP
WRITE(*, 56) ITYP

IF(MOD(ITYP, 5).NE.0) GO TO 30
WRITE(*, *) ' Give the number of blocks'
READ(*, 56) IBLOCK
WRITE(*, 56) IBLOCK

WRITE(*, *) ' Give for each block I-MIN, J-MIN, I-MAX, J-MAX '
WRITE(*, *) ' (INTEGER VALUES), and Actual value of parameter'
WRITE(*, *) ' (REAL WITH DECIMAL POINT)'

DO 20 IBL=1, IBLOCK
READ(*, 57) IMN, JMN, IMX, JMX, C
WRITE(*, 57) IMN, JMN, IMX, JMX, C
DO 20 I=IMN, IMX
DO 20 J=JMN, JMX
A(I, J)=C
20 CONTINUE

30 IF(MOD(ITYP, 7).NE.0) GO TO 50
WRITE(*, *) ' Give the number of single cells'
READ(*, 56) NUMEX
WRITE(*, 56) NUMEX

```

WRITE(*,*)' Give for each single cell I,J, Actual value'
DO 40 NUM=1,NUMEX
  READ(*,58) I,J,C
  WRITE(*,58) I,J,C
  A(I,J)=C
40 CONTINUE

```

```

50 CONTINUE

```

```

RETURN
END

```

SUBROUTINE INFAC(MAUT)

```

*****

```

```

C*--This subroutine acts as an interface between the SST program *
C*--and the grid preprocessor, reading from LUN 20. If the pre- *
C*--processor program is not used, then MAUT must equal 1. *
C*-- D. Kozlowski, Solar Energy Laboratory, January 1989. *

```

```

*****

```

```

COMMON /WST1/ AREAR(20,30),AREAZ(20,30),CIN(20,30),FR(20,30),
1 FZ(20,30),GFR(20,30),GFZ(20,30),R(20),RISOR(20,30),
2 RISOZ(20,30),RLAM(20,30),RM(20),T(20,30),Z(30),
3 ZM(30),IMAX,IMAX1,JMAX,JMAX1
COMMON /WST2/ IMN(20),IMX(20),JMN(20),JMX(20),NA
COMMON /WST4/ ARESTO(101),CCSTO1,CINSTO,DISPER,DTDEM,
1 DTSTOX,DTSUR,FBSTO(101),FRACC1(30),FRACC2(30),FSTO(101),
2 FZACC1(20),FZACC2(20),GFSTO(101),ISTOMN,ISTOMX(30),JJMAX,
3 JJPMP1,JJPMP2,JSTMIN,RLAMST,TAIR,TIME,TIMSTO,TIMSUR,
4 TSTO(101),TWIN,TWOUT,VDARCY(101),VOLCEL,WFLOW,WFLOWX,
5 ZMSTO(101),ZSTO(101),JSTMAX
COMMON /WST5/ DTOKAY,DTOKST,LCOORD,IND,CSTO,CWATER,RLSTO
1 ,LFCV,TAIRM,LPOND
COMMON/WST6/RLAML(10),CL(10),D(10),THL(10),RADIUS,HEIGHT,
1 DEPTH,IRR,FAC,DRMIN,DRMAX,ZDMIN,RIST,RISS,RISB,VOLST,
2 THISO,FRIST,FRISS,FRISB,RISLAM,TSTIN,TIMO3,TSTART,TGRAD,
3 ILAY

```

```

COMMON/DIMEN/IDIM,JDIM,JJDIM,PI
COMMON/OPTS/LB24,LTOP,LBOT,SMTME

```

```

96 FORMAT(10I8)
98 FORMAT(10G12.6)

```

C* Data for buffer & extraction options

```

      READ(20,96) I1
      IF(I1.EQ.0) GOTO 100
      READ(20,96) LB24
      READ(20,96) LTOP
      READ(20,96) LBOT

100  CONTINUE
C*-- 1=AUTOMATIC MESH GENERATION
      READ(20,96) MAUT
      IF(MAUT.EQ.1) RETURN

      READ(20,96) IMAX,JMAX,LCOORD
      IMAX1=IMAX+1
      JMAX1=JMAX+1

      READ(20,96) NA

      DO 130 IA=1,NA
130  READ(20,96) IMN(IA),JMN(IA),IMX(IA),JMX(IA)

      DO 131 I=1,IMAX1
131  READ(20,98) R(I),RM(I)

      DO 132 J=1,JMAX1
132  READ(20,98) Z(J),ZM(J)

C*-- CHECK IF WANT DECK GROUND VALUES
      READ(20,96) IDFLT
      IF (IDFLT .EQ. 1) GOTO 55

C*-- SOIL2: RLAM,CIN

      IM1=IDIM/10
      M1 = 0
      IF (IM1*10 .NE. IDIM) M1=IM1*10 + 1
      DO 50 J=1,JDIM
      DO 40 L1=1,IM1
40  READ(20,98) (RLAM(I,J),I=(L1-1)*10+1,L1*10)

      IF (M1 .NE. 0) READ(20,98) (RLAM(I,J),I=M1,JDIM)
50  CONTINUE

      DO 51 J=1,JDIM
      DO 41 L1=1,IM1

```

```

41  READ(20,98) (CIN(I,J),I=(L1-1)*10+1,L1*10)

      IF (M1 .NE. 0) READ(20,98) (CIN(I,J),I=M1,IDIM)
51  CONTINUE

C*-- INPUT2: RISOR
      DO 52 J=1,JDIM
      DO 42 L1=1,IM1
42  READ(20,98) (RISOR(I,J),I=(L1-1)*10+1,L1*10)

      IF (M1 .NE. 0) READ(20,98) (RISOR(I,J),I=M1,IDIM)
52  CONTINUE

C*-- INPUT2: RISOZ
      DO 53 J=1,JDIM
      DO 43 L1=1,IM1
43  READ(20,98) (RISOZ(I,J),I=(L1-1)*10+1,L1*10)

      IF (M1 .NE. 0) READ(20,98) (RISOZ(I,J),I=M1,IDIM)
53  CONTINUE

C*-- INPUT2: T
      DO 54 J=1,JDIM
      DO 44 L1=1,IM1
44  READ(20,98) (T(I,J),I=(L1-1)*10+1,L1*10)

      IF (M1 .NE. 0) READ(20,98) (T(I,J),I=M1,IDIM)
54  CONTINUE

      CALL UTDAT2
55  CONTINUE

      CALL THEPRO

C*-- ***SST*** DATA FOR HEAT STORAGE VOLUME
      READ(20,96) ISTOMN,JSTMIN,JSTMAX,NR

      J2=JSTMIN-1
      DO 70 N=1,NR
      J1=J2+1
      READ(20,96) I2,J2
      DO 60 J=J1,J2

```

```
60  ISTOMX(J)=I2
70  CONTINUE

      READ(20,96) JJMAX

      JJ2=JJMAX+1
      DO 20 JJ=1,JJ2
20   READ(20,98) ZSTO(JJ),ZMSTO(JJ)

      *C-- SET OTHER PARAMETERS FROM INDAT2; IF LPOND=2, USE MAUT=1

      WFLOWX=WFLOWX*VOLST/86400.
      LFCV=2
      LPOND=0
      DTOKST=86400.
      DTOKAY=3.*86400.
      DO 90 JJ=1,JJMAX
90   TSTO(JJ)=TSTIN

      RETURN
      END
```

Appendix C: Computer Code for Selected SST Subroutines

and for Other Models Used in This Study

Part 1: TRNSYS SST SUBROUTINES FOR MINSUN-TRNSYS COMPARISON

Main TRNSYS Type

WSTSB2

WSTSB1

BUFVOL

ENSUM

PMPSTO

```

SUBROUTINE TYPE39(SIMTIM,XIN,OUT,TDUM,DTDT,PAR,INFO)
C*****C
C  LUND-SST: Lund University Seasonal Storage Tank      C
C  STRATIFIED TEMPERATURE STORAGE MODEL                C
C  Main Authors: Claesson, Efring, and Hellstrom      C
C               Dept. of Mathematical Physics          C
C               Lund Institute of Technology           C
C               Box 725, S-220 07 Lund, Sweden        C
C               C
C  TRNSYS Adaptation by: D. Kozlowski                 C
C  University of Wisconsin Solar Energy Laboratory     C
C               May, 1989                             C
C  From MINSUN Version Update 850114                  C
C*****C
  DIMENSION XIN(20),OUT(20),PAR(30),INFO(10),TTTT(1),DTDT(1)
  COMMON /WST1/ AREAR(20,30),AREAZ(20,30),CIN(20,30),FR(20,30),
  1 FZ(20,30),GFR(20,30),GFZ(20,30),R(20),RISOR(20,30),
  2 RISOZ(20,30),RLAM(20,30),RM(20),T(20,30),Z(30),
  3 ZM(30),IMAX,IMAX1,JMAX,JMAX1
  COMMON /WST2/ IMN(20),IMX(20),JMN(20),JMX(20),NA
  COMMON /WST4/ ARESTO(101),CCSTO1,CINSTO,DISPER,DTDEM,
  1 DTSTOX,DTSUR,FBSTO(101),FRACC1(30),FRACC2(30),FSTO(101),
  2 FZACC1(20),FZACC2(20),GFSTO(101),ISTOMN,ISTOMX(30),JJMAX,
  3 JJPMP1,JJPMP2,JSTMIN,RLAMST,TAIR,TIME,TIMSTO,TIMSUR,
  4 TSTO(101),TWIN,TWOUT,VDARCY(101),VOLCEL,WFLOW,WFLOWX,
  5 ZMSTO(101),ZSTO(101),JSTMAX
  COMMON /WST5/ DTOKAY,DTOKST,LCOORD,IND,CSTO,CWATER,RLSTO
  1 ,LFCV,TAIRM,LPOND
  COMMON/WST6/RLAML(10),CL(10),D(10),THL(10),RADIUS,HEIGHT,
  1 DEPTH,IRR,FAC,DRMIN,DRMAX,ZDMIN,RIST,RISS,RISB,VOLST,
  2 THISO,FRIST,FRISS,FRISB,RISLAM,TSTIN,TIMO3,TSTART,TGRAD,
  3 ILAY

  COMMON/WST3/VOLBF2,TBUFU2,VOLBF1,TBUFU1,JJEXT2,JJEXT1
  COMMON/OPTS/LB24,LTOP,LBOT,SMTME
  COMMON/SIM/TIME0,TFINAL,DELT
  COMMON/INIT/IPRE,TCMAX
  COMMON/CAVE1/NSTOC,NEQM,LHP,VCEL,NEQ,TSTOLD(101)
  COMMON/DIMEN/IDIM,JDIM,JJDIM,PI
  IDIM=20
  JDIM=30
  JJDIM=101
  PI=3.141592654
  SMTME=SIMTIM
C

```



```

INF7=INFO(7)
IF (INFO(7) .GE. 0 ) GO TO 100
*  INITIALIZE NEW SIMULATION
INFO(6)=13

VOLST=PAR(1)
HEIGHT=PAR(2)
THISO=PAR(3)
FRIST=PAR(4)
FRISS=PAR(5)
FRISB=PAR(6)
RISLAM=PAR(7)
DEPTH=PAR(8)
TSTIN=PAR(9)
CWATER=PAR(10)
WFLOWX=PAR(11)
RLSTO=PAR(12)
DISPER=PAR(13)
RLAMST=PAR(14)
CSTO=PAR(15)
TIMO3=PAR(16)
IPRE=PAR(17)
TCMAX=PAR(18)
TSURF=PAR(19)
TSTART=PAR(20)
TGRAD=PAR(21)
NEQ=PAR(22)
ILAY=PAR(23)
J=24
DO 20 I=1,ILAY
  RLAML(I)=PAR(J)
  CL(I)=PAR(J+1)
  THL(I)=PAR(J+2)
20  J=J+3

JJMAX=NEQ
TAIR = TSURF
CALL WSTIN(TMSTOR,TSTMX,TSTMN,SIMTIM)

OUT(15)=TMSTOR
VCEL=VOLCEL
GO TO 764
100 CONTINUE

*C  SYNCHRONIZE CLOCKS

```

```

IF (SIMTIM .EQ. TIME0) THEN
TIMSTO=(SIMTIM+DELT)*3600.
TIMSUR=(SIMTIM+24.)*3600.
TIMBUF=SIMTIM*3600.
DELTS=DELT*3600.
GOTO 764
END IF

```

```

TIME=SIMTIM*3600.
TAWST=XIN(5)

```

C** CALCULATIONS FOR SOLAR COLLECTOR LOOP

```
TFWST=XIN(1)
```

C** NEXT LINE FLUID DENSITY = 1000. KG/M**3

```
QWWST2=XIN(2)/3.6E+06
```

```
IF(QWWST2.EQ.0.) GO TO 40
```

```
IF(ABS(QWWST2).LE.WFLOWX) GO TO 6667
```

```
QW1=QWWST2*86400./VOLST
```

```
WF1=WFLOWX*86400./VOLST
```

```
WRITE(6,6666) QW1,WF1
```

```
6666 FORMAT(
```

```
1 ' *** PROGRAM STOPPED BECAUSE OF AN ERROR IN SST INPUT. ***',
```

```
2 ' *** FLOW RATE IN SOLAR LOOP ',E12.4,' VOLUME/DAY ***',
```

```
3 ' *** EXCEEDS MAXIMUM FLOW RATE ',E12.4,' VOLUME/DAY ***',
```

```
4 ' *** WHICH WAS GIVEN AS INPUT. ***')
```

```
STOP 221
```

```
6667 CONTINUE
```

```
LOD=1
```

```
GO TO 45
```

```
40 CONTINUE
```

```
LOD=0.
```

```
45 CONTINUE
```

```
DEN2=0.
```

```
TOUTM=0.
```

C**The collector side extraction node is set at bottom of store

```
JJEXT2 = JJMAX
```

```
TOUT2 = TSTO(JJEXT2)
```

```
CALL WSTSB2(LOD,QWWST2,TFWST,TOUT2,QWST2,TAWST,TIME,DELTS,
```

```
1 TBUFU2,VOLBF2,DEN2,TSTMX,TSTMN,TMSTOR,INF7)
```

C** CALCULATION FOR LOAD LOOP

C** FS=Flow through storage, F2=Flow through bypass

C** FS+F2=Total flow in loop

C** HOUSE HEATING

F2H=0.

FSH=0.

TFSH=0.

JJEXT1=1

TOUT1=TSTO(JJEXT1)

TTH=XIN(3)

C* Convert from kg/hr to m3/s

IF (LHP.EQ. 1) XIN(6)=0.

FWSH=(XIN(6)+XIN(10))/3.6E+06

IF(FWSH.EQ.0.) GO TO 52

TFSH=(XIN(6)*XIN(4)+XIN(10)*XIN(13))/(FWSH*3.6E+06)

C* HEAT PUMP LOOP

C* The extraction node NEQM and number of nodes required NSTOC are

C* determined in the Heat Pump Subroutine

IF(LHP.EQ.1) THEN

JJEXT1=NEQM

FSH=FWSH

THPG=TSTO(JJEXT1)

TOUT1=THPG

IF(NSTOC.EQ.1) GO TO 52

XX=0.

JJEXT2=JJEXT1+NSTOC-1

DO 51 JJ=JJEXT1,JJEXT2

51 XX=XX+TSTO(JJ)

THPG=XX/FLOAT(NSTOC)

DO 53 JJ=JJEXT1,JJEXT2

53 TSTO(JJ)=THPG

TOUT1=THPG

GO TO 52

END IF

*C Find node >= to demand; demand temperature is delivered exactly

*C by mixing appropriate amount of return water (F2H), if possible

IF(TFSH.GE.TSTMX) THEN

F2H=FWSH

TOUT1=TFSH

ELSE

FSH=FWSH

TOUT1=TSTO(1)

ENDIF

IF(TTH.GE.TSTMX) GO TO 52

IF(TSTMX.EQ.TFSH) GO TO 52

IF(TSTMN.GT.TTH) GO TO 62

```

JJEXT1=1
IF(LTOP.EQ.1)GOTO 63
61 CONTINUE
IF(TSTO(JJEXT1+1).LT.TTH) GO TO 63
JJEXT1=JJEXT1+1
GO TO 61
62 CONTINUE
JJEXT1=JJMAX-1
63 CONTINUE
TSTEXT=TSTO(JJEXT1)
IF(TSTEXT.EQ.TFSH) THEN
  TOUT1=TSTO(JJEXT1)
  GO TO 52
END IF
F2H=(TSTEXT-TTH)*FWSH/(TSTEXT-TFSH)
FSH=FWSH-F2H
TOUT1=TTH

C** TAP WATER IN PARALLEL OPTION
C** Not used if XIN(7 and (9 or 11))=0
52 CONTINUE
F2T=0.
FST=0.
TFST=0.
TTT=XIN(7)
FWST=(XIN(9)+XIN(11))/3.6E+06
IF(FWST.EQ.0.) GO TO 71
TFST=(XIN(9)*XIN(8)+XIN(11)*XIN(12))/(FWST*3.6E+06)
IF(XIN(11).EQ.0.) GO TO 69
FST=FWST
GO TO 70
69 IF(TFST.GE.TSTMX) F2T=FWST
IF(TFST.LT.TSTMX) FST=FWST
IF(TTT.GE.TSTMX) GO TO 70
IF(TSTMX.EQ.TFST) GO TO 70
F2T=(TSTMX-TTT)*FWST/(TSTMX-TFST)
FST=FWST-F2T
70 TOUT3=AMIN(TSTMX,TTT)
71 CONTINUE

C** NEXT LINE FLUID DENSITY = 1000. KG/M**3
QWWST1=ABS(FSH+FST)
IF(QWWST1.LE.WFLOWX) GO TO 7667
QW1=QWWST1*86400./VOLST
WF1=WFLOWX*86400./VOLST
WRITE(16,7666) QW1,WF1

```

```

7666 FORMAT(
  1 ' *** PROGRAM STOPPED BECAUSE OF AN ERROR IN SST INPUT. ***',
  2 ' *** FLOW RATE IN LOAD LOOP  'E12.4,' VOLUME/DAY ***',
  3 ' *** EXCEEDS MAXIMUM FLOW RATE 'E12.4,' VOLUME/DAY ***',
  4 ' *** WHICH WAS GIVEN AS INPUT.          ***')
  WRITE(6,7665) FWSH,FWST,FSH,F2H,FST,F2T,TSTMX,TTH,TFSH,TTT,TFST
7665 FORMAT(/11E12.3)
  STOP 222
7667 CONTINUE

```

```

  IF(QWWST1.EQ.0.) GO TO 75
  TFWST=(FSH*TFSH+FST*TFST)/(FSH+FST)
  LOD=-1
  GO TO 80
75 CONTINUE
  QWWST1=0.
  TFWST=0.
  LOD=0.
80 CONTINUE
  DEB=0.

```

*C--Enter WSTSB1, even if QWWST1=0; else iterations are bad

```

  CALL WSTSB1(LOD,QWWST1,TFWST,TSTEXT,QWST1,TAWST,TIME,DELTS,
  1 TBUFU1,VOLBF1,DEN1,DEB,TSTMX,TSTMN,TMSTOR,INF7)

```

```

  IF(XIN(10).NE.0.)DEN1=(THPG-TFWST)*QWWST1*CWATER*DELTS

```

C** Calculation of MAX,MIN and MEAN storage temperatures
 C** Update Mean daily instead of hourly because changes are small

```

  TSTMX=TSTO(1)
  TSTMN=TSTO(JJMAX)
  TSTMIX=.0

  IF (AMOD(SIMTIM,24.).EQ.0.)THEN
    DO 300 JJ=1,JJMAX
300  TSTMIX=TSTMIX+TSTO(JJ)*VOLCEL
    TSTMIX=TSTMIX+(TBUFU2-TSTO(JJEXT2))*VOLBF2
    1  +(TBUFU1-TSTO(JJEXT1))*VOLBF1
    TSTMIX=TSTMIX/(JJMAX*VOLCEL)
    TMSTOR=TSTMIX
  END IF

  C* !LFCV=Convection mode: 3=mixed cell temp.
  IF(LFCV.EQ.3) TSTMX=TSTMIX
  IF(LFCV.EQ.3) TSTMN=TSTMIX

```

TMAX=TSTO(1)

OUT(1)=TOUT2
 OUT(2)=QWWST2*3.6E+06
 OUT(3)=TOUT1
 OUT(4)=QWWST1*3.6E+06
 OUT(5)=(FSH+F2H+FST+F2T)*3.6E+06
 OUT(6)=(DEB)*1.E-3/DELT
 OUT(7)= DEN1*0.001/DELT
 OUT(8)= ((TMSTOR-OUT(15))*0.001)*CSTO*VOLST
 OUT(9)= DEN2*0.001/DELT
 OUT(10)=TMSTOR
 OUT(11)=TSTO(1)
 OUT(12)=TSTO(JJMAX)
 OUT(13)=TOUT3

764 CONTINUE

C* The first of these two subroutines prints out ground parameters and
 C* grid characteristics (after the pre-heating subroutine). The second
 C* of these subroutines will print out the store temperature profile
 C* and average store temperature for the last day of the month to LUN25.
 * IF (INFO(8) .EQ. 2) CALL ARRYWT
 * CALL MNTHWT(SIMTIM,TMSTOR)

RETURN
 END

SUBROUTINE WSTSB2(LOD,WFLW,TWN,TWOT,QWST,TAR,TIM,DTDM,
 1 TBUFU,VOLBFU,DEN,TSTMX,TSTMN,TMSTOR,INF7)
 DIMENSION FRACO1(30),FRACO2(30),FSTOO(101),FZACO1(20),
 1 FZACO2(20),TOLD(20,30)
 COMMON /WST1/ AREAR(20,30),AREAZ(20,30),CIN(20,30),FR(20,30),
 1 FZ(20,30),GFR(20,30),GFZ(20,30),R(20),RISOR(20,30),
 2 RISOZ(20,30),RLAM(20,30),RM(20),T(20,30),Z(30),
 3 ZM(30),IMAX,IMAX1,JMAX,JMAX1
 COMMON /WST4/ ARESTO(101),CCSTO1,CINSTO,DISPER,DTDEM,
 1 DTSTOX,DTSUR,FBSTO(101),FRACC1(30),FRACC2(30),FSTO(101),
 2 FZACC1(20),FZACC2(20),GFSTO(101),ISTOMN,ISTOMX(30),JJMAX,
 3 JJPMP1,JJPMP2,JSTMIN,RLAMST,TAIR,TIME,TIMSTO,TIMSUR,
 4 TSTO(101),TWIN,TWOUT,VDARCY(101),VOLCEL,WFLOW,WFLOWX,
 5 ZMSTO(101),ZSTO(101),JSTMAX
 COMMON /WST5/ DTOKAY,DTOKST,LCOORD,IND,CSTO,CWATER,RLSTO
 1 ,LFCV,TAIRM,LPOND
 COMMON/WST6/RLAML(10),CL(10),D(10),THL(10),RADIUS,HEIGHT,

```

1 DEPTH,IRR,FAC,DRMIN,DRMAX,ZDMIN,RIST,RISS,RISB,VOLST,
2 THISO,FRIST,FRISS,FRISB,RISLAM,TSTIN,TIMO3,TSTART,TGRAD,
3 ILAY
COMMON/WST3/VOLBF2,TBUFU2,VOLBF1,TBUFU1,JJEXT2,JJEXT1
COMMON/OPTS/LB24,LTOP,LBOT,SMTME
COMMON/CAVE1/NSTOC,NEQM,LHP,VCEL,NEQ,TSTOLD(101)
IF (INF7 .GT. 0) GOTO 8

```

```

TMOLD=TMSTOR

```

```

OLD1=VOLBFD
OLD2=VOLBFU
OLD3=TBUFU
OLD4=TBUFD
OLD5=TIMSTO
OLD6=TIMSUR
OLD7=TAIRM
OLD8=TIMBUF
DO 9 JJ=1,JJMAX
9 TSTOLD(JJ)=TSTO(JJ)
DO 11 J=JSTMIN,JSTMAX
FRACO1(J)=FRACC1(J)
FRACO2(J)=FRACC2(J)
FSTOO(J)=FSTO(J)
11 CONTINUE
I2=ISTOMX(JSTMIN)
DO 12 I=ISTOMN,I2
12 FZACO1(I)=FZACC1(I)
I2=ISTOMX(JSTMAX)
DO 13 I=ISTOMN,I2
13 FZACO2(I)=FZACC2(I)
DO 14 I=1,IMAX
DO 14 J=1,JMAX
14 TOLD(I,J)=T(I,J)
GO TO 18

```

C--SEND ITERATIONS HERE-- GIVE ORIGINAL VALUES

```

8 CONTINUE
VOLBFD=OLD1
VOLBFU=OLD2
TBUFU=OLD3
TBUFD=OLD4
TIMSTO=OLD5
TIMSUR=OLD6
TAIRM=OLD7
TIMBUF=OLD8

```

```

      DO 19 JJ=1,JJMAX
19 TSTO(JJ)=TSTOLD(JJ)
      DO 21 J=JSTMIN,JSTMAX
      FRACC1(J)=FRACO1(J)
      FRACC2(J)=FRACO2(J)
      FSTO(J)=FSTOO(J)
21 CONTINUE
      I2=ISTOMX(JSTMIN)
      DO 22 I=ISTOMN,I2
22 FZACC1(I)=FZACO1(I)
      I2=ISTOMX(JSTMAX)
      DO 23 I=ISTOMN,I2
23 FZACC2(I)=FZACO2(I)
      DO 24 I=1,IMAX
      DO 24 J=1,JMAX
24 T(I,J)=TOLD(I,J)

```

```

18 CONTINUE

```

```

      LOAD=LOD
      WFLOW=WFLW
      TWIN=TWN
      TWEXT=TWOT
      TAIR=TAR
      TIME=TIM
      DTDEM=DTDM
      TIMDEM=TIME+DTDEM

```

```

      TIMBUF=TIME
      TIMX=AMIN1(TIMDEM,TIMSUR+DTSUR)

```

```

      DEN=0.
      TAIRM=TAIRM+TAIR*(TIMX-TIME)
      IF(LOAD.EQ.0) WFLOW=.0

```

C** DETERMINATION OF TIME TO PASS UNTIL THE INLET BUFFER IS FILLED

** VOLBF=Momentary vol of buffer at bottom of storage volume

** VOLCEL=Cell volume; max vol of buffers

** Here dtbuf does not include current timestep

```

      DTBUF=1.E30
      IF(LOAD.EQ.1.AND.WFLOW.NE.0.) DTBUF=(VOLCEL-VOLBFU)/WFLOW

```

*TIMSUR = time at which ground temps are calculated

```

70 TSURNX=TIMSUR+DTSUR
      TBUFNX=TIMBUF+DTBUF

```



```

TIME1=TSURNX
IF(TBUFNX.LT.TIME1) TIME1=TBUFNX
IF(TIMDEM.LT.TIME1) TIME1=TIMDEM

C** START OF THE TIME ITERATION LOOP
  LSUR=1
  IF(TSURNX.GT.TIME1) LSUR=0
  LBUF=1
  IF(TBUFNX.GT.TIME1) LBUF=0
  LRETUR=1
  IF(TIMDEM.GT.TIME1) LRETUR=0
  IF(LBUF.EQ.0) GO TO 90

C** A BUFFER IS FILLED;CALC NEW VOLUMES OF THE TWO BUFFERS
  CALL BUFVOL(DTBUF,VOLBFU,TBUFU,TWIN,LOAD)
C** CALC ACCUMULATED ENERGIES AND THERMALITY CONSUMPTION.
  CALL ENSUM(DTBUF,TWIN,TWEXT,WFLOW,DEN,LOAD)
C** MOVE ALL TEMPS OF STORAGE VOLUME ONE CELL IN FLOW DIRECTION
  CALL PMPSTO(VOLBFU,TBUFU,VOLBF1,TBUFU1,TOUT2,
  1 TOUT1,JJEXT2,JJEXT1)

  TIMBUF=TIMBUF+DTBUF
  DTBUF=VOLCEL/WFLOW

  CALL FCVSTO(1,TSTO,JJMAX,TBUFU,VOLBFU,TBUFD,VOLBFD,
  1 VOLCEL)
  TBUFU=0.
  TBUFD=0.
  90 IF(LSUR.EQ.0) GO TO 100
*****
C** CONDUCTIVE CALCULATIONS IN THE SURROUNDING GROUND
*FLOW2 calcs the heat flows in the ground outside the sto vol
*NEWT2 calcs new temps outside the storage volume

  TAIRX=TAIR
  TAIR=TAIRM/DTSUR

  CALL FLOW2
  CALL NEWT2
  TIMSUR=TIMSUR+DTSUR

  TAIR=TAIRX
  TIMX=AMIN1(TIMDEM,TIMSUR+DTSUR)
  TAIRM=TAIR*(TIMX-TIMSUR)

100 CONTINUE

```

```
IF(LRETUR.EQ.1) GO TO 200
GO TO 70
```

```
200 CONTINUE
C** INJECTION OF WATER TO TIME TIMDEM INTO BUFFER
DTBUF=TIMDEM-TIMBUF
CALL BUFVOL(DTBUF,VOLBFU,TBUFU,TWIN,LOAD)
CALL ENSUM(DTBUF,TWIN,TWEXT,WFLOW,DEN,LOAD)
```

```
TWOUT=TWEXT
TWOT=TWEXT
TAR=TAIR
RETURN
END
```

```
SUBROUTINE WSTSB1(LOD,WFLW,TWN,TWOT,QWST,TAR,TIM,DTDM,
1 TBUFU,VOLBFU,DEN,DEB,TSTMX,TSTMN,TMSTOR,INF7)
```

```
COMMON /WST1/ AREAR(20,30),AREAZ(20,30),CIN(20,30),FR(20,30),
1 FZ(20,30),GFR(20,30),GFZ(20,30),R(20),RISOR(20,30),
2 RISOZ(20,30),RLAM(20,30),RM(20),T(20,30),Z(30),
3 ZM(30),IMAX,IMAX1,JMAX,JMAX1
COMMON /WST4/ ARESTO(101),CCSTO1,CINSTO,DISPER,DTDEM,
1 DTSTOX,DTSUR,FBSTO(101),FRACC1(30),FRACC2(30),FSTO(101),
2 FZACC1(20),FZACC2(20),GFSTO(101),ISTOMN,ISTOMX(30),JJMAX,
3 JJPMP1,JJPMP2,JSTMIN,RLAMST,TAIR,TIME,TIMSTO,TIMSUR,
4 TSTO(101),TWIN,TWOUT,VDARCY(101),VOLCEL,WFLOW,WFLOWX,
5 ZMSTO(101),ZSTO(101),JSTMAX
COMMON /WST5/ DTOKAY,DTOKST,LCOORD,IND,CSTO,CWATER,RLSTO
1 ,LFCV,TAIRM,LPOND
COMMON/WST6/RLAML(10),CL(10),D(10),THL(10),RADIUS,HEIGHT,
1 DEPTH,IRR,FAC,DRMIN,DRMAX,ZDMIN,RIST,RISS,RISB,VOLST,
2 THISO,FRIST,FRISS,FRISB,RISLAM,TSTIN,TIMO3,TSTART,TGRAD,
3 ILAY
COMMON/WST3/VOLBF2,TBUFU2,VOLBF1,TBUFU1,JJEXT2,JJEXT1
COMMON/OPTS/LB24,LTOP,LBOT,SMTME
IF (INF7 .GT. 0) GOTO 8
OLD1=VOLBFD
OLD2=VOLBFU
OLD3=TBUFU
OLD4=TBUFD
OLD8=TIMBUF
GO TO 18
```

C--ITERATIONS TO HERE--, SO SAVE ORIGINAL VALUES

```

8 CONTINUE
VOLBFD=OLD1
VOLBFU=OLD2
TBUFU=OLD3
TBUFD=OLD4
TIMBUF=OLD8

```

```

18 CONTINUE

```

```

LOAD=LOD
WFLOW=WFLW
TWIN=TWN
TWEXT=TSTO(JJEXT1)
TIME=TIM
DTDEM=DTDM
TIMDEM=TIME+DTDEM
TIMBUF=TIME
DEN=0.
DEB=0.

```

```

C** DETERMINATION OF TIME TO PASS UNTIL THE INLET BUFFER IS FILLED

```

```

DTBUF=1.E30
IF(LOAD.EQ.-1.AND.WFLOW.NE.0.) DTBUF=(VOLCEL-VOLBFU)/WFLOW

```

```

70 TBUFNX=TIMBUF+DTBUF
TIME1=TBUFNX
IF(TIMDEM.LT.TIME1) TIME1=TIMDEM

```

```

C** START OF THE TIME ITERATION LOOP

```

```

LBUF=1
IF(TBUFNX.GT.TIME1) LBUF=0
LRETUR=1
IF(TIMDEM.GT.TIME1) LRETUR=0

```

```

IF(LBUF.EQ.0) GO TO 100

```

```

C** A BUFFER IS FILLED;CALC NEW VOLUMES OF THE TWO BUFFERS

```

```

CALL BUFVOL(DTBUF,VOLBFU,TBUFU,TWIN,LOAD)

```

```

C** CALC ACCUMULATED ENERGIES AND THERMALITY CONSUMPTION.

```

```

CALL ENSUM(DTBUF,TWIN,TWEXT,WFLOW,DEN,LOAD)

```

```

C** MOVE ALL TEMPS OF STORAGE VOLUME ONE CELL IN FLOW DIRECTION

```

```

CALL PMPSTO(VOLBF2,TBUFU2,VOLBFU,TBUFU,TOUT2,
1 TOUT1,JJEXT2,JJEXT1)

```

```

TIMBUF=TIMBUF+DTBUF
DTBUF=VOLCEL/WFLOW
CALL FCVSTO(1,TSTO,JJMAX,TBUFU,VOLBFU,TBUFD,VOLBFD,
1 VOLCEL)

```

```

100 CONTINUE
IF(LRETUR.EQ.1) GO TO 200
GO TO 70

```

```

200 CONTINUE
C** INJECTION OF WATER TO TIME TIMDEM
DTBUF=TIMDEM-TIMBUF
CALL BUFVOL(DTBUF,VOLBFU,TBUFU,TWIN,LOAD)
CALL ENSUM(DTBUF,TWIN,TWEXT,WFLOW,DEN,LOAD)

```

```

*****

```

```

C**PURGE BUFFERS AT END OF DAY IF LB24=1

```

```

IF (LB24.EQ.1.AND.AMOD(SMTME,24.) .EQ. 0)THEN
CALL PMPSTO(VOLBF2,TBUFU2,VOLBFU,TBUFU,TOUT2,
1 TOUT1,JJEXT2,JJEXT1)
CALL FCVSTO(1,TSTO,JJMAX,TBUFU,VOLBFU,TBUFD,VOLBFD,
1 VOLCEL)
END IF

```

```

IF (LB24.EQ.0.)THEN
CALL PMPSTO(VOLBF2,TBUFU2,VOLBFU,TBUFU,TOUT2,
1 TOUT1,JJEXT2,JJEXT1)
CALL FCVSTO(1,TSTO,JJMAX,TBUFU,VOLBFU,TBUFD,VOLBFD,
1 VOLCEL)
END IF

```

```

*****

```

```

ITER=(TIME1-TIMSTO)/DTSTOX+1

```

```

C** CONDUCTIVE CALCULATIONS IN THE STORAGE VOLUME

```

```

*DTSTOX = max time step for storage volume
*TIMSTO = time at which conductive calcs are performed
*DTSTO = time step for storage volume simulation
*TMPSTO calcs new temperatures in the storage volume
*DEB=Heat losses to ground

```

```

DO 88 IT=1,ITER
DTSTO=DTSTOX
IF(TIMSTO+DTSTO .GT. TIMDEM) GOTO 88
CALL TMPSTO(DTSTO,LOAD)

```

```

DO 85 JJ=1,JJMAX

```

```

85 DEB=DEB-FBSTO(JJ)*DTSTO
   TIMSTO=TIMSTO+DTSTO

```

C** CONVECTIVE CALCULATIONS IN THE STORAGE VOLUME.

*LFCV = Parameter to determine how the effect of free convection in
 * storage volume is accounted

```

   CALL FCVSTO(LFCV,TSTO,JJMAX,TBUFU,VOLBFU,TBUFD,VOLBFD,
1  VOLCEL)

```

```

*C!TWOT=Outlet fluid temp at end of call
88  CONTINUE

```

```

   TWOT=TWEXT
   RETURN
   END

```

```

C  MEMBER      BUFVOL
C BUFVOL

```

```

   SUBROUTINE BUFVOL(DTST,VOLBFU,TBUFU,TWIN,LOAD)

```

*Calculates new volumes of the two buffers when water is pumped through the
 *storage system. New temperature of the inlet buffer is calculated.

```

   COMMON /WST4/ ARESTO(101),CCSTO1,CINSTO,DISPER,DTDEM,
1  DTSTOX,DTSUR,FBSTO(101),FRACC1(30),FRACC2(30),FSTO(101),
2  FZACC1(20),FZACC2(20),GFSTO(101),ISTOMN,ISTOMX(30),JJMAX,
3  JJPMP1,JJPMP2,JSTMIN,RLAMST,TAIR,TIME,TIMSTO,TIMSUR,
4  TSTO(101),TWIN,TWOUT,VDARCY(101),VOLCEL,WFLOW,WFLOWX,
5  ZMSTO(101),ZSTO(101),JSTMAX

```

```

   WVOL=WFLOW*DTST
   IF (LOAD .EQ. 0 ) GOTO 20

```

```

   TBUFU=(VOLBFU*TBUFU+WVOL*TWIN)/(VOLBFU+WVOL)
   VOLBFU=VOLBFU+WVOL

```

```

20  RETURN
   END

```

```

C  MEMBER      ENSUM
C ENSUM

```

```

   SUBROUTINE ENSUM(DT,TWN,TWEXT,WFLW,DEN,LOAD)

```

*Calculates accumulated energies.
 *C!LOAD=1 for injection of energy from heat source
 *C!LOAD=0 for rest mode

```
*C!LOAD=-1 for extraction of energy to load
COMMON /WST5/ DTOKAY,DTOKST,LCOORD,IND,CSTO,CWATER,RLSTO
1 ,LFCV,TAIRM,LPOND
```

```
IF(LOAD.EQ.0) RETURN
IF(LOAD.EQ.-1) GO TO 100
X=(TWN-TWEXT)*WFLW*CWATER*DT
DEN=DEN+X
GO TO 200
```

```
100 X=(TWEXT-TWN)*WFLW*CWATER*DT
DEN=DEN+X
```

```
200 CONTINUE
```

```
RETURN
END
```

```
C MEMBER PMPSTO
```

```
C PMPSTO
```

```
SUBROUTINE PMPSTO(VOLBF2,TBUFU2,VOLBF1,TBUFU1,TOUT2,
1 TOUT1,JJEXT2,JJEXT1)
```

```
*When the inlet buffer is full, the routine moves all temperatures
```

```
*of the storage volume one cell in the flow direction. The
```

```
*buffer temperature is moved to the inlet cell. The buffer volume
```

```
*is set to zero.
```

```
COMMON /WST4/ ARESTO(101),CCSTO1,CINSTO,DISPER,DTDEM,
1 DTSTOX,DTSUR,FBSTO(101),FRACC1(30),FRACC2(30),FSTO(101),
2 FZACC1(20),FZACC2(20),GFSTO(101),ISTOMN,ISTOMX(30),JJMAX,
3 JJPMP1,JJPMP2,JSTMIN,RLAMST,TAIR,TIME,TIMSTO,TIMSUR,
4 TSTO(101),TWIN,TWOUT,VDARCY(101),VOLCEL,WFLOW,WFLOWX,
5 ZMSTO(101),ZSTO(101),JSTMAX
COMMON/OPTS/LB24,LTOP,LBOT,SMTME
```

```
IF(LBOT.EQ.1)THEN
JJINJ2=1
JJINJ1=JJMAX
GOTO 35
END IF
```

```
C ** Find injection cell for downwards pumping
```

```
DO 10 JJ=1,JJMAX
IF(TBUFU2.GE.TSTO(JJ)) GO TO 15
10 CONTINUE
```

```

      JJ=JJMAX
15  JJINJ2=JJ

C ** Find injection cell for upwards pumping

      DO 25 N=1,JJMAX
      JJ=JJMAX+1-N
      IF(TBUFU1.LE.TSTO(JJ)) GO TO 30
25  CONTINUE
      JJ=1
30  JJINJ1=JJ

*C--GET TBUFU'S OUT
35  TOUT2 = TSTO(JJEXT2)
      TOUT1 = TSTO(JJEXT1)

C** UPWARD PUMPING

      IF (JJINJ1 .EQ. JJMAX) TMXOLD=TSTO(JJMAX)

      TUNDER=TBUFU1
      DO 110 N=JJEXT1,JJINJ1
      JJ=JJINJ1+JJEXT1-N
      TOLD=TSTO(JJ)
      TSTO(JJ)=(VOLBF1*TUNDER+(VOLCEL-VOLBF1)*TSTO(JJ))/VOLCEL
      TUNDER=TOLD
110  CONTINUE

*C Switch routine necessary for 24 hour buffer use.
      IF (JJINJ1 .EQ. JJMAX) THEN
      TMXSAV = TSTO(JJMAX)
      TSTO(JJMAX) = TMXOLD
      END IF

*C ** DOWNWARD PUMPING
      TOVER=TBUFU2
      DO 101 JJ=JJINJ2,JJEXT2
      TOLD=TSTO(JJ)
      TSTO(JJ)=(VOLBF2*TOVER+(VOLCEL-VOLBF2)*TSTO(JJ))/VOLCEL
      TOVER=TOLD
101  CONTINUE

      IF (JJINJ1 .EQ. JJMAX) THEN
      TSTO(JJMAX) = TSTO(JJMAX) - (TMXOLD-TMXSAV)
      END IF

```

```
200 VOLBF2=0.  
    VOLBF1=0.  
    TBUFU2=0.  
    TBUFU1=0.  
*C!The fluid is pumped betw cells JJPMP1 and JJPMP2  
    JJPMP1=JMIN(JJINJ1,JJINJ2,JJEXT1,JJEXT2)  
    JJPMP2=JMAX(JJINJ1,JJINJ2,JJEXT1,JJEXT2)  
  
300 RETURN  
    END
```


**Part 2: ADDITIONAL TRNSYS SUBROUTINES USED
FOR MINSUN-TRNSYS COMPARISON**

House Load Model

Heat Pump Model

Pipe Model

Determination of Heating Season

Massflow Determination for Constant Collector Outlet Temperature

Massflow Determination for Constant Load Outlet Temperature

* House Load Model

```

SUBROUTINE TYPE12(TIME,XIN,OUT,T,DTDT,PAR,INFO)
DIMENSION PAR(15),XIN(10),OUT(20),INFO(10)
COMMON/TOPTMP/TSTMX
COMMON /SIM/ TIME0,TIMEF,DELT

```

C* This subroutine simulates a house-heating thermal load;
 C* it uses the energy per degree-day concept. There is no
 C* heat exchanger in this subroutine.
 C* UA - is the overall loss conductance for the house
 C* TRBAR - is the temperature of the interior of the house
 C* FLOW - is the flow rate of the heating fluid
 C* CP - is the specific heat of the heating fluid
 C* TAMB - is the ambient outside air temperature
 C* THOT - is the inlet heating fluid temperature
 C* LGAM - is on/off controller for space heating season

C FIRST CALL OF SIMULATION

```

IF (INFO(7).GE.0) GO TO 5
INFO(9)=1
INFO(6)=5
NP=5
NI=5
CALL TYPECK(1,INFO,NI,NP,0)

```

C SET PARAMETERS

```

TRET=PAR(1)
UA=PAR(2)
TRBAR=PAR(3)
DHW=PAR(4)
CP=PAR(5)
RETURN

```

C SET INPUTS

```

5  THOT=XIN(1)
   FLOW=XIN(2)
   TAMB=XIN(3)
   QGAIN=XIN(4)
   LGAM=INT(XIN(5)+0.1)
   QAUX = 0.0
   TCOLD = THOT

C ENERGY RATE CONTROL
  if (tamb .ge. 10.0) tamb=trbar
  Q = UA*(TRBAR-TAMB) - QGAIN
  Q = AMAX1(Q,0.0)

C PARALLEL AUXILIARY
  QTOT = LGAM*Q + DHW      !TOTAL LOAD
  QT = FLOW*CP*(THOT-TRET)  !ENERGY TRANSFERRED
  QT = AMAX1(QT,0.0)
  IF (FLOW.NE.0.) THEN
    TCOLD = THOT - QT/FLOW/CP
  ELSE
    TCOLD = THOT
  END IF
  QAUX = QTOT - QT
  QAUX = AMAX1(QAUX,0.0)
  IF (TIME.EQ.TIME0+1.AND.INFO(7).EQ.0) TCOLD=TSTMX

C OUTPUTS
40  OUT(1) = TCOLD
    OUT(2) = FLOW
    OUT(3) = QTOT
    OUT(4) = QT
    OUT(5) = QAUX
    RETURN
    END

```

```
*****
* Theoretical Heat Pump: Based on IEA routines. Modified and *
* Incorporated into TRNSYS for use with SST by D. Kozlowski 2/5/89 *
*****
```

```
SUBROUTINE TYPE20(TIME,XIN,OUT,TDUM,DTDUM,PAR,INFO)
DIMENSION XIN(10),OUT(10),PAR(10),INFO(10)
DIMENSION TSTO(101)
COMMON/CAVE1/NSTOC,NEQM,LHP,VCEL,NEQ,T(101)
COMMON/SIM/TIME0,TIMEF,DEL T
```

*C--COMMON block CAVE1 is passed from SST subroutine MAIN & WSTSB2

```
C THIS ROUTINE MODELS A HEAT PUMP WITH EVAPORATOR MASS FLOW CONSTANT
C ETATCF=EFFICIENCY OF EL-MOTOR
C AKC=K*A CONDENSER
C FITOT=COEFFICIENT OF PERFORMANCE
C FLOWE=(MASSFLOW EVAPORATOR)*CPF
C FLOWC=(MASSFLOW CONDENSER)*CPF
C
C EQUATION SYSTEM
C PAR(7)=MIN FITOT FOR OPERATION
C FITOT={(TCUT+XCN)/(TCUT+XCN-TFUT+XFN)}*ETATCF
C PPEL=PPC/FITOT
C PPF=PPC-PPEL
C XFN=PPF*AA
C XCN=PPC*AC
C AA=1/AKF+0.5/FLOWE
C AC=AMAX1((1./AKC-0.5/FLOWC),0.)
C ETATCF=ETATCF-AMAX1(TTC-TTE-ETADEL,0.)*ETACON
```

C FIRST CALL OF SIMULATION

```
IF (INFO(7).GE.0) GO TO 5
INFO(9)=1
INFO(6)=8
NP=8
NI=3
CALL TYPECK(1,INFO,NI,NP,0)
```

C SET PARAMETERS

C Values of AKF, AKC, and PPC assume units of KJ/HR-C

```

ETATCF=PAR(1)
TBROK=PAR(2)
TSTAG=PAR(3)
AKF=PAR(4)
AKC=PAR(5)
TFMIN=PAR(6)
CPF=PAR(8)
NEQM=NEQ-1
ETACON=ETATCF/(TSTAG-TBROK)
ETADEL=TBROK+273.
RETURN

```

*C-- SET INPUTS

```

5 QLOAD=XIN(1)
TCUT=XIN(2)+273.
FLOWC=XIN(3)*CPF
QAUX=0.

```

*C-- Tell SST to use Heat Pump

```

LHP=1
IF (TIME.EQ.TIME0)GOTO 50

```

```

PPC=QLOAD
FLOWE=AKF
IF(PPC.LE.0.) GO TO 50
TTC=TCUT+PPC*AMAX1((1/AKC-0.5/FLOWC),0.)

```

*C-- NSTOC = Number of nodes necessary for extraction

*C-- Next line density of water = 1000 kg/m3

```

HPVOL=FLOWE/1000./CPF
NSTOC=INT(HPVOL/VCEL)+1
IF (NSTOC .GT. 1) THEN
WRITE(*,*)Heat Pump requires average temperature of more than

```

1 one SST node. Do not use buffers.'

END IF

*C-- Check if store can directly supply load

DO 12 I=1,NEQ

TSTO(I)=T(I)

IF (TSTO(I).GE.(TCUT-273.)) THEN

LHP=0

GOTO 50

END IF

12 CONTINUE

NEQM=MIN0(NEQ-1,NEQ-NSTOC+1)

TFIN=TSTO(NEQM)+273.

AA=1/AKF-0.5/FLOWE

TKF=TTC*FLOWE

PKF=PPC*(1+FLOWE*AA)

10 CONTINUE

TPF=TTC*(PPC-FLOWE*TFIN)

TRES=PPC*TTC+PPC*FLOWE*AA*TFIN

TFUT=(TRES-ETATCF*TPF)/(ETATCF*TKF+PKF)

XFN=FLOWE*(TFIN-TFUT)*AA

IF(TTC-TFUT+XFN.LT.ETADEL)GOTO 11

ETANOL=ETATCF+ETACON*(ETADEL-TTC-FLOWE*AA*TFIN)

ETAONE=ETACON*(1+FLOWE*AA)

RA=ETAONE*TKF

RB=ETANOL*TKF+ETAONE*TPF+PKF

RC=ETANOL*TPF-TRES

RX=RB*RB-4*RA*RC

IF(RX.LT.0) GOTO 15

TFUT=(-RB+SQRT(RX))/2./RA

11 CONTINUE

OUT(1)=TFUT-273.

```

      IF(OUT(1).GT.TFMIN) GOTO 17
15  CONTINUE
      IF(NEQM.LE.1) THEN
        QAUX=QLOAD
        IF(TIME.GT.9550) THEN
          WRITE(16,*)'NEQM LE 1 @ TIME=',TIME
          DO 16 J=1,NEQ
16  WRITE(16,*)TSTO(J)
          END IF
          GOTO 50
        END IF
        NEQM=NEQM-1
        TFIN=TSTO(NEQM)+273.
        GOTO 10

```

```

17  CONTINUE
*C   Ready for output
      PPF=FLOWE*(TFIN-TFUT)
      PPEL=PPC-PPF

      OUT(2)=FLOWE/CPF
      OUT(3)=PPF
      OUT(4)=PPC
      OUT(5)=PPEL
      OUT(6)=PPC/PPEL
      IF(OUT(6).LE.PAR(7))THEN
        QAUX=QLOAD
        GOTO 50
      END IF
      OUT(7)=TFIN-273.
      OUT(8)=0.
      RETURN

```

```

50  CONTINUE

```

```

C   AUX HEATER USED OR NO LOAD
      OUT(1)=TFIN-273.

```

```
OUT(2)=0.  
OUT(3)=0.  
OUT(4)=0.  
OUT(5)=0.  
OUT(6)=1.  
OUT(7)=0.  
OUT(8)=QAUX  
RETURN  
END
```

* Log mean temperature difference Pipe Model

SUBROUTINE TYPE31(TIME,XIN,OUT,T,DT,PAR,INFO)

DIMENSION XIN(2),OUT(4),PAR(6),INFO(10)

PI = 3.14159265

OUT(6)=3

TENV = PAR(1)

ROUT = PAR(2)

RIN = PAR(3)

COND = PAR(4)

PLEN = PAR(5)

CPF = PAR(6)

TIN = XIN(1)

FLW = XIN(2)

IF (FLW .GT. 0.) THEN

UA = 3.6*(2*PI*COND*PLEN)/(ALOG(ROUT/RIN)) !kJ/Hr-C

CAP = FLW*CPF

DTIN = (TIN - TENV)

DTOUT = DTIN*(1.-EXP(-UA/CAP))

TOUT = TIN - DTOUT

QLOSS = FLW*CPF*(TIN - TOUT)

ELSE

TOUT = TIN

QLOSS = 0.

END IF

OUT(1) = TOUT

OUT(2) = FLW

OUT(3) = QLOSS

RETURN

END

```

*****
* Subroutine to determine heating season. The value of gamma
* (1 for heating season) determines the load in house model
*****
      SUBROUTINE TYPE40(SIMTIM,XIN,OUT,TDUM,DTDUM,PAR,INF)
      REAL PAR(4),OUT(2),XIN(1)
      INTEGER INF(10)
      INTEGER GAMMA

      IF (INF(7) .GE. 0) GOTO 5
      INF(6) = 2
      INF(9) = 1

      NI=1
      NP=4
      ND=0

      CALL TYPECK(1,INF,NI,NP,ND)
5      CONTINUE

      LASTDAY=PAR(1)
      FIRSTDAY=PAR(2)
      TTH=PAR(3)
      Adjust=PAR(4)
      XIN(1)=TA

C*!Hour 1 is from midnite to 1 a.m.
      HOUR=SIMTIM-1.
      LDAY=INT(HOUR/24.)+1
      DO WHILE (LDAY .GT. 365)
        LDAY=LDAY - 365
      END DO

      DEG=0.
      IF (LDAY .GT. LASTDAY .AND. LDAY .LT. FIRSTDAY) THEN
        GAMMA = 0
      ELSE
        GAMMA = 1
      IF (TA.LT.0.)DEG=INT(TA)
      TTH = TTH - 0.5*DEG
      END IF

      OUT(1) = TTH
      OUT(2) = GAMMA
      RETURN
END

```

```

*****
* Subroutine to determine flowrate for constant outlet
* temperature collector
*****

SUBROUTINE TYPE22(TIME,XIN,OUT,T,DTDT,PAR,INFO)
DIMENSION XIN(10), PAR(10), OUT(10), INFO(10)
REAL THOT,CPF,MAXFLW,MINFLW,TINC,QU,TOUTC,QUMIN

IF (INFO(7) .GE. 0) GOTO 5
INFO(6) = 3
INFO(9) = 1
NI=4
NP=4
ND=0
* CALL TYPECK(1,INF,NI,NP,ND)

THOT = PAR(1)
CPF = PAR(2)
MAXFLW = PAR(3)
MINFLW = PAR(4)

5 TINC = XIN(1)
QU = XIN(2)
TOUTC = XIN(3)
GAMMA = XIN(4)

IF (INFO(7) .GT. 48) OUT(1) = QU/(CPF*(TOUTC-TINC))
IF (OUT(1) .LT. MINFLW) OUT(1) = MINFLW
IF (OUT(1) .GT. MAXFLW) OUT(1) = MAXFLW

IF((TOUTC - TINC).LT.10..AND.OUT(1).EQ.MAXFLW)THEN
OUT(1)=MINFLW
END IF

IF (TOUTC .LT.(THOT-35.)) THEN
OUT(1) = 0.
END IF

OUT(2) = QU
RETURN
END

```

```

*****
*   Constant Load Outlet Temperature Subroutine
*****
      SUBROUTINE TYPE23(TIME,XIN,OUT,T,DTDT,PAR,INFO)
      REAL XIN(3), PAR(2), OUT(2)
      INTEGER INFO(10)
      COMMON/SIM/TIME0,TIMEF,DELT

      IF (INFO(7) .GE. 0) GOTO 5
      INFO(9) = 1
      NP=2
      ND=0
      NI=5
*C-- WITHOUT HEAT PUMP
      INFO(6) = 1
*C-- WITH HEAT PUMP
*   INFO(6)=2

      CALL TYPECK(1,INFO,NI,NP,ND)

      TSET=PAR(1)
      CPF = PAR(2)

5      THOT = XIN(1)
      TRET = XIN(2)
      QPIPE1 = XIN(3)
      QLOAD = XIN(4)
      TSTMX = XIN(5)

      QRET = QPIPE1 + QLOAD

*C-- NEXT LINE WITHOUT HEAT PUMP
      IF (TSTMX.LE. TSET+1.53 .OR. INFO(7).GT.46) QRET=0.

      IF (THOT.NE.TSET) OUT(1)=QRET/(CPF*(THOT-TSET))
      OUT(1)=AMAX1(OUT(1),0.)

*C-- This code added for heat pump model only (remember to change
*C-- TYPECK call.
*   QPIPE2=XIN(5)
*   QTOT=QRET+QPIPE2
*   OUT(2)=QTOT

      RETURN
      END

```

Appendix D: Comparison of April 15 Radiation Components

Key:

IH = global horizontal radiation (kJ/hr-m²)

IDN = direct normal radiation (kJ/hr-m²)

IBT = beam radiation on tilted surface (kJ/hr-m²)

IDT = diffuse radiation on tilted surface (kJ/hr-m²)

IT = total tilted surface radiation (kJ/hr-m²)

FRTAN = $F_R(\tau\alpha)_N$ = collector gain coefficient

LOSS = collector losses

AF = array factor = 0.88

FLW1 = minimum collector flowrate = 1E-3 (kg/s-m²)

- {1} MINSUN daily total collected energy/area before array factor or interpolation
- {2} TRNSYS daily total collected energy/area before array factor or collector control
- {3} MINSUN daily total collected energy/ area after interpolation [$T_i = 10^\circ\text{C}$,
 $T_o = 90^\circ\text{C}$, $(T_i + T_o) / 2 = 50^\circ\text{C}$]
- {4} MINSUN final daily total collected energy/ area after array factor
- {5} TRNSYS daily total collected energy/ area after collector control
- {6} TRNSYS final daily total collected energy/ area after array factor

TIME	IH	IDN	IBT	IDT	IT	FRTAN	LOSS@10°C	QU/A	
								(kJ/hr-m2)	
				MIN	SUN				
6	352.8	1526	59.8	132.1	191.8	0.75	142.6	1.3	
7	882.0	2462	707.7	176.6	884.3	0.75	123.8	539.4	
8	1458.0	2948	1529.1	216.9	1746	0.75	102.2	1207.3	
9	1958.4	3175	2276.7	253.4	2530	0.75	80.6	1816.9	
10	2307.6	3236	2812.9	280.7	3094	0.75	60.5	2259.7	
11	2574.0	3215	3100.9	369.3	3470	0.75	59.0	2543.6	
12	2638.8	3290	3280.0	328.0	3608	0.75	50.4	2655.6	
13	2610.0	3312	3191.8	345.5	3537	0.75	-1.4	2654.4	
14	2419.2	3283	2848.1	355.8	3204	0.75	-11.5	2414.4	
15	1972.8	2855	2040.2	416.0	2456	0.75	-17.3	1859.5	
16	1155.6	1836	946.8	353.7	1300	0.75	-23.0	998.4	
17	536.4	964.8	274.2	237.1	511.2	0.75	-20.2	403.6	
18	255.6	421.2	15.1	175.1	190.2	0.75	-14.4	157.0	
19	*0	97.2							
						Total MINSUN QU/A:		19511.1	{1}
*below critical value of 50 kJ/hr-m2									
				TRN	SYS				
6	352.8	1526	0.0	219.3	219.3	0.75	142.6	21.9	
7	882.0	2462	401.6	326.3	727.9	0.75	123.8	422.1	
8	1458.0	2948	1194.0	380.4	1574	0.75	102.2	1078.3	
9	1958.4	3175	1974.0	399.9	2374	0.75	80.6	1699.9	
10	2307.6	3236	2585.0	389.3	2974	0.75	60.5	2170.0	
11	2574.0	3215	2970.0	428.7	3399	0.75	59.0	2490.2	
12	2638.8	3290	3254.0	334.5	3588	0.75	50.4	2640.6	
13	2610.0	3312	3275.0	296.3	3572	0.75	-1.4	2680.4	
14	2419.2	3283	3035.0	254.7	3289	0.75	-11.5	2478.3	
15	1972.8	2855	2282.0	288.1	2570	0.75	-17.3	1944.8	
16	1155.6	1836	1142.0	250.9	1393	0.75	-23.0	1067.8	
17	536.4	964.8	391.3	175.8	567.1	0.75	-20.2	445.5	
18	255.6	421.2	69.0	146.9	215.9	0.75	-14.4	176.3	
19	46.8	97.2	0.0	35.16	35.16	0.75	8.6	17.7	
				Total TRNSYS QU/A (before Operational Control) :				19333.8	{2}

TIME	QU/A	LOSS@10°C (subtract)	LOSS@50°C (add)	QU/A (interpolated)		QU*AF (final)			
		MIN	SUN						
6	1.3	142.6	718.6	0.0		0.0			
7	539.4	123.8	699.8	0.0		0.0			
8	1207.3	102.2	678.2	631.3		555.5			
9	1816.9	80.6	656.6	1240.9		1092.0			
10	2259.7	60.5	636.5	1683.7		1481.7			
11	2543.6	59.0	635.0	1967.6		1731.5			
12	2655.6	50.4	626.4	2079.6		1830.1			
13	2654.4	-1.4	574.6	2078.4		1829.0			
14	2414.4	-11.5	564.5	1838.4		1617.8			
15	1859.5	-17.3	558.7	1283.5		1129.4			
16	998.4	-23.0	553.0	422.4		371.7			
17	403.6	-20.2	555.8	0.0		0.0			
18	157.0	-14.4	561.6	0.0		0.0			
	Total MINSUN QU/A:			13225.9	{3}	11638.8	{4}	Collector hours on = 9	
		TRN	SYS						
TIME	QU/A		QU*AF	Max To@Flw1	Collector on?	QU*AF (final)			
6	21.9		19.2852	11.3	No	0			
7	422.1		371.4	34.7	No	0			
8	1078.3		948.9	73.1	Yes	948.9			
9	1699.9		1495.9	109.4	Yes	1495.9			
10	2170.0		1909.6	136.9	Yes	1909.6			
11	2490.2		2191.4	155.6	Yes	2191.4			
12	2640.6		2323.7	164.4	Yes	2323.7			
13	2680.4		2358.8	166.8	Yes	2358.8			
14	2478.3		2180.9	154.9	Yes	2180.9			
15	1944.8		1711.4	123.7	Yes	1711.4			
16	1067.8		939.7	72.4	Yes	939.7			
17	445.5		392.0	36.1	No	0			
18	176.3		155.2	20.3	No	0			
19	17.7		15.6	11.0	No	0			
	Total TRNSYS QU/A:		17013.7	{5}		16060.2	{6}	Collector hours on = 9	

Appendix E: April 15 House Load Comparison

Shows difference in TRNSYS and MINSUN total daily house load is gain subtracted from MINSUN load for hours with no space heating.

Key:

UA and parameters from Appendix F

Copenhagen TMY data

Total Load is House Heating + DHW

Daily DHW Load is $2340 \text{ kJ/hr} * 550 \text{ houses} * 24 \text{ hours} = 3.088\text{E}07 \text{ kJ}$

Hourly Gain is $1440 \text{ kJ/hr} * 550 \text{ houses} = 7.920\text{E}05 \text{ kJ/hr}$

Total Values Match Those Reported in TRNSYS Summary and UMSORT Routines

Ta (°C)	Ta,r Ta<10. or 18.	UA Load UA*(18-Ta,r)	UA Load - GAIN
1.9	1.9	4.574E+06	3.782E+06
1.3	1.3	4.745E+06	3.953E+06
0.8	0.8	4.887E+06	4.095E+06
0.2	0.2	5.058E+06	4.266E+06
-0.2	-0.2	5.171E+06	4.379E+06
0.1	0.1	5.086E+06	4.294E+06
1.4	1.4	4.717E+06	3.925E+06
2.9	2.9	4.290E+06	3.498E+06
4.4	4.4	3.864E+06	3.072E+06
5.8	5.8	3.466E+06	2.674E+06
5.9	5.9	3.438E+06	2.646E+06
6.5	6.5	3.267E+06	2.475E+06
10.1	18.0	0.000E+00	0.000E+00
10.8	18.0	0.000E+00	0.000E+00
11.2	18.0	0.000E+00	0.000E+00
11.6	18.0	0.000E+00	0.000E+00
11.4	18.0	0.000E+00	0.000E+00
11.0	18.0	0.000E+00	0.000E+00
9.4	9.4	2.444E+06	1.652E+06
8.4	8.4	2.728E+06	1.936E+06
6.4	6.4	3.296E+06	2.504E+06
6.5	6.5	3.267E+06	2.475E+06
5.7	5.7	3.495E+06	2.703E+06
5.0	5.0	3.694E+06	2.902E+06
Average =	7.5167	7.149E+07	5.723E+07
		<u>MINSUN</u>	<u>TRNSYS</u>
UA Load		5.248E+07	5.723E+07
DHW Load		3.088E+07	3.088E+07
TOTAL	1)	8.336E+07	2) 8.812E+07

1) Daily UA + 24*(DHW - GAIN) = 7.149E+07 - 24*(7.92E+05)

2) Sum ((hourly UA - GAIN) > 0) + 24*DHW

**Appendix F TRNSYS Deck for Comparison Simulation
of Lyckebo System**

```
*****
*      MINSUN COMPARISON SIMULATION PROGRAM      *
*      LYCKEBO SYSTEM          JAN 89  DLK        *
*****
```

```
* 1 YEAR SIMULATION
SIMULATION 2160 10920 1.0
TOLERANCES .00001 .00001
LIMITS 50 10 50
```

```
CONSTANTS 20
  START = 2160
  FTIME = 1E6
*---Collector parameters
  AREA = 28.8E03
  LAT = 55.68
  FUL = 4.0 * 3.6
  SLOCOLL = 42.
  ACON = 0.75
  GTEST = 50.
  TOUT = 90.
  CPF = 4.18
  MINFLW = 0.002 * 3600. * AREA
  MAXFLW = .2 * 3600. * AREA
*---Storage Volume parameters
  VOLSTO = 105E03
  HT = 30.0
*---House load parameters
  TSET = 18.0
  UAHSE = 516.6 * 550
  FLOAD = 1E5
  DHW = 2340 * 550
  GAIN = 1440 * 550
  TENV = 10.
```

WIDTH 72

UNIT 9 TYPE 9 CARD READER

*For weather data

PARAMETERS 13

*READ IN DRY TA, DNI, IH LUN of input data, fmt

3 1 -1 0.1 0 -2 3.6 0 -3 3.6 0 10 1

(T23,F5.0,T35,F4.0,T39,F4.0)

*TRACE START FTIME

UNIT 16 TYPE 16 RAD PCR

PARAMETERS 6

*1:I and Idn as input

*2:Fixed surface

*3:Start day 1

*4:Latitude

*5:Solar constant

*6:Hour angle shift

5 1 91 LAT 4871.0.

INPUTS 7

*1:Global rad

*2:Direct Normal

*3:Last reading

*4:Next reading

*5:Ground reflectance

*6:Collector Slope

*7:Gamma

9,3 9,2 9,19 9,20 0,0 0,0 0,0
0 0 0 2.0 0.0 SLOCOLL 0.0

*TRACE START FTIME

UNIT 33 TYPE 3 PUMP

*Pump into collector from tank

PARAMETERS 1

*Max coldside flow

MINFLW

INPUTS 3

*Ti, Mi, cntrl fnc

32,1 22,1 2,1
0.0 0.0 0.0

*TRACE START FTIME

UNIT 1 TYPE 1 COLLECTOR

PARAMETERS 11

*1:Linear efficiency mode

*2: Number of collectors in series
 *3: Total collector area
 *4: Specific heat of collector fluid
 *5: Efficiency mode
 *6: Test flowrate
 *7: Intercept efficiency
 *8: Slope efficiency
 *9: Effectiveness of heat exchanger
 *10: Cold side of htex fluid
 *11: No Bo

1.0 1.0 AREA CPF 1.0 GTEST
 ACON FUL -1 0.0 0.0

INPUTS 5

*1: Temp of inlet to cold side htex
 *2: Mass flowrate of collector
 *3: Mass flowrate of htex cold side
 *4: Ambient temp
 *5: Tilted incident radiation
 *6: Global horizontal
 *7: Horiz diffuse
 *8: ground reflectance
 *9: incidence angle
 *10: collector slope

33,1 33,2 0,0 9,1 16,6
 * 16,4 16,5 0,0 16,9 0,0

0.0 0.0 0.0 0.0 0.0
 * 0.0 0.0 0.0 0.0 SLOCOLL

*TRACE START FTIME

UNIT 2 TYPE 2 CONTROLLER

PARAMETERS 3

5 1 1

INPUTS 3

*upper input, lower input, control fcn
 1,1 0,0 2,1
 0.0 60. 0.0

*TRACE START FTIME

UNIT 22 TYPE 22 CONS

PARAMETERS 4

*1:Desired Tout

*2:CPF

*3:Initial flowrate

*4:Min flowrate

TOUT CPF MAXFLW MINFLW

INPUTS 3

*1:T_in of collector

*2:Qu of collector

*3:T_out of collector

33,1 1,3 1,1

0.0 0.0 0.0

*TRACE START FTIME

UNIT 31 TYPE 31 COLLECTOR RETURN PIPE

PARAMETERS 6

*1:TENV (C)

*2:Outside pipe diameter (m)

*3:Inside pipe diameter (m)

*4:Conductivity of insulation (W/m-K)

*5:Length of pipe (m)

*6:Fluid heat capacity (kJ/kg-C)

TENV 0.16 0.1 0.04 5000 CPF

INPUTS 2

*1:Inlet temp

*2:Mass flow rate

1,1 1,2

0.0 0.0

*TRACE START FTIME

UNIT 35 TYPE 31 LOAD RETURN PIPE

PARAMETERS 6

*1:TENV (C)

*2:Outside pipe diameter (m)

*3:Inside pipe diameter (m)

*4:Conductivity of insulation (W/m-K)

*5:Length of pipe (m)
 *6:Fluid heat capacity (kJ/kg-C)

TENV 0.165 0.045 0.04 3700 CPF

INPUTS 2

*1:Fluid Inlet Temperature
 *2:Mass flow rate

12,1 12,2
 0.0 0.0

UNIT 39 TYPE 39 SST TANK

PARAMETERS 26

*VOLST=PAR(1)	TANK VOLUME (m3)
*HEIGHT=PAR(2)	TANK HEIGHT (m)
*THISO=PAR(3)	THICKNESS INSULATION
*FRIST=PAR(4)	REL. WT. OF INSULATION (TOP)
*FRISS=PAR(5)	" " " " (SIDES)
*FRISB=PAR(6)	" " " " (BOTTOM)
*RISLAM=PAR(7)	THERMAL COND. OF INSULATION (W/M-K)
*DEPTH=PAR(8)	DISTANCE BETW GROUND & TOP OF TANK
*TSTIN=PAR(9)	INITIAL TEMP IN STORAGE VOLUME
*CWATER=PAR(10)	VOLUMETRIC HEAT CAP. OF FLUID (J/C-M3)
*WFLOWX=PAR(11)	(IF RLSTO>0) (M3 H2O/DAY)/VOLUME
*RLSTO=PAR(12)	CHAR. LENGTH OF DISPERSION TERM (M)
*DISPER=PAR(13)	DARCY POWER
*RLAMST=PAR(14)	THERMAL COND. OF STORAGE VOL (W/M-K)
*CSTO=PAR(15)	VOLUMETRIC HEAT CAPACITY FOR STORAGE (J/C M3)
*TIMO3=PAR(16)	DURATION OF SIMULATION (YEARS)
*IPRE=PAR(17)	NO. OF PRE-HEAT CYCLES
*TCMAX=PAR(18)	MAX PRE-HEAT STORE TEMP
*TA_IN=PAR(19)	AIR TEMP DURING PRE-HEAT
*TSTART=PAR(20)	INITIAL GROUND SURFACE TEMP (C)
*TGRAD=PAR(21)	TEMP GRADIENT OF TSTART (usually negative)
*NEQ = PAR(22)	NUMBER OF NODES
*ILAY=PAR(23)	NO. GROUND LAYERS W/ DIFF THERMAL PROPS
*RLAML=PAR(24+3)	THERMAL COND. IN A LAYER (W/mK)
*CL=PAR(25+3)	VOLUMETRIC HEAT CAP IN A LAYER (J/m3K)
*THL=PAR(26+3)	THICKNESS OF A LAYER (M)

VOLST 30 0.0 1 1
 1 0.05 30 45. 4.18E06
 1.0 0 1 0.6 4.18E06
 1 2.0 80 2.8 10 0.

10 1 3.5 2.0E6 2000.

INPUTS 13

*1:Fluid temp from solar collector
 *2:Fluid flow rate in collector loop
 *3:Demand temp for house heating loop
 *4:Return temp from house heating loop
 *5:Boundary temp at ground surface
 *6:Fluid flow rate in house heating loop
 *7:Demand temp for tap water loop
 *7:Collector extraction temperature
 *8:Return temp form tap water loop
 *9:Fluid flow rate in tap water loop
 *10:House heating evaporator flow
 *11:Tap water evaporator flow
 *12:Return temp from tap evaporator
 *13:Return temp from house evaporator

31,1 31,2 40,1 35,1 9,1
 35,2 0,0 0,0 0,0 0,0
 0,0 0,0 0,0

0 0 0 0 0
 0 0 0 0 0
 0 0 0

*TRACE START FTIME

UNIT 32 TYPE 31 COLLECTOR FORWARD PIPE PARAMETERS 6

*1:TENV (C)
 *2:Outside pipe diameter (m)
 *3:Inside pipe diameter (m)
 *4:Conductivity of insulation (W/m-K)
 *5:Length of pipe (m)
 *6:Fluid heat capacity (kJ/kg-C)
 TENV 0.16 0.1 0.04 5000 CPF

INPUTS 2

*1:Inlet temp
 *2:Mass flow rate
 39,1 39,2
 0.0 0.0

*TRACE START FTIME

UNIT 34 TYPE 31 LOAD FORWARD PIPE
PARAMETERS 6

*1:TENV (C)
*2:Outside pipe diameter (m)
*3:Inside pipe diameter (m)
*4:Conductivity of insulation (W/m-K)
*5:Length of pipe (m)
*6:Fluid heat capacity (kJ/kg-C)

TENV 0.165 0.045 0.04 3700 CPF

INPUTS 2

*1:Fluid Inlet Temperature
*2:Mass flow rate

39,3 39,5
0.0 0.0

*TRACE 2184. 2232

UNIT 40 TYPE 40 SEASON
PARAMETERS 4

*1:Last day of Heating Season
*2:First day of Heating Season
*3:TTH On
*4:TTH Off

135 255 60. 60.

INPUTS 1

9,1
0.0

*TRACE START FTIME

UNIT 12 TYPE 12 HOUSE
PARAMETERS 5

*1:Nominal TRET
*2:UA
*3:T_room set temp
*4:DHW hourly load
*5:Cp of heat source fluid

45. UAHSE TSET DHW CPF

INPUTS 5

*1:Temp of fluid from heat source

*2:Mass flow fluid from heat source

*3:Tamb

*4:Q_gain

*5:Seasonal controller

34,1 23,1 9,1 0,0 40,2

0 0 0 GAIN 0

*TRACE START FTIME

UNIT 23 TYPE 23 CONST

PARAMETERS 2

*1:Desired load return temp

*2:CPF

45. CPF

INPUTS 5

*1:T_hot to load (from store)

*2:T_ret from load (from HOUSE)

*3:Pipe loss

*4:House load

*5:Max Store Temp

39,3 12,1 34,3 12,3 39,11

0.0 0.0 0.0 0.0

*TRACE START FTIME

UNIT 24 TYPE 28 SIM SUM

PARAMETERS 9

*1:No. of hours for summary

*2:Begin time

*3:End time

*4:Logical Unit Number for Output

*5:Output mode

*6:1st input on top

*7:Output

*8:Next input on top

*9:Output

-1 START FTIME 6 2 -11 -4 -12 -4

INPUTS 2

34,3 35,3
 LABELS 2
 QLFWD QLRET

UNIT 25 TYPE 28 SIM SUM
 PARAMETERS 14
 *1:No. of hours for summary
 *2:Begin time
 *3:End time
 *4:Logical Unit Number for Output
 *5:Output mode
 *6:1st input on top
 *7:Output
 *8:Next input on top
 *9:Output

-1 START FTIME 6 2 1 0
 0 -4 -4 0 -4 0 -4 0 -4

INPUTS 4
 39,8 39,9 39,6 39,7
 LABELS 4
 QINJ DU QENV QEXT
 CHECK 2, 1, -2, -3, -4

UNIT 27 TYPE 28 SIM SUM
 PARAMETERS 22
 *1:No. of hours for summary
 *2:Begin time
 *3:End time
 *4:Logical Unit Number for Output
 *5:Output mode
 *6:1st input on top
 *7:Output
 *8:Next input on top
 *9:Output

-1 START FTIME 6 2 -11 -12
 3 -13 3 -3 -14 -3 -7 2 7
 -1 1. 3 -4 -15 -4

INPUTS 5
 12,3 34,3 35,3 12,5 1,3
 LABELS 4

QLOAD QAUX FSOL QCOLL

UNIT 28 TYPE 28 SIM SUM

PARAMETERS 13

*1:No. of hours for summary

*2:Begin time

*3:End time

*4:Logical Unit Number for Output

*5:Output mode

*6:1st input on top

*7:Output

*8:Next input on top

*9:Output

-1 START FTIME 6 2 -11 -4

-12 -4 -13 -4 -14 -4

INPUTS 4

1,2 1,3 32,3 31,3

LABELS 4

KGFLWC QU QCFWD QCRET

UNIT 26 TYPE 28 SIM SUM

PARAMETERS 21

*1:No. of hours for summary

*2:Begin time

*3:End time

*4:Logical Unit Number for Output

*5:Output mode

*6:1st input on top

*7:Output

*8:Next input on top

*9:Output

-1 START FTIME 6 2 -11 -1 CPF 1 -4

-12 -3 -13 -3 3 -14 -3 3 -4 -15 -4

INPUTS 5

12,2 12,3 34,3 35,3 12,5

LABELS 6

HCF HLOAD P31L P32L QLTOT QAUX

END

Appendix G TRNSYS Deck for Comparison Simulation
of Franklin System

NOLIST

* MINSUN COMPARISON SIMULATION PROGRAM *

* FRANKLIN SYSTEM JAN 89 DLK *

* 1 YEAR SIMULATION

SIMULATION 2160 10920 1.0

TOLERANCES .00001 .00001

LIMITS 50 10 50

CONSTANTS 18

START = 2160.

FTIME = 1E6

*---Collector parameters

AREA = 3500.

LAT = 42.0

FUL = 3.5 * 3.6

SLOCOLL = 42.

ACON = 0.77

GTEST = 50.

CPF = 4.18

MINFLW = 0.005 * 3600. * AREA

*---Storage Volume parameters

VOLSTO = 15000.

HT = 10.0

*---House load parameters

TSET = 18.0

UAHSE = 1260. * 100

FLOAD = 1E5

DHW = 278.64 * 100

GAIN = 1440 * 100

TENV = 10.

WIDTH 72

UNIT 9 TYPE 9 CARD READER

*For weather data

PARAMETERS 13

*READ IN GLOBAL, DRY TA, DNI, LUN of input data, frmt

3 1 -1 1 0 -2 1 0 -3 1 0 10 1

(T10,F7.2,T20,F6.2,T30,F7.2)

*TRACE START FTIME

UNIT 16 TYPE 16 RAD PCR

PARAMETERS 6

- *1:I and Idn as input
- *2:Fixed surface
- *3:Start day 1
- *4:Latitude
- *5:Solar constant
- *6:Hour angle shift

5 1 91 LAT 4871. 0.

INPUTS 7

- *1:Global rad
- *2:Direct Normal
- *3>Last reading
- *4:Next reading
- *5:Ground reflectance
- *6:Collector Slope
- *7:Gamma

9,1 9,3 9,19 9,20 0,0 0,0 0,0
0 0 0 2.0 0.0 SLOCOLL 0.0

*TRACE START FTIME

UNIT 33 TYPE 3 PUMP

*Pump into collector from tank

PARAMETERS 1

*Max coldside flow

MINFLW

INPUTS 3

*Ti, Mi, cntrl fnc

32,1 0,0 2,1
0.0 MINFLW 0.0

*TRACE START FTIME

UNIT 1 TYPE 1 COLLECTOR

PARAMETERS 12

- *1:Linear efficiency mode
- *2:Number of collectors in series
- *3:Total collector area

*4:Specific heat of collector fluid
 *5:Efficiency mode
 *6:Test flowrate
 *7:Intercept efficiency
 *8:Slope efficiency
 *9:Effectiveness of heat exchanger
 *10:Cold side of htex fluid

1.0 1.0 AREA CPF 1.0 GTEST
 ACON FUL -1 0.0 1.0 0.1

INPUTS 10

*1:Temp of inlet to cold side htex
 *2:Mass flowrate of collector
 *3:Mass flowrate of htex cold side
 *4:Ambient temp
 *5:Tilted incident radiation
 *6:Global horizontal
 *7:Horiz diffuse
 *8:ground reflectance
 *9:incidence angle
 *10:collector slope

33,1	33,2	0,0	9,2	16,6
16,4	16,5	0,0	16,9	0,0
0.0	0.0	0.0	0.0	0.0
0.0	0.0	0.2	0.0	SLOCOLL

*TRACE START FTIME

UNIT 2 TYPE 2 CONTROLLER

PARAMETERS 3

3 2 2

INPUTS 3

*upper input, lower input, control fcn
 1,1 39,1 2,1
 0.0 0.0 0.0

*TRACE START FTIME

UNIT 31 TYPE 31 COLLECTOR RETURN PIPE

PARAMETERS 6

*1:TENV (C)
 *2:Outside pipe diameter (m)
 *3:Inside pipe diameter (m)
 *4:Conductivity of insulation (W/m-K)
 *5:Length of pipe (m)
 *6:Fluid heat capacity (kJ/kg-C)
 TENV 0.16 0.1 0.04 350 CPF

INPUTS 2

*1:Inlet temp
 *2:Mass flow rate
 1,1 1,2
 0.0 0.0

*TRACE START FTIME

UNIT 35 TYPE 31 LOAD RETURN PIPE

PARAMETERS 6

*1:TENV (C)
 *2:Outside pipe diameter (m)
 *3:Inside pipe diameter (m)
 *4:Conductivity of insulation (W/m-K)
 *5:Length of pipe (m)
 *6:Fluid heat capacity (kJ/kg-C)

TENV 0.20 0.1 0.04 225 CPF

INPUTS 2

*1:Fluid Inlet Temperature
 *2:Mass flow rate

12,1 12,2
 0.0 0.0

*TRACE START FTIME

UNIT 39 TYPE 39 SST TANK

PARAMETERS 26

*VOLST=PAR(1)	TANK VOLUME (m3)
*HEIGHT=PAR(2)	TANK HEIGHT (m)
*THISO=PAR(3)	THICKNESS INSULATION
*FRIST=PAR(4)	REL. WT. OF INSULATION (TOP)
*FRISS=PAR(5)	" " " " (SIDES)
*FRISB=PAR(6)	" " " " (BOTTOM)
*RISLAM=PAR(7)	THERMAL COND. OF INSULATION (W/M-K)

*DEPTH=PAR(8) DISTANCE BETW GROUND & TOP OF TANK
 *TSTIN=PAR(9) INITIAL TEMP IN STORAGE VOLUME
 *CWATER=PAR(10) VOLUMETRIC HEAT CAP. OF FLUID (J/C-M3)
 *WFLOWX=PAR(11) (IF RLSTO>0) (M3 H2O/DAY)/VOLUME
 *RLSTO=PAR(12) CHAR. LENGTH OF DISPERSION TERM (M)
 *DISPER=PAR(13) DARCY POWER
 *RLAMST=PAR(14) THERMAL COND. OF STORAGE VOL (W/M-K)
 *CSTO=PAR(15) VOLUMETRIC HEAT CAPACITY FOR STORAGE (J/C M3)
 *TIMO3=PAR(16) DURATION OF SIMULATION (YEARS)
 *IPRE=PAR(17) NO. OF PRE-HEAT CYCLES
 *TCMAX=PAR(18) MAX PRE-HEAT STORE TEMP
 *TA_IN=PAR(19) AIR TEMP DURING PRE-HEAT
 *TSTART=PAR(20) INITIAL GROUND SURFACE TEMP (C)
 *TGRAD=PAR(21) TEMP GRADIENT OF TSTART (usually negative)
 *NEQ = PAR(22) NUMBER OF NODES
 *ILAY=PAR(23) NO. GROUND LAYERS W/ DIFF THERMAL PROPS
 *RLAML=PAR(24+3) THERMAL COND. IN A LAYER (W/mK)
 *CL=PAR(25+3) VOLUMETRIC HEAT CAP IN A LAYER (J/m3K)
 *THL=PAR(26+3) THICKNESS OF A LAYER (M)

VOLST	HT	1.0	0.4	0.1
0.0	0.05	.0	20.	4.18E06
5.0	0	1	0.6	4.18E06
2	2.0	80	7.04	10 0.033
10	1	2.0	2.0E6	2000.

INPUTS 13

*1:Fluid temp from solar collector
 *2:Fluid flow rate in collector loop
 *3:Demand temp for house heating loop
 *4:Return temp from house heating loop
 *5:Boundary temp at ground surface
 *6:Fluid flow rate in house heating loop
 *7:Demand temp for tap water loop
 *7:Collector extraction temperature
 *8:Return temp form tap water loop
 *9:Fluid flow rate in tap water loop
 *10:House heating evaporator flow
 *11:Tap water evaporator flow
 *12:Return temp from tap evaporator
 *13:Return temp from house evaporator

31,1	31,2	40,1	35,1	9,2
35,2	0,0	0,0	0,0	20,2
0,0	0,0	20,1		

0 0 0 0 0
 0 0 0 0 0
 0 0 0

*TRACE START FTIME

UNIT 32 TYPE 31 COLLECTOR FORWARD PIPE

PARAMETERS 6

*1:TENV (C)
 *2:Outside pipe diameter (m)
 *3:Inside pipe diameter (m)
 *4:Conductivity of insulation (W/m-K)
 *5:Length of pipe (m)
 *6:Fluid heat capacity (kJ/kg-C)

TENV 0.16 0.1 0.04 350 CPF

INPUTS 2

*1:Inlet temp
 *2:Mass flow rate

39,1 39,2

0.0 0.0

*TRACE START FTIME

UNIT 20 TYPE 20 HEAT PUMP

PARAMETERS 8

*1:Value of constant portion of efficiency curve
 *2:Temperature difference between TH and TL at which efficiency declines (C)
 *3:Temperature difference between TH and TL at which stagnation occurs (C)
 *4:Evaporator heat transfer coefficient times area (kJ/Hr-K)
 *5:Condenser heat transfer coefficient times area (kJ/Hr-K)
 *6:Minimum temperature for operation of heat pump (C)
 *7:Minimum COP for operation
 *8:Heat capacity of water from store and in house loop (kJ/kg-C)

0.6 50. 100. 3.6E5 2.16E5 20. 1. CPF

INPUTS 3

*1:Total system Load
 *2:Desired temperature to load
 *3:Load flowrate

23,2 40,1 23,1

0.0 0.0 0.0

*TRACE START FTIME

UNIT 34 TYPE 31 LOAD FORWARD PIPE
PARAMETERS 6

*1:TENV (C)
*2:Outside pipe diameter (m)
*3:Inside pipe diameter (m)
*4:Conductivity of insulation (W/m-K)
*5:Length of pipe (m)
*6:Fluid heat capacity (kJ/kg-C)

TENV 0.20 0.1 0.04 225 CPF

INPUTS 2

*1:Fluid Inlet Temperature
*2:Mass flow rate

40,1 23,1
0.0 0.0

*TRACE 5088 8016

UNIT 40 TYPE 40 SEASON
PARAMETERS 4

*1:Last day of Heating Season
*2:First day of Heating Season
*3:TTH
*4:TTH Adjust

152 258 70. 0.5

INPUTS 1

9,2
0.0

*TRACE START FTIME

UNIT 12 TYPE 12 HOUSE
PARAMETERS 5

*1:Nominal TRET
*2:UA
*3:T_room set temp
*4:DHW hourly load
*5:Cp of heat source fluid

55. UAHSE TSET DHW CPF

INPUTS 5

*1:Temp of fluid from heat source

*2:Mass flow fluid from heat source

*3:Tamb

*4:Q_gain

*5:Seasonal controller

34,1	23,1	9,2	0,0	40,2
0	0	0	GAIN	0

*TRACE 2184. 2232

UNIT 23 TYPE 23 CONST

PARAMETERS 2

*1:Desired load return temp

*2:CPF

55. CPF

INPUTS 5

*1:T_hot to load (from store)

*2:T_ret from load (from HOUSE)

*3:Pipe loss

*4:House load

*5:Pipe2 loss

40,1 12,1 34,3 12,3 35,3

0.0 0.0 0.0 0.0 0.0

*TRACE START FTIME

UNIT 24 TYPE 28 SIM SUM

PARAMETERS 13

*1:No. of hours for summary

*2:Begin time

*3:End time

*4:Logical Unit Number for Output

*5:Output mode

*6:1st input on top

*7:Output

*8:Next input on top

*9:Output

-1 START FTIME 6 2 -11 -3 -12 -3 2 -4 -13 -4

INPUTS 3

20,4 20,5 20,3

LABELS 4

Qcond Wel COP QEVP

UNIT 25 TYPE 28 SIM SUM
PARAMETERS 14

*1:No. of hours for summary
*2:Begin time
*3:End time
*4:Logical Unit Number for Output
*5:Output mode
*6:1st input on top
*7:Output
*8:Next input on top
*9:Output

-1 START FTIME 6 2 1 0
0 -4 -4 0 -4 0 -4 0 -4

INPUTS 4
39,8 39,9 39,6 39,7
LABELS 4
QINJ DU QENV QEXT
CHECK 2, 1, -2, -3, -4

UNIT 27 TYPE 28 SIM SUM
PARAMETERS 22

*1:No. of hours for summary
*2:Begin time
*3:End time
*4:Logical Unit Number for Output
*5:Output mode
*6:1st input on top
*7:Output
*8:Next input on top
*9:Output

-1 START FTIME 6 2 -11 -12
3 -13 3 -3 -14 -3 -7 2 7
-1 1. 3 -4 -15 -4

INPUTS 5
12,3 34,3 35,3 20,8 1,3
LABELS 4
QLOAD QAUX FSOL QCOLL

UNIT 28 TYPE 28 SIM SUM

PARAMETERS 17

*1:No. of hours for summary

*2:Begin time

*3:End time

*4:Logical Unit Number for Output

*5:Output mode

*6:1st input on top

*7:Output

*8:Next input on top

*9:Output

-1 START FTIME 6 2 -11 -4

-12 -4 -13 -4 -14 -4 -15 -4 -16 -4

INPUTS 6

1,3 32,3 31,3 12,3 34,3 35,3

LABELS 6

QU QCFWD QCRET QHSE QLFWD QLRET

END

List of Figures

Figure	Page
2.1	Node Representation of Net Flow Model
2.2	Plug Flow Model
2.3	Example Cross-Sectional Storage Volume Shapes Compatible with the SST
2.4	Example Ground Mesh Generated by the SST
2.5	Heat Flow Between Adjacent Ground Cells
2.6	Conduction Flow from Ground Cell (i,j) to Storage Node jj is Proportional to Fraction XX_j
2.7	Storage Volume Cells in the Ground
2.8	24 Hour Buffer System
2.9	Demand Temperature Delivered to Load is Available With Either Fixed or Variable Extraction
2.10	Sinusoidally Varying Lumped Temperature Imposed on Store During Pre-Heat
2.11	Heat Pump Model
2.12	Heat Pump Effectiveness Curve
3.1	The Lyckebo CSHPSS System
3.2a	Hourly Heat Source Injection Temperatures for September, 1987; Electric

	Boiler Energy Mimics the Daily Contribution of Solar Energy	48
3.2b	Hourly Heat Source Injection Temperatures for November, 1987: Electric Boiler Continuously Supplies Energy to the Storage Volume	48
3.2c	Hourly Heat Source Temperatures for January, 1987; No Energy is Supplied to the Storage Volume	49
3.2d	Hourly Load Flowstream Storage Extraction and Return Injection Temperatures for January, 1987	49
3.3	Lyckebo Cavern Temperature Profiles for March 1 and November 1, 1987	50
3.4	Schematic of Lyckebo Heating Plant Showing Locations for Data Measurement	52
3.5	Chronology of Lyckebo Data Use for SST Model Validation	55
3.6	Crack System in Lyckebo Cavern Act as a Thermosiphon	58
3.7	Daily Average Density of Water in Cavern vs. Day of Simulation	60
3.8a	Measured and Simulation (without Buffers) June 1987 Storage Profiles	66
3.8b	Measured and Simulation (without Buffers) Sept. 1987 Storage Profiles	66
3.9	Thermosiphon Flowrate vs. Density	67
3.10a	Measured and Simulation (with Buffers) June 1987 Storage Profiles	69
3.10b	Measured and Simulation (with Buffers) Sept. 1987 Storage Profiles	69
3.11	Predicted 1987 Annual Losses at Higher Rock Conductivities	73
3.12	Monthly 1987 Measured Losses for Lyckebo Cavern and Simulated Losses with $k=7.0$ and for Thermosiphon Loss Model	75
3.13a	10 Node Profiles After 4 Months for No, 24 Hour and Full Buffers	78
3.13b	30 Node Profiles After 4 Months for No, 24 Hour and Full Buffers	78
3.14a	Storage Profiles after 5 Months Simulation for 10, 30, and 100 Nodes	82
3.14b	Monthly Ground Losses for 10, 30, and 100 Nodes	82

4.1	Schematic of Agreed Configuration for TRNSYS vs. MINSUN Comparison	87
4.2	Comparison of Lyckebo Cavern Average Storage Temperatures on Last Day of Month	108
4.3a,b	Comparison of Useful Collected and Ground Loss Energies for Lyckebo Simulation	109
4.3c,d	Comparison of Load and Auxiliary Energies for Lyckebo Simulation	110
4.4	Schematic of Configuration for Franklin School Comparison	112
4.5	Comparison of Franklin School Average Storage Temperatures on Last Day of Month	116
4.6a,b	Monthly System Load and Q_u for Franklin System	117
4.6c,d	Monthly Ground Losses and Auxiliary Energies for Franklin System	118
4.7a,b	Heat Pump Condenser and Direct to Load Energies	119
4.8	Monthly Heat Pump Compressor Energies	120

List of Tables

Table	Page
1.1 Comparison of Small and Large CSHPSS Systems	8
2.1 SST Versions and Their Features	16
3.1 Description of Lyckebo CSHPSS System	46
3.2 Annual Energy Balances for the Lyckebo Cavern	50
3.3 Available Lyckebo Data	51
3.4 Lyckebo Operational Data Monthly Energy Balance for 1987 Simulation Year	54
3.5 TRNSYS SST Parameters Used in Validation Simulation	62
3.6 Preliminary Results for Validation Simulation	64
3.7 Thermosiphon Losses as Percent of Total Ground Losses	67
3.8 Full Buffer Results for Validation Simulation	71
4.1 Schedule of TRNSYS vs. MINSUN Test Simulations	89
4.2 TRNSYS vs. MINSUN SST Design of Daily Updates	91
4.3 TRNSYS Collector Strategy for Constant Temperature Outlet	94

		208
4.4	"UMSORT" Example Output	96
4.5	MINSUN Collector Strategy for Constant Temperature Outlet	97
4.6	List of MINSUN Collector Subsystem Assumptions	99
4.7	Summary of April 15 Total Qu/A Calculation Results	101
4.8	List of MINSUN Load Subsystem Assumptions	102
4.9	MINSUN Load Calculations	104
4.10	Annual Summaries of Franklin School System Performance	114

Nomenclature

English Letter Symbols

COP	= coefficient of performance
C_p	= specific heat ($J/kg^{\circ}C$)
E_{env}	= storage energy losses to surrounding ground (kJ)
E_{in}	= energy injected into storage (kJ)
E_{out}	= energy extracted from storage (kJ)
ΔE_s	= internal energy change of storage (kJ)
f	= solar fraction
$F_R U_L$	= negative of slope of efficiency vs. $(T_i - T_a)/I_T$ ($W/m^2^{\circ}C$)
G	= conductance ($W/^{\circ}C$)
h	= heat transfer coefficient ($W/m^2-^{\circ}C$)
h_{jj}	= height of storage volume node (m)
H_{jj}	= conductive energy flow from ground cell to node jj
H_s	= height of store (m)
I	= integrated hourly radiation on a horizontal surface ($kJ/hr-m^2$)
I_b	= integrated hourly beam radiation on a horizontal surface ($kJ/hr-m^2$)
I_{dn}	= integrated hourly direct normal radiation on a horizontal surface ($kJ/hr-m^2$)

I_d	= integrated hourly diffuse radiation on a horizontal surface (kJ/hr-m^2)
I_T	= integrated hourly radiation on a tilted surface (kJ/hr-m^2)
k	= thermal conductivity ($\text{W/m-}^\circ\text{C}$)
L	= length (m)
\dot{m}	= mass flow (kg/hr)
Q	= energy flow (kJ/hr or W)
Q_u	= useful collected energy (kJ)
R	= inner radial coordinate of ground cell (m)
RI	= heat resistance due to thermal insulation between ground cells ($\text{m}^2\text{-}^\circ\text{C/W}$)
RM	= radial coordinate of midpoint of ground cell (m)
T	= temperature ($^\circ\text{C}$)
$\Delta\tau$	= timestep (seconds)
t	= time (seconds)
T_a	= ambient temperature ($^\circ\text{C}$)
UA	= total heat transfer coefficient - area product ($\text{kJ/hr-}^\circ\text{C}$)
V	= volume (m^3)
\dot{V}	= volumetric flowrate (m^3/s)
W	= work (kJ)
Z	= vertical coordinate (m)
ZM	= vertical coordinate of midpoint of ground cell (m)

Greek Letter Symbols

ϵ = effectiveness

θ_z = solar azimuth angle (degrees)

ω = solar hour angle (degrees)

References

Andersson, B., "Opening Address", *Proceedings*, North Sun '88 - Solar Energy at High Latitudes International Conference, Swedish Council for Building Research, Stockholm, Sweden, pp. 23-24, 1988.

Bankston, C., "Central Solar Heating Plants with Seasonal Storage - Evaluation of Concepts", International Energy Agency Solar Heating and Cooling Task VII, U.S. Department of Energy Report #T.7.2.B., Washington, D.C., 1986.

Bankston, C. "A Summary of Central Solar Heating Plants with Seasonal Storage", *Advances in Solar Energy Technology*, Proceedings of the Biennial Congress of the International Solar Energy Society, Hamburg, FRG, Vol. 2, pp. 1227-1231, 1987.

Breger, D., "Preliminary Design Report - A Central Solar Heating Plants with Seasonal Storage for the Tri-County Regional Vocational Technical School in Franklin, Massachusetts", Seasonal Storage Development Company, Millers Falls, Ma., 1988.

Breger, D., personal communication, April, 1989.

Brunström, C. and Hillström, C., "The Lyckebo Project: Solar District Heating with Seasonal Storage in a Rock Cavern - Evaluation and Operational Experience", Swedish

Council for Building Research, Document D20, 1987(a).

Brunström, C., Efring, B., and Claesson, J., "The Lyckebo Project: Heat Losses from the Rock Cavern Storage", *Advances in Solar Energy Technology*, Proceedings of the Biennial Congress of the International Solar Energy Society, Hamburg, FRG, Vol. 2, pp. 1262-1266, 1987(b).

Brunström, C., personal communication, August, 1988.

Chant, V., "Central Solar Heating Plants with Seasonal Storage - The MINSUN Simulation and Optimization Program Application and User's Guide", International Energy Agency Solar Heating and Cooling Task VII, National Research Council, Document #CENSOL2, Ottawa, Ontario Canada, 1985.

(CRC), *Handbook of Chemistry and Physics*, Chemical Rubber Company, Cleveland, Ohio, 54th ed., 1973.

Dalenbäck, J., "Large- Scale Swedish Solar Heating Technology - System Design and Rating", Swedish Council for Building Research, Stockholm, Sweden, Report D6, 1987(a).

Dalenbäck, J. and Jilar, T., "Swedish Solar Heating with Seasonal Storage - Economical Prospects Today", *Advances in Solar Energy Technology*, Proceedings of the Biennial Congress of the International Solar Energy Society, Hamburg, FRG, Vol. 2, pp. 1252-1255, 1987(b).

Duffie, J. and Beckman, W., *Solar Engineering of Thermal Processes*, Wiley-Interscience, New York, 1980.

Eftring, B., "Stratified Storage Temperature Model - Manual for Computer Code", Department of Mathematical Physics, University of Lund, Sweden, 1983.

Erbs, D., *Models and Applications for Weather Statistics Related to Building Heating and Cooling Loads*, Dissertation, University of Wisconsin - Madison, 1984.

Krischel, D., "Comparison of Concepts for Central Solar Heating Plants with Seasonal Storage", *Intersol 85*, Proceedings of the Ninth Biennial Congress of the International Solar Energy Society, Montreal, Vol. 2, pp. 848-852, 1985.

Krischel, D. and H. Kiupel, "Solare Wärmeversorgung mit zentralem Kollektorfeld und Langzeitspeicher", Bundesministerium für Forschung und Technologie, Report FB-T 86-202, December 1986.

Krischel, D., personal communication, May, 1988.

Kuhn, J., von Fuchs, G., and Zob, A., "Developing and Upgrading of Solar System Thermal Energy Storage Simulation Models", Boeing Computer Services Company, Report BCS-40319, Seattle, WA., 1980.

Lund, P., "Performance Comparison of Storage Control Strategies in CSH PSS

Systems", *Journal of Solar Energy Engineering*, Vol. 109, pp. 185-191, 1987.

Öfverholm, E., "The Swedish Solar Heating Program", *Proceedings*, North Sun '88 - Solar Energy at High Latitudes International Conference, Swedish Council for Building Research, Stockholm, Sweden, pp. 25-30, 1988.

Sellberg, B., "Energy Storage - A Necessity for Solar Heating Systems", *Proceedings*, North Sun '88 - Solar Energy at High Latitudes International Conference, Swedish Council for Building Research, Stockholm, Sweden, pp. 145- 150, 1988.

Wallentun, H., Holst, P., and Zinko, H., "Performance and Operating Results for the Solar District Heating Plant at Lyckebo, Uppsala Sweden", Studsvik Energiteknik AB, Nyköping, Sweden, Report EI-85/46, 1985.

Wallentun, H. and Östergren, A., "The Lyckebo Rock Cavern Storage", Studsvik Energiteknik AB, Nyköping, Sweden, (Format III - A level), 1986.

Wallentun, H., "MINSUN Simulation of the Lyckebo Plant", *Advances in Solar Energy Technology*, Proceedings of the Biennial Congress of the International Solar Energy Society, Hamburg, FRG, Vol. 2, pp. 1267-1271, 1987.